Robust Gain-Scheduled Observer Design with Application to Vehicle State Estimation

by

Yan Wang

A dissertation submitted to the Graduate Faculty of
Auburn University
in partial fulfillment of the
requirements for the Degree of
Doctor of Philosophy

Auburn, Alabama
December 13th, 2014

Keywords: Linear Matrix Inequalities (LMIs), Linear Parameter Varying (LPV) Systems, Vehicle State Estimation

Approved by

David M. Bevly, chair, Mechanical Engineering
John Y. Hung, Electrical and Computer Engineering
Subhash Sinha, Mechanical Engineering
George Flowers, Mechanical Engineering

Abstract

This dissertation develops an application of the state-of-the-art convex optimization algorithms to the vehicle state estimation problem. The main challenge in this field is that the time-varying uncertain parameters and nonlinearity are both contained in the vehicle dynamical models. In the automotive control systems products, the gain-scheduled control and estimation algorithms are widely used to deal with these difficult components. However, the tuning of the stable controller and observer parameters is a heuristic and time-consuming task. A vast amount of simulation and validation experiments have to be implemented to verify the performance of the algorithm. Sometimes, the trial-and-error cycle is inevitable. Therefore, an efficient gain-scheduled observer design methodology for both linear and nonlinear systems is the main topic of this dissertation.

First, the linear-parameter-varying (LPV) representation of the three degree-of-freedom (DOF) bicycle model is presented, where the longitudinal velocity and acceleration are treated as the online measurable time-varying parameters. The LPV design methodology overcomes some eminent drawbacks of the traditional gain scheduled design methods. In the LPV framework, the search of the globally convergent observer parameters are resorted to a semidefinite programming problem. It is also shown that some robust controller design methods can be applied to develop an optimal unstructured LPV observer.

Next, the LPV observer is extended to a gain-scheduled interval observer where the variation range of the uncertain cornering stiffness parameters is incorporated into the observer design. Instead of a single estimation curve for each state variable, the interval observer computes the lower and upper bounds of all the admissible values of the states in the presence of parametric uncertainty. For automotive active safety systems, this envelope provides

an estimation of the worst case bounds for the critical vehicle state under uncertain road conditions.

Although the gain-scheduled interval observer directly takes the uncertain cornering stiffness parameters into consideration, the tire-road friction is a highly complex nonlinear phenomenon such that the linear observer is far from satisfactory in some extreme maneuvers. To further improve the performance of the estimation algorithm, a nonlinear observer design methodology is also developed for a class of differentiable Lipschitz continuous nonlinear systems. Since the nonlinear bicycle model also contains the time-varying parameters, the time invariant nonlinear observer is further augmented to a gain scheduled nonlinear observer.

The simulation results demonstrate the validity of the proposed gain-scheduled observer design to provide accurate and robust estimation of vehicle states, such as tire slip angles in the presence of time-varying parameters and nonlinearities.

All the vehicle state estimation algorithms proposed in this dissertation are verified by using the simulation data from CarSim, a commercial vehicle simulation software package. Additionally, all the observer design methodologies are formulated in a high-level systematic approach, which allow them to be applied to other systems.

Acknowledgments

First and foremost, I would like to thank all of people who encouraged and supported me during the undertaking of this research.

I would present my deep appreciation to my supervisor Prof. David M. Bevly, for giving me the precious opportunity to join in the GPS and Vehicle Dynamics Lab and conduct such an interesting Ph.D. dissertation project. He, with his strong scientific personality, guided this work and discussed with me in many aspects.

I would like to express my sincere gratitude to my Ph.D. program committee members, Dr. John Y. Hung, Dr. Subhash Sinha, and Dr. George Flowers, for their guidance and advice. They have been a constant source of inspiration, encouragement and assistance during this dissertation work, both in my academic studies and more.

Special thanks to my wife Jinjin Wu and my parents, relatives and all my friends for their continuous support and stimulation of my perseverance in my research activities. Without them this work would have been monumentally harder to carry out.

Table of Contents

Abstract ii

Acknowledgments iv

List of Figures viii

List of Tables xi

1 Introduction 1

1.1 Motivation 1

1.2 Contributions 2

1.3 Dissertation Outline 4

2 Preliminaries 5

2.1 Linear Fractional Representation (LFR) 5

2.2 Linear Matrix Inequalities (LMIs) 7

2.2.1 Definition of LMI and BMI 8

2.2.2 Convexity 9

2.2.3 Congruence Transformation and Schur Complement 9

2.2.4 Feasibility and Optimization 11

2.2.5 Application of LMIs in Observer Design for LTI Systems 13

2.3 Dissipativity 16

2.3.1 Definition 16

2.3.2 Applications in Control 18

2.4 S-Procedure 22

2.5 Stability Analysis of A Lure System 23

2.6 Conclusions 27

3 Linear Parameter Varying (LPV) Observer Design for Three DOF Bicycle Model 28

3.1 Introduction of LPV Technique 28
3.1.1 LPV Modeling 29
3.1.2 Stability Analysis of LPV Systems 31
3.1.3 LPV Controller 34
3.1.4 A Numerical Example 37
3.2 LPV Observer Design for The Bicycle Model 41
3.2.1 LPV Representation of The Bicycle Model 42
3.2.2 LPV Observer Design with Perfect Knowledge of Scheduling Parameter 46
3.2.3 LPV Observer Design with Uncertain Scheduling Parameter 48
3.3 Simulation Results 69
3.4 Conclusions 78
4 LPV Interval Observer Design with Uncertain cornering Stiffness 79
4.1 Introduction 79
4.2 Notation and Background 81
4.2.1 Metzler Matrix 82
4.2.2 Positive Linear Systems 82
4.2.3 Interval Observer for A LTI System with Uncertain Input 82
4.2.4 Lyapunov Stability for The Positive Linear Systems 83
4.3 Interval Observer Design for LTI Systems with Parametric Uncertainty . . . 83
4.3.1 LTI Interval Observer Design 84
4.4 Interval Observer Design for LPV Systems 88
4.4.1 Gain-Scheduled Interval Observer 89
4.4.2 Gain-Scheduled Interval Observer with L2 Gain Minimization 93
4.5 Robust Slip Angle Estimation 94
4.5.1 3 DOF Bicycle Model 95
4.5.2 LPV Interval Observer Design 97
4.5.3 Simulation Results 98

4.6 Conclusions 100
5 Gain Scheduled Nonlinear Observer Design 102
5.1 Introduction 102
5.2 Observer Design for Nonlinear Time Invariant Systems 106
5.2.1 Problem Statement 106
5.2.2 Sector Condition for e and $\phi(t, e)$ 108
5.2.3 Sufficient Stability Condition for *Lure* System 111
5.2.4 Search for The Observer Gains L_1, L_2 112
5.2.5 Nonlinear Optimal *L2* Observer Design 116
5.3 Observer Design for Parameter Varying Nonlinear (PVNL) Systems 119
5.3.1 Convergent Gain-Scheduled Nonlinear Observer Design 120
5.3.2 Gain-Scheduled Nonlinear Optimal *L2* Observer Design 122
5.3.3 Finite Dimensional Relaxation 123
5.4 Simulation Examples 129
5.4.1 Van der Pol Oscillator 129
5.4.2 Slip Angle Estimation 132
5.5 Conclusions 138
6 Conclusions and Future Work 140
6.1 Concluding Remarks 140
6.2 Future Work 141
6.2.1 Sensor Fusion with Camera, Radar and Lidar 141
6.2.2 Moving Horizon Estimation using Multi-Parametric Programming . . 142
Bibliography 144

List of Figures

2.1 Upper and lower linear fractional representation 5

2.2 Lure System 24

2.3 Sector Condition 25

2.4 Passivity Condition 26

3.1 The state trajectory with fixed parameters 33

3.2 The state trajectory with varying parameters 34

3.3 Simulation results of the tank lever control system with a gain scheduled PI controller. 42

3.4 Bicycle Model 42

3.5 The block diagram of the uncertain plant model and the unstructured observer 55

3.6 The polytopic space for the scheduling parameters $\frac{1}{v_x}$ and $\frac{a_x}{v_x}$. 64

3.7 The screen shot of the simulation. 70

3.8 Longitudinal velocity and acceleration profile in the simulation. 70

3.9 The simulation results of gain scheduled observer in tire side angle estimation. . 72

3.10 The simulation results of the optimal H_2 LPV Luenberger observer with $\epsilon_1 = -0.04$, $\epsilon_2 = 0.06$. 74

3.11 The simulation results of the optimal H_∞ LPV Luenberger observer with $\epsilon_1 = -0.04$, $\epsilon_2 = 0.06$. 74

3.12 The simulation results of the optimal H_2 LPV unstructured observer with $\epsilon_1 = -0.04$, $\epsilon_2 = 0.06$. 75

3.13 The simulation results of the optimal H_∞ LPV unstructured observer with $\epsilon_1 = -0.04$, $\epsilon_2 = 0.06$. 75

3.14 The simulation results of the optimal H_2 LPV Luenberger observer with $\epsilon_1 = -0.10$, $\epsilon_2 = 0.15$. 76

3.15 The simulation results of the optimal H_∞ LPV Luenberger observer with $\epsilon_1 = -0.10$, $\epsilon_2 = 0.15$. 77

3.16 The simulation results of the optimal H_2 LPV unstructured observer with $\epsilon_1 = -0.10$, $\epsilon_2 = 0.15$. 77

3.17 The simulation results of the optimal H_∞ LPV unstructured observer with $\epsilon_1 = -0.10$, $\epsilon_2 = 0.15$. 78

4.1 Bicycle Model 95

4.2 Trajectory of double lane change maneuver 98

4.3 Cornering stiffness curves for the front and rear tires 99

4.4 Relationship between slip angles and lateral tire forces 99

4.5 Simulation results of the nominal observer 100

4.6 Simulation results of the interval observer 101

5.1 Lure-System Representation of the Observer Error System 107

5.2 Simulation Results for The State Observation 131

5.3 Simulation Results for The Phase Portrait 131

5.4 A typical curve of the nonlinear tire model in Eq. (5.63) 133

5.5 The lookup table for the longitudinal velocity and acceleration scheduled observer gains. 137

5.6 The steering angle of fishhook. 137

5.7 The longitudinal velocity and acceleration profile in the simulation. 138

5.8 The simulation results of gain scheduled nonlinear observer and the LPV observer in the fishhook maneuver. 139

List of Tables

Chapter 1

Introduction

1.1 Motivation

The first automobile powered by an internal combustion engine was built by Karl Benz more than one hundred years ago. Since then, the vehicle technologies have been continuing to evolve such that the motor vehicle always represents the latest technical achievements in the fields of mechanical, material, electrical and information engineering. Nowadays, the automobile has already become a computer-driven high-tech product. Hundreds of micro controllers are mounted on a single vehicle that govern the operation from complex power-train systems to body control systems. Especially, the ever-increasing demand for safety and driving comfort makes the major OEMs and suppliers invest heavily on the research and development of safety and advanced driver assistance systems (ADAS). Various automotive active safety systems, such as anti-lock braking systems (ABS), traction control (TC), cruise control (CC) and electronic stability control (ESC), are becoming standard installations for all the vehicles on the market. All these electronic control units (ECU) aim at keeping the vehicle away from crash and maintaining the stability. The stability of the vehicle is affected by crucial factors, such as tire-road friction forces, side slip angle, rollover index and so on. However, no commercial vehicles are equipped with sensors that can directly measure these signals due to either cost concerns or technical challenges. This dilemma provides a need for an algorithm that can efficiently and accurately estimate those critical vehicle states. Therefore, vehicle state estimation attracts numerous researchers both from industry and academia. It is also an important technique in one of today's most popular research fields — autonomous vehicle driving systems.

Generally, the vehicle state estimation algorithm can be classified as two categories: kinematic approach and dynamical model based approach. The kinematic approach relies on the geometry of motion together with the measurements from inertial measurement units (IMU) and some advanced vehicle velocity sensors, such as GPS receiver, lidar and radar, to estimate the speed related signals. Due to the lack of verification from physical laws, the measurement error has a huge impact on the estimation accuracy in this approach. The dynamical model based approach incorporates a physical model in the estimator, which partially overcomes the disadvantage of high sensitivity to the quality of sensor signals in the kinematic approach. However, the highly nonlinear and uncertain vehicle dynamic models make the design of the robust controller or estimator extremely challenging. This dissertation aims at providing a systematic approach for the robust nonlinear vehicle state estimator design such that those nonlinear and time-varying uncertain dynamical models can be treated in a rigorous way. The research results also prove that the linear matrix inequalities (LMIs) based convex optimization algorithms is a powerful tool in the systems and control theory.

1.2 Contributions

The main contributions of this dissertation are the following three aspects:

1) The linear parameter varying (LPV) modeling and control design technique aims at overcoming some critical weak points of the traditional gain-scheduled controller, such as local stability rather than global stability. Various significant theoretical breakthrough and successful applications were achieved in the past twenty years. Although the gain-scheduled controllers are very common in automotive control systems, old design techniques still dominate in real-world applications. The elegant LPV theoretical method has just appeared in automotive literature for a few years. This dissertation contributes an example that applies the LPV design methodology to develop the gain scheduled observer, in which the measured inertia signals, such as longitudinal velocity and acceleration, are treated as the scheduling parameters for slip angle estimation.

This result also relaxes the assumption of the constant longitudinal velocity that is used by many previous research papers. The robust design methods that minimize the estimation error resulting from the uncertainty of scheduling parameters are also discussed.

2) Another contribution is that a systematic interval observer design method for both linear-time-invariant (LTI) and linear-parameter-varying (LPV) systems with parametric uncertainty has been proposed and applied to the bicycle model, where the cornering stiffnesses are the uncertain parameters with known variation ranges. Unlike previous methods reported in the literature for LTI/LPV interval observers, the well-developed semidefinite programming (SDP) approach [58] [54] is proposed to search for the qualified observer gains, which result in a robustly stable and cooperative observer error dynamical system.

3) To take the nonlinearity in the tire-road friction model into consideration, a nonlinear observer design technique is developed in a unified framework for both time invariant and parameter varying Lipschitz nonlinear systems that are differentiable with respect to state variables. In addition to ensuring asymptotic convergence, extension of this observer design technique to optimization of a L_2 performance criterion is presented, which enables the observer to handle the unknown disturbance inputs. Next, augmentation of this technique to parameter varying nonlinear (PVNL) systems is developed. Different from methods suggested in the LPV literature, a simple but non-conservative finite dimensional relaxation method for quadratic parameter dependent LMIs is presented. These results constitute the first systematic observer design methodology in literature for PVNL systems to the best of the author's knowledge.

1.3 Dissertation Outline

This dissertation is organized as follows. First, some background knowledge in control theory is reviewed in Chapter 2. Next, linear parameter varying (LPV) modeling and observer design methodology is applied to the bicycle model for slip angle estimation in Chapter 3. Both perfect measurement and imperfect measurement with bounded error of the scheduling parameters is discussed in detail. In Chapter 4, the focus is on the gain-scheduled interval observer with uncertain cornering stiffness parameters. Finally, nonlinear tire-road friction is incorporated into the bicycle model in Chapter 5. With this nonlinearity, the observer development for time invariant differentiable nonlinear system and its augmentation to the parameter varying nonlinear (PVNL) system is presented in this chapter. The conclusions of this dissertation and recommendation for future research directions are stated in Chapter 6.

Chapter 2

Preliminaries

In this chapter, some background knowledge in control theory are briefly reviewed. These concepts will be referred to frequently in the later chapters of observer development.

2.1 Linear Fractional Representation (LFR)

Linear fractional representation (LFR) is a widely used modeling method in classical robust control theory. The basic idea is to represent the feedback loop as the interconnection of the generalized plant P and the controller K (lower LFR), or represent the uncertain process model as the interconnection of nominal model P and the uncertainty block Δ (upper LFR) [56] [38].

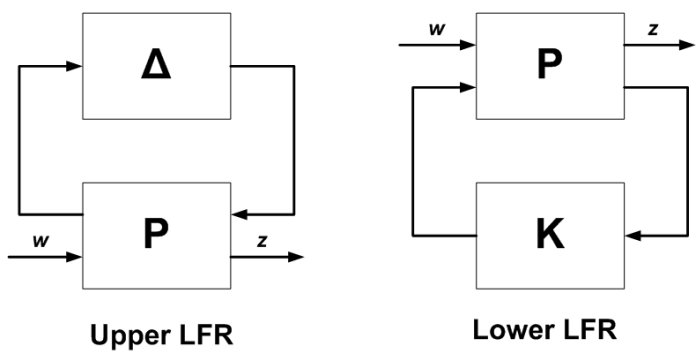

Figure 2.1: Upper and lower linear fractional representation

The transfer functions from the exogenous input w to the performance output z in the two cases are shown below.

- **Transfer Function for Upper LFR**

$$z = [P_{22} + P_{21}\Delta(I - P_{11}\Delta)^{-1}P_{12}]w \tag{2.1}$$

- **Transfer Function for Lower LFR**

$$z = [P_{11} + P_{12}K(I - P_{22}K)^{-1}P_{21}]w \tag{2.2}$$

where the transfer function matrix of the generalized plant P has the following form.

$$P(s) = \begin{pmatrix} P_{11}(s) & P_{12}(s) \\ P_{21}(s) & P_{22}(s) \end{pmatrix} \tag{2.3}$$

Here, it is implicitly assumed that the inter-connection in both cases are well-posed (no singular algebraic loop). LFR is the basis of many well-developed methods in linear robust control theory, such as μ analysis, H_∞ controller design and so on [56]. In this dissertation, the focus is the interconnection of the nominal model and the uncertainty block. In what follows, an example to illustrate how to derive the upper linear fractional representation for an uncertain LTI system whose state space matrices depend on the uncertainty parameter $\delta = (\delta_1, \ldots, \delta_k)^T$ affinely will be presented [54].

Suppose the following state space model with parametric uncertainty is given.

$$\begin{pmatrix} \dot{x} \\ z \end{pmatrix} = \begin{pmatrix} A(\delta) & B(\delta) \\ C(\delta) & D(\delta) \end{pmatrix} \begin{pmatrix} x \\ w \end{pmatrix} \tag{2.4}$$

The affine δ dependence implies

$$\begin{pmatrix} A(\delta) & B(\delta) \\ C(\delta) & D(\delta) \end{pmatrix} = \begin{pmatrix} A_0 & B_0 \\ C_0 & D_0 \end{pmatrix} + \sum_{i=1}^{k} \delta_i \begin{pmatrix} A_i & B_i \\ C_i & D_i \end{pmatrix} \tag{2.5}$$

The above matrices can be factorized as

$$\begin{pmatrix} A_i & B_i \\ C_i & D_i \end{pmatrix} = \begin{pmatrix} L_{i,1} \\ L_{i,2} \end{pmatrix} \begin{pmatrix} R_{i,1} & R_{i,2} \end{pmatrix} \tag{2.6}$$

where $\begin{pmatrix} L_{i,1} \\ L_{i,2} \end{pmatrix}$ and $\begin{pmatrix} R_{i,1} & R_{i,2} \end{pmatrix}$ have full column and row rank respectively. Such a factorization can be obtained by hand calculation and it is not unique in general. Then, the original system can be described as

$$\begin{aligned} \begin{pmatrix} \dot{x} \\ z \end{pmatrix} &= \begin{pmatrix} A_0 & B_0 \\ C_0 & D_0 \end{pmatrix} \begin{pmatrix} x \\ w \end{pmatrix} + \begin{pmatrix} L_{1,1} & \cdots & L_{k,1} \\ L_{1,2} & \cdots & L_{k,2} \end{pmatrix} \begin{pmatrix} w_1 \\ \vdots \\ w_k \end{pmatrix} \\ \begin{pmatrix} z_1 \\ \vdots \\ z_k \end{pmatrix} &= \begin{pmatrix} R_{1,1} & R_{1,2} \\ \vdots & \vdots \\ R_{k,1} & R_{k,2} \end{pmatrix} \begin{pmatrix} x \\ w \end{pmatrix} \end{aligned} \tag{2.7}$$

The vectors $(w_1 \cdots w_k)^T$ and $(z_1 \cdots z_k)^T$ are related by

$$\begin{pmatrix} w_1 \\ \vdots \\ w_k \end{pmatrix} = \begin{pmatrix} \delta_1 I & & \\ & \ddots & \\ & & \delta_k I \end{pmatrix} \begin{pmatrix} z_1 \\ \vdots \\ z_k \end{pmatrix} \tag{2.8}$$

where the size of the diagonal matrix $\delta_i I$ is equal to the number of columns or rows of $\begin{pmatrix} L_{i,1} \\ L_{i,2} \end{pmatrix}$ or $\begin{pmatrix} R_{i,1} & R_{i,2} \end{pmatrix}$ respectively. In the next chapter, this method to derive the linear fraction representation of the bicycle model with uncertain longitudinal velocity and acceleration parameters will be applied.

2.2 Linear Matrix Inequalities (LMIs)

Linear matrix inequalities (LMIs) were first applied in control system analysis by Yakubovich in the 1960s. Since 1990, the appearance of efficient numerical solvers, such as the ellipsoid method and the interior point algorithm, accelerated the application of LMIs to various engineering problems. Nowadays, it has become a standard numerical tool in control community

[58] [35] [54]. Many important methodologies in mathematical system theory and control, such as H_2/H_∞ control, robust model predictive control, linear-parameter-varying (LPV) controller design, system identification, hybrid control system analysis and development are based on this technique.

Although the LMIs used in some papers may have a very large dimension and look quite complicated, the application of LMIs can make the system analysis and controller design easier. In what follows, this powerful method is quickly reviewed.

2.2.1 Definition of LMI and BMI

A linear matrix inequality (LMI) is a special semidefinite constraint that has the following form [58] [54]:

$$F(x) = F_0 + x_1 F_1 + \cdots + x_m F_m \leq 0 \tag{2.9}$$

where $x = (x_1, \ldots, x_m)^T$ with $x_i \in R$ denotes the collection of all the decision variables. $F_i = F_i^T$, $i = 0, 1, \ldots, m$ are fixed symmetric real matrices. The symbol "$\leq$" represents a negative semidefinite constraint. Similarly, the positive semidefinite constraint can be defined by the symbol "$\geq$". From the above definition, the two following properties for $F(x)$ are obvious:

1. Each element in the matrix $F(x)$ is an affine function of x;

2. $F(x)$ is a symmetric matrix;

A bilinear matrix inequality is another special semidefinite constraint that has the following form [65]:

$$F(x, y) = F_0 + \sum_{i=1}^{m} x_i F_i + \sum_{j=1}^{n} y_i G_i + \sum_{i=1}^{m} \sum_{j=1}^{n} x_i y_j F_{i,j} \leq 0 \tag{2.10}$$

where $x = (x_1, \ldots, x_m)^T$, $y = (y_1, \ldots, y_n)^T$ with x_i, $y_j \in R$ denote the collection of all the decision variables. $F_i = F_i^T$, $G_i = G_i^T$, $F_{i,j} = F_{i,j}^T$, $i = 0, 1, \ldots, m$, $j = 1, \ldots, n$ are all fixed

symmetric real matrices. Similar as the LMI, $F(x, y)$ is a symmetric matrix. Different from the LMI, each element in the matrix $F(x, y)$ is a bi-affine function of x and y, which implies that the BMI degenerates to a LMI in x for fixed y and a LMI in y for fixed x.

Because the BMI is a more general semidefinite constraint than the LMI, they can describe much wider classes of constraint sets and can be used to represent more types of optimization and control problems. However, the main drawback of the BMI is that it is much more difficult to handle computationally than the LMI. In the application of control, several mathematical tricks are developed to transfer the BMI constraint to a LMI constraint. In what follows, concentration will be on the review of mathematical background of LMIs and its application in control. The BMI will be occasionally referred.

2.2.2 Convexity

As demonstrated in the following, the semidefinite condition for $F(x)$ is indeed a convex set for the x [54].

Lemma 1 *If the LMI in Eq. (2.9) is feasible, all the feasible points constitute a convex set.*

Proof: Suppose x and y are two feasible points, such as $F(x) \geq 0$ and $F(x) \geq 0$. Any point in the line segment between x and y can be represented as $\lambda x + (1 - \lambda)y$, $0 \leq \lambda \leq 1$. Then, the affine matrix function $F(\lambda x + (1 - \lambda)y)$ can be evaluated as

$$F(\lambda x + (1 - \lambda)y) = \lambda F(x) + (1 - \lambda)F(y) \geq 0 \tag{2.11}$$

2.2.3 Congruence Transformation and Schur Complement

Congruence transformation and Schur complement are two frequently used methods that transfer a BMI constraint to an equivalent LMI constraint [65]. From matrix theory, it is known that the congruence transformation does not change the number of positive, negative

and zero eigenvalues of a symmetric matrix. Therefore, an infinite number of equivalent LMIs can be derived.

Lemma 2 ***(Congruence Transformation)*** *The semidefinite condition $F(x) \leq 0$ in Eq. (2.9) or $F(x,y) \leq 0$ is feasible if and only if its congruence transformation is feasible.*

$$M^T F(x) M \leq 0, \quad N^T F(x,y) N \leq 0 \tag{2.12}$$

where M and N are both non-singular real matrices.

Lemma 3 ***(Schur Complement)*** *The real symmetric block matrix shown below is negative definite*

$$\begin{pmatrix} Q & S^T \\ S & R \end{pmatrix} \prec 0 \tag{2.13}$$

if and only if either of the following two sets of semidefinite constraints is feasible.

1) $Q \prec 0$ ***and*** $R - S^T Q^{-1} S \prec 0$

2) $R \prec 0$ ***and*** $Q - S R^{-1} S^T \prec 0$

where the symbol $\prec$ represents a negative definite constraint.

Proof: The Schur complement can be proven from the following two congruence transformations for the matrix $\begin{pmatrix} Q & S^T \\ S & R \end{pmatrix}$.

$$\begin{pmatrix} I & 0 \\ -SQ^{-1} & I \end{pmatrix} \begin{pmatrix} Q & S^T \\ S & R \end{pmatrix} \begin{pmatrix} I & -Q^{-1}S^T \\ 0 & I \end{pmatrix} = \begin{pmatrix} Q & 0 \\ 0 & R - SQ^{-1}S^T \end{pmatrix}$$

$$\begin{pmatrix} I & -S^T R^{-1} \\ 0 & I \end{pmatrix} \begin{pmatrix} Q & S^T \\ S & R \end{pmatrix} \begin{pmatrix} I & 0 \\ -R^{-1}S & I \end{pmatrix} = \begin{pmatrix} Q - S^T R^{-1} S & 0 \\ 0 & R \end{pmatrix}$$

Hence, the negative definite constraint in Eq. (2.13) is equivalent to the negative definite constraints on the diagonal blocks of its two congruence transformations.

One of the most frequently used applications of Schur complement in robust control theory is the linearization of the algebraic Riccati inequality (ARI).

$$A^T P + PA + PBR^{-1}B^T P + Q \prec 0 \tag{2.14}$$

where $R = R^T \succ 0$. The symmetric matrix P is the decision variable. This is a quadratic matrix inequality rather than a LMI due to its quadratic dependence on P. By applying Schur complement, the following equivalent LMI can be obtained

$$\begin{pmatrix} A^T P + PA + Q & PB \\ B^T P & -R \end{pmatrix} \prec 0 \tag{2.15}$$

where each element of the matrix on the left side depends affinely on the elements of P. It will be shown later that this LMI is the basis of H_∞ analysis of the LTI systems.

2.2.4 Feasibility and Optimization

Generally, the application of LMIs in control can be classified into two categories: feasibility and optimization problems [54].

1. **Feasibility Problem:** This aims at verifying whether there exists at least one point in the decision parameter space such that the given LMI constraint in Eq. (2.9) is feasible. The search for the candidate Lyapunov function for stability analysis is such an example, which will be shown later.

2. **Optimization Problem:** This aims at minimizing a linear cost function of x with the LMI in Eq. (2.9) as a constraint.

$$\begin{aligned} &\textbf{minimize } c^T x \\ &\textbf{subject to } F(x) \geq 0 \end{aligned} \tag{2.16}$$

Due to the convexity of the LMI constraint, this is indeed a convex optimization problem. The local minimum is just the global minimum [57].

Once the LMI problem is formulated, the numerical solvers, such Sedumi 1.3 or SDPT3, can be applied to verify the feasibility of the LMIs. If a linear cost function is given, the solver will return the global minimum of the convex optimization problem. To demonstrate the application of LMIs in control, a few examples are shown below.

1) **Lyapunov Stability Analysis**

This is a LMI feasibility problem, which aims at searching for a qualified Lyapunov function to verify the asymptotic stability of the LTI system, whose state equation has the form of $\dot{x} = Ax$. The LMIs for this problem are shown as what follows

$$P \succ 0, \quad A^T P + PA \prec 0 \tag{2.17}$$

where all the elements in the matrix P constitute the decision variables which the numerical solver searches for.

2) **Least Square with Linear Inequality Constraints**

This is an optimization problem, whose mathematical formulation is shown below

$$\begin{aligned} &\textbf{minimize } \|y - Hx\|_2^2 \\ &\textbf{subject to } Ax \leq b \end{aligned} \tag{2.18}$$

where y represents the measurement sequence and x denotes the collection of parameters to be estimated. H is assumed to be a matrix with full-column rank. The equivalent LMI optimization problem is formulated as the following form

$$\begin{aligned} &\textbf{minimize } \gamma \\ &\textbf{subject to } \begin{pmatrix} \gamma & (y-Hx)^T \\ y-Hx & I \end{pmatrix} \geq 0, \quad Ax \leq b \end{aligned} \tag{2.19}$$

where the LMI constraint comes from Schur complement of the scalar quadratic polynomial inequality $\gamma - \|y - Hx\|_2^2 \geq 0$. Due to reformulation, an additional decision variable γ is added to the original set of decision variables x.

2.2.5 Application of LMIs in Observer Design for LTI Systems

Due to the focus of this dissertation on the application of the LMIs in the observer design, an example to illustrate the LMI based observer design for the LTI system is presented in the remaining part of this section. The Luenberger observer is a well-structured estimator for a linear system. It is composed of a copy of the plant model and a linear output correction term.

Luenberger Observer: Given a linear system

$$\begin{aligned} \dot{x} &= Ax \\ y &= Cx \end{aligned} \tag{2.20}$$

The Luenberger observer has the following form

$$\dot{\hat{x}} = A\hat{x} + L(y - C\hat{x}) \tag{2.21}$$

where L is an observer gain such that $(A-LC)$ is a Hurwitz matrix. The stability region of L is defined by a set of polynomial inequalities, which is a non-convex set in general. Classical

ways of tuning the observer gain L are pole placement, steady-state continuous-time Kalman filter, etc. Tuning of the observer gain L can also be done through solving a set of matrix inequalities.

Convergence Conditions for Luenberger Observer: The observer state $\hat{x}$ in Eq. (2.21) will converge to the state x of the original system in Eq. (2.20) asymptotically, if the following define constraints are feasible

$$\begin{gathered} P \succ 0 \\ (A^T - C^T L^T)P + P(A - LC) \prec 0 \end{gathered} \tag{2.22}$$

where P and L are matrix decision variables. Unfortunately, the 2nd inequality in Eq. (2.22) is a bilinear matrix inequality due to the term PL, which is difficult to solve. Fortunately, the change of variable method (a 30-year old trick) helps us to linearize this matrix inequality [54].

Change of Variable Method: Suppose the matrix Q is defined as

$$Q = PL \tag{2.23}$$

Then, the bilinear matrix inequality condition in Eq. (2.22) becomes a linear matrix inequality condition as

$$\begin{gathered} P \succ 0 \\ (A^T P - C^T Q^T) + (PA - QC) \prec 0 \end{gathered} \tag{2.24}$$

where P and Q are matrix decision variables. If this LMI is feasible, the observer gain L can be constructed as

$$L = P^{-1} Q \tag{2.25}$$

However, the structured Luenberger observer is not the only option. In the robust control literature, the unstructured observer is often more popular [55] [48] [12].

Unstructured Observer: Given a linear system

$$\begin{aligned} \dot{x} &= Ax \\ y &= Cx \end{aligned} \tag{2.26}$$

The generalized unstructured observer has the following form

$$\dot{\hat{x}} = A_o\hat{x} + B_o y \tag{2.27}$$

where A_o, B_o are matrix decision variables that make the observer output signal $\hat{x}$ converge to x asymptotically. The observer error state equation is

$$\begin{aligned} \dot{x} - \dot{\hat{x}} &= (A - B_oC)x - A_o\hat{x} \\ &= (A - B_oC)(x - \hat{x}) + (A - A_0 - B_oC)\hat{x} \end{aligned} \tag{2.28}$$

If the Lyapunov function is chosen as $V = (x-\hat{x})^T P(x-\hat{x})$, $P \succ 0$, then the quadratic form of its derivative along the trajectory becomes

$$\begin{pmatrix} x - \hat{x} \\ \hat{x} \end{pmatrix}^T \begin{pmatrix} (A - B_oC)^T P + P(A - B_oC) & P(A - A_o - B_oC) \\ (A - A_o - B_oC)^T P & 0 \end{pmatrix} \begin{pmatrix} x - \hat{x} \\ \hat{x} \end{pmatrix} \tag{2.29}$$

The semidefinite constraint that guarantees the asymptotic convergence must has the following form

$$P \succ 0, \quad \begin{pmatrix} (A - B_oC)^T P + P(A - B_oC) & P(A - A_o - B_oC) \\ (A - A_o - B_oC)^T P & 0 \end{pmatrix} \prec 0 \tag{2.30}$$

where the matrices P, A_o and B_o are the decision variables. However, this semidefinite constraint depends on the decision variables bilinearly, which is difficult to find a feasible solution in general. Fortunately, the change variable method can still be applied to obtain

an equivalent LMI constraint shown below.

$$P \succ 0, \quad \begin{pmatrix} (A^T P + PA) - (C^T Q_2^T + Q_2 C) & PA - Q_1 - Q_2 C) \\ A^T P - Q_1^T - C^T Q_2^T) & 0 \end{pmatrix} \prec 0 \tag{2.31}$$

Once, the feasible matrix variables P, Q_1 and Q_2 are returned by the solver, the observer state space matrices A_o, B_o can be derived as

$$A_o = P^{-1} Q_1, \quad B_o = P^{-1} Q_2 \tag{2.32}$$

Unsurprisingly, the resulting observer always has exactly the same structure with the Luenberger observer

$$A_o = A - LC, \quad B_o = LC \tag{2.33}$$

where L is the feedback gain in the Luenberger observer. However, it will be shown that the unstructured observer may not have the same structure with the Luenberger observer in the presence of model uncertainty in the next chapter.

2.3 Dissipativity

Dissipativity theory has achieved much attention in the analysis of dynamical systems and controller design in the past twenty years [54]. The powerfulness of this method lies in the fact that it does not discriminate the linear and nonlinear systems in general. Therefore, many methods developed for linear systems can be easily extended to nonlinear systems. It is shown that many popular system analysis methods, such as L_2 gain analysis and integral quadratic constraint (IQC), are the special cases of dissipativity [45].

2.3.1 Definition

First, this section begins with a review of the definition of passivity which is a special case of the generalized dissipativity.

Definition of Passivity:

Passivity theory is an energy based method to analyze the stability of the ODE system using input-output relationship. It is one of the most commonly used design methodologies in nonlinear control literature.

Definition of Passivity [8]: *For the dynamical system represented by the state space model*

$$\begin{aligned} \dot{x} &= f(x,u) \\ y &= h(x,u) \end{aligned} \tag{2.34}$$

where $f : R^n \times R^p \to R^n$ *is locally Lipschitz,* $h : R^n \times R^p \to R^m$ *is continuous,* $f(0,0) = 0$*, and* $h(0,0) = 0$*. This system is said to be passive if there exists a continuously differentiable positive semidefinite function* $V(x)$ *(called a storage function) such that*

$$\dot{V} = \frac{\partial V}{\partial x} f(x,u) \leq u^T y, \quad \forall (x,u) \in R^n \times R^p \tag{2.35}$$

or

$$V(T) - V(0) \leq \int_0^T (u^T y) dt, \quad \forall (x,u) \in R^n \times R^p \tag{2.36}$$

Usually, the Lyapunov function is used as a storage function. Also, similar to the Lyapunov function, it is not necessary for the storage function to have physical interpretations [5]. For example, the inner product $\int_0^T (u^T y) dt$ may not represent the true energy flow into the system. However, many stability analysis results in physics are based on the the storage function and energy flow with clear physical interpretations, such as Hamiltonian mechanics and electrical circuit theory. In general, passivity is a conservative condition for stability.

Definition of Dissipativity:

Besides the inner product of input and output, other types of energy flow can also be applied. This leads to the more general dissipativity theory, which is the basis of some optimal control design methodologies.

Definition of Dissipativity [54] [3]: *For the dynamical system represented by the state space model in Eq. (2.34), this system is said to be dissipative w.r.t. the supply rate function $S(u, y)$ if there exists a continuously differentiable positive semidefinite function $V(x)$ (called the storage function) such that*

$$\dot{V} = \frac{\partial V}{\partial x} f(x, u) \leq S(u, y), \quad \forall (x, u) \in R^n \times R^p \tag{2.37}$$

or

$$V(T) - V(0) \leq \int_0^T S(u, y) dt, \quad \forall (x, u) \in R^n \times R^p \tag{2.38}$$

The supply rate function $S(u, y)$ is usually chosen as a general quadratic polynomial of u and y.

$$\begin{aligned} S(u, y) &= y^T Q y + 2 y^T S^T u + u^T R u \\ &= \begin{pmatrix} y^T & u^T \end{pmatrix} \begin{pmatrix} Q & S^T \\ S & R \end{pmatrix} \begin{pmatrix} y \\ u \end{pmatrix} \end{aligned} \tag{2.39}$$

$S(u, y) = u^T y$ in the passivity condition and $S(u, y) = 0$ in the stability condition are just special cases of the generalized supply rate function.

2.3.2 Applications in Control

In the remaining part of this section, a few examples that apply the dissipativity theory to the system analysis and design of control systems is presented.

Kalman-Yakubovich-Popov Lemma

For linear systems, the dissipativity inequality in terms of the state space model is connected with the frequency domain inequality through the Kalman-Yakubovich-Popov (KYP) Lemma [3].

Lemma 4 *(**Kalman-Yakubovich-Popov Lemma:**) For the following LTI system*

$$\dot{x} = Ax + Bu,\ y = Cx + Du \Longleftrightarrow T(s) = D + C(sI - A)^{-1}B \tag{2.40}$$

Suppose $(A,\, B)$ *is controllable. Then, there exists a positive definite matrix* P *satisfying the following dissipativity inequality,*

$$\begin{pmatrix} A^TP + PA & PB \\ B^TP & 0 \end{pmatrix} - \begin{pmatrix} C & D \\ 0 & I \end{pmatrix}^T \begin{pmatrix} Q & S^T \\ S & R \end{pmatrix} \begin{pmatrix} C & D \\ 0 & I \end{pmatrix} \leq 0 \tag{2.41}$$

if and only if the transfer matrix $T(s)$ *satisfies the frequency domain inequality (FDI) shown below.*

$$\begin{pmatrix} T(i\omega) \\ I \end{pmatrix}^* \begin{pmatrix} Q & S^T \\ S & R \end{pmatrix} \begin{pmatrix} T(i\omega) \\ I \end{pmatrix} \geq 0,\ \ \forall \omega \in R \cup \{\infty\},\ i\omega \notin \lambda(A) \tag{2.42}$$

The semidefinite condition in Eq. (2.41) is simply the multiplier matrix for the quadratic form of the dissipativity inequality in Eq. (2.37).

$$\begin{aligned} &\frac{\partial V}{\partial x} f(x,u) - S(u,y) = \\ &\begin{pmatrix} x \\ u \end{pmatrix}^T \left(\begin{pmatrix} A^TP + PA & PB \\ B^TP & 0 \end{pmatrix} - \begin{pmatrix} C & D \\ 0 & I \end{pmatrix}^T \begin{pmatrix} Q & S^T \\ S & R \end{pmatrix} \begin{pmatrix} C & D \\ 0 & I \end{pmatrix} \right) \begin{pmatrix} x \\ u \end{pmatrix} \end{aligned} \tag{2.43}$$

Positive Real Lemma

For linear systems, the positive real lemma relates the frequency domain inequality with the passivity condition in time domain [8]. It can be treated as a special case of the Kalman-Yakubovich-Popov lemma.

Lemma 5 ***(Positive Real Lemma:)*** *For the LTI system in Eq. (2.40), the following positive real condition is satisfied*

$$T^*(i\omega) + T(i\omega) \geq 0 \Longleftrightarrow \begin{pmatrix} T(i\omega) \\ I \end{pmatrix}^* \begin{pmatrix} 0 & 0.5I \\ 0.5I & 0 \end{pmatrix} \begin{pmatrix} T(i\omega) \\ I \end{pmatrix} \geq 0 \tag{2.44}$$

if and only if the LMI constraint shown below is feasible

$$\begin{pmatrix} A^TP + PA & PB \\ B^TP & 0 \end{pmatrix} - \begin{pmatrix} C & D \\ 0 & I \end{pmatrix}^T \begin{pmatrix} 0 & 0.5I \\ 0.5I & 0 \end{pmatrix} \begin{pmatrix} C & D \\ 0 & I \end{pmatrix} \leq 0 \tag{2.45}$$

Note: The LMI in Eq. (2.45) is just the multiplier matrix of the quadratic form of the following dissipativity inequality.

$$\dot{V} - u^Ty = x^T(A^TP + PA)x + 2x^TPBu - u^Ty \leq 0 \tag{2.46}$$

where the storage function $V = x^TPx$.

Bounded Real Lemma

The bounded real lemma is used for L_2 gain analysis of a LTI system in robust control theory [38] [54]. It is also treated as a special case of Kalman-Yakubovich-Popov lemma.

Lemma 6 ***(Bounded Real Lemma:)*** *For the LTI system in Eq. (2.40), its L_2 gain is upper bounded by γ as shown below,*

$$T^*(i\omega)T(i\omega) \geq \gamma^2 I \Longleftrightarrow \begin{pmatrix} T(i\omega) \\ I \end{pmatrix}^* \begin{pmatrix} -I & 0 \\ 0 & \gamma^2 I \end{pmatrix} \begin{pmatrix} T(i\omega) \\ I \end{pmatrix} \geq 0 \tag{2.47}$$

if and only if the LMI constraint shown below is feasible

$$\begin{pmatrix} A^T P + PA & PB \\ B^T P & 0 \end{pmatrix} - \begin{pmatrix} C & D \\ 0 & I \end{pmatrix}^T \begin{pmatrix} -I & 0 \\ 0 & \gamma^2 I \end{pmatrix} \begin{pmatrix} C & D \\ 0 & I \end{pmatrix} \leq 0 \tag{2.48}$$

The LMI in Eq. (2.48) is just the multiplier matrix of the quadratic form of the following dissipativity inequality

$$\dot{V} - (\gamma^2 u^T u - y^T y) = x^T (A^T P + PA)x + 2x^T PBu - (\gamma^2 u^T u - y^T y) \leq 0 \tag{2.49}$$

where the storage function $V = x^T P x$.

The bounded real lemma is the basis of the linear H_∞ control theory. By using Schur Complement and congruence transformation, a few matrix inequalities, each of which is equivalent to Eq. (2.48), can be derived [54].

- Two LMI conditions:

$$\begin{pmatrix} A^T P + PA + C^T C & PB + C^T D \\ B^T P + D^T C & D^T D - \gamma^2 I \end{pmatrix} \leq 0 \tag{2.50}$$

$$\begin{pmatrix} A^T P + PA & PB & C^T \\ B^T P & -\gamma I & D^T \\ C & D & -\gamma I \end{pmatrix} \leq 0 \tag{2.51}$$

- One quadratic matrix condition (algebraic Riccati inequality):

$$A^T P + PA + C^T C + (PB + C^T D)(\gamma^2 I - D^T D)^{-1}(B^T P + D^T C) \leq 0 \tag{2.52}$$

The semidefinite constraints in Eq. (2.50) and (2.52) are the same as those in Eq. (2.15) and (2.14) respectively, if the matrices D, Q and R satisfy the following conditions.

$$D = 0, \quad Q = C^T C, \quad R = \gamma^2 I$$

2.4 *S*-Procedure

The S-Procedure is a LMI related approach that is widely used in robust control theory and stability analysis of nonlinear systems [58]. Let $\sigma_0(x), \ldots, \sigma_k(x)$ be scalar quadratic functions of the variable $x \in \mathbf{R}^n$. The following condition is satisfied

$$\sigma_0(x) \leq 0 \textbf{ for all } x \textbf{ such that } \sigma_i(x) \leq 0,\ i = 1, \ldots, k \tag{2.53}$$

if there exist $\tau_1, \ldots, \tau_k \geq 0$, such that

$$\sigma_0(x) - \sum_{i=1}^{k} \tau_i \sigma_i(x) \leq 0 \tag{2.54}$$

If the quadratic function $\sigma_i(x)$ is represented as $\sigma_i(x) = x^T A_i x + B_i x + C_i$, then Eq. (2.54) can be written as the linear matrix inequality (LMI) form as

$$\begin{pmatrix} A_0 & B_0^T \\ B_0 & C_0 \end{pmatrix} - \sum_{i=1}^{k} \tau_i \begin{pmatrix} A_i & B_i^T \\ B_i & C_i \end{pmatrix} \leq 0 \tag{2.55}$$

In optimization theory, Eq. (2.54) is the Lagrange dual of Eq. (2.53). It is also important to remember that all the quadratic polynomials $\sigma_i(x)$, $i = 0, \ldots, k$ should be indefinite to make the S-Procedure non-trivial.

The two conditions in Eq. (2.53) and Eq. (2.54) are not equal, in general, except for some special cases [35]. Therefore, S-Procedure just gives us a sufficient condition for the negativeness of $\sigma_0(x)$ on the semi-algebraic set defined by $\sigma_i(x) \leq 0$, **for all** $i = 1, \ldots, k$. However, this trade off can lead to numerical tractable conditions in the application of systems and control theory.

A few typical applications of the S-Procedure in control application are listed below.

$\sigma_0(x) \leq 0$	$\sigma_1(x), \ldots, \sigma_k(x) \leq 0$	Application
Derivative of a Candidate Lyapunov Function	Interested Domain in the state space	Estimation of Domain of Attraction
Dissipativity Inequality	Semi-Algebraic Set for Uncertainty	Robust Optimal Control
Expected Least Square Level for Curve Fitting	Pre-Specified Range for Parameter Search	System Identification

However, the S-Procedure results in a conservative sufficient condition for the non-positiveness of $\sigma_0(x)$. In many control applications, one single quadratic polynomial constraint, such as $\sigma_1(x) \leq 0$, is enough. Surprisingly, the S-Procedure becomes lossless in this case. If multiple quadratic polynomial constraints are unavoidable, the conservatism can be relieved by substituting the positive semidefinite functions as the multipliers for $\tau_1, \ldots, \tau_k$ in Eq. (2.54) or (2.55). This leads to the Generalized S-Procedure [63].

2.5 Stability Analysis of A Lure System

Stability analysis of a Lure system, which is composed of a LTI system in the forward loop and a memoryless nonlinear block in the feedback loop, is an old but important research topic in robust control theory and nonlinear system analysis. Its block diagram is shown in Fig. 2.2 below. In some standard textbooks of nonlinear systems and control, Circle

Criterion, Popov Criterion and Small Gain Theorem are commonly used for stability analysis. In the later chapters of this dissertation, the LMI based asymptotic stability criterion for Lure system will be applied to design the nonlinear observer. Therefore, it is worth presenting a brief review of this type of system.

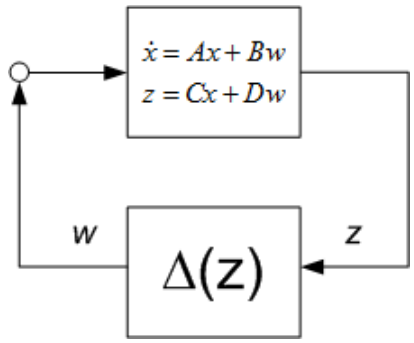

Figure 2.2: Lure System

The state space model of the Lure system is shown as

$$\begin{aligned} \dot{x} &= Ax + Bw \\ z &= Cx + Dw \\ w &= \Delta(z) \end{aligned} \tag{2.56}$$

where $\Delta(\cdot)$ is a nonlinear Lipschitz continuous time-varying function. The relationship of its input and output signals z and w is covered by a homogeneous quadratic polynomial inequality in the form of Eq. (5.17).

$$\begin{pmatrix} z \\ w \end{pmatrix}^T \begin{pmatrix} Q & S^T \\ S & R \end{pmatrix} \begin{pmatrix} z \\ w \end{pmatrix} \leq 0 \tag{2.57}$$

where Q, R are real symmetric matrices. S is a real matrix with a compatible dimension. This quadratic polynomial inequality can be used to represent many important semi-algebraic sets, such as the sector condition, passivity and the L_2 gain of a Lipschitz continuous function.

- The sector condition can be interpreted geometrically as shown in Fig. 2.3 below.

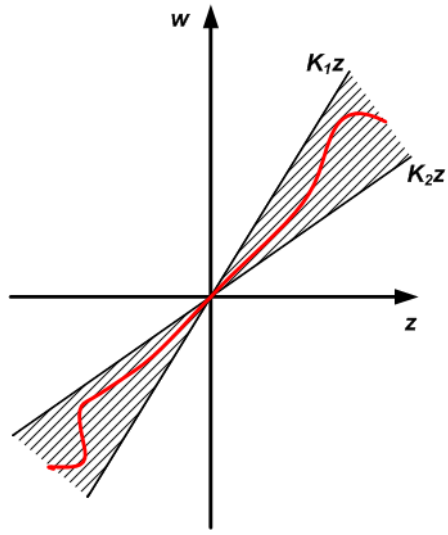

Figure 2.3: Sector Condition

The corresponding algebraic condition for the sector condition is

$$
\begin{gathered}
(w - K_1 z)^T (w - K_2 z) \leq 0 \\
\Updownarrow \\
\begin{pmatrix} z \\ w \end{pmatrix}^T \begin{pmatrix} \dfrac{K_1^T K_2 + K_2^T K_1}{2} & -\dfrac{K_1^T + K_2^T}{2} \\ -\dfrac{K_1 + K_2}{2} & I \end{pmatrix} \begin{pmatrix} z \\ w \end{pmatrix} \leq 0
\end{gathered}
\tag{2.58}
$$

where K_1, K_2 are constant matrices. It is also easy to see that the L_2 gain constraint for z and w is just a special case of this general sector condition

$$
w^T w - \gamma^2 z^T z \leq 0, \quad \gamma > 0 \tag{2.59}
$$

where γ denotes the L_2 gain.

- The passivity condition can be interpreted geometrically as shown in Fig. 2.4 below. The corresponding algebraic condition for the passivity condition is

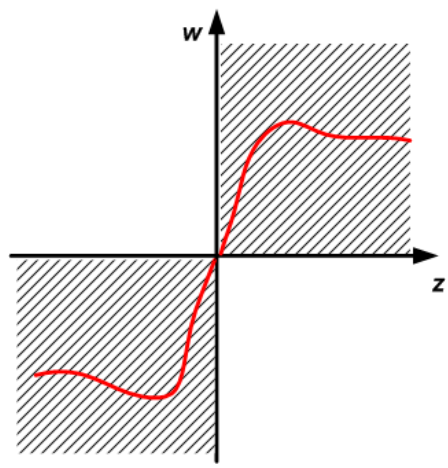

Figure 2.4: Passivity Condition

$$
\begin{gathered}
w^T z \geq 0 \\
\Updownarrow \\
\begin{pmatrix} z \\ w \end{pmatrix}^T \begin{pmatrix} 0 & -I \\ -I & 0 \end{pmatrix} \begin{pmatrix} z \\ w \end{pmatrix} \leq 0
\end{gathered}
\tag{2.60}
$$

The following theorem shows the LMI based sufficient conditions for the asymptotic stability of this *Lure* system.

Theorem 1 ([18]) *The feedback interconnected system in Eq. (2.56), where the input-output relationship of the operator $\Delta(\cdot)$ satisfies the homogeneous quadratic polynomial inequality in the form of Eq. (2.57), is asymptotically stable if the following linear matrix inequalities (LMIs) are feasible.*

$$
\begin{gathered}
P \succ 0 \\
\begin{pmatrix} A^T P + PA & PB \\ B^T P & 0 \end{pmatrix} - \begin{pmatrix} C & D \\ 0 & I \end{pmatrix}^T \begin{pmatrix} Q & S^T \\ S & R \end{pmatrix} \begin{pmatrix} C & D \\ 0 & I \end{pmatrix} \prec 0
\end{gathered}
\tag{2.61}
$$

Proof: If the quadratic Lyapunov function $V(x) = x^T P x$ with $P \succ 0$ is chosen, its derivative is

$$\dot{V}(x) = \begin{pmatrix} x \\ w \end{pmatrix}^T \begin{pmatrix} A^T P + PA & PB \\ B^T P & 0 \end{pmatrix} \begin{pmatrix} x \\ w \end{pmatrix} \tag{2.62}$$

From the state space model in Eq. (2.56), the vector $(x \;\; w)^T$ and $(z \;\; w)^T$ are related by a linear mapping as

$$\begin{pmatrix} z \\ w \end{pmatrix} = \begin{pmatrix} C & D \\ 0 & I \end{pmatrix} \begin{pmatrix} x \\ w \end{pmatrix} \tag{2.63}$$

Then, the quadratic polynomial constraint in the form of Eq. (2.57) is equivalent to

$$\begin{pmatrix} x \\ w \end{pmatrix}^T \begin{pmatrix} C & D \\ 0 & I \end{pmatrix}^T \begin{pmatrix} Q & S^T \\ S & R \end{pmatrix} \begin{pmatrix} C & D \\ 0 & I \end{pmatrix} \begin{pmatrix} x \\ w \end{pmatrix} \leq 0 \tag{2.64}$$

Finally, applying the S-Procedure to Eq. (2.62) and (2.64), the second LMI in Eq. (2.61) can be obtained.

2.6 Conclusions

Some basic concepts in control theory that are discussed frequently in this dissertation were briefly reviewed in this chapter. Many of them resort to a LMIs based optimization problem. As shown above, one of the important applications of LMIs is to search for a candidate Lyapunov function such that the asymptotic stability of the linear or some special nonlinear systems can be proven. In the later chapters, these LMIs based optimization algorithms will applied to search for the Lyapunov function and convergent observer gains in a systematic way.

Chapter 3

Linear Parameter Varying (LPV) Observer Design for Three DOF Bicycle Model

From this chapter, the state-of-the-art convex optimization algorithms will be applied to develop the robust observer for vehicle state estimation. Although the focus is constrained on the three degree-of-freedom bicycle model, the observer design procedure is formalized in a high-level systematic way which allows it to be applied to other systems. First, the linear tire-road friction model will be considered in this chapter. The observer design with the consideration of uncertain cornering stiffness and nonlinear tire model will be discussed in the next two chapters.

The research on linear parameter varying (LPV) modeling and control design techniques started in late of the 1980s. It aims at overcoming some critical weak points of the traditional gain-scheduled controller, such as local stability rather than global stability. Various significant theoretical breakthroughs and successful applications were achieved in the past twenty years. Although the gain-scheduled controllers are very common in automotive control systems, old design techniques still dominate in real-world applications. This elegant theoretical method has just recently appeared in automotive literature in the last few years. Before the discussion of the applications of the LPV design technique in observer design, a brief overview of this method is presented.

3.1 Introduction of LPV Technique

LPV models are the basis of modern gain-scheduling control algorithms. It was initiated by Dr. Jeff Shamma (now a professor in Georgia Tech) and his Phd advisor Michael Athans at Massachusetts Institute of Technology (MIT) in the late 1980s. In classical gain-scheduling control methods, the controller gains are the function of linearized model parameters around

each equilibrium point. Therefore, only local stability and performance is guaranteed [24]. Some ad hoc methods of interpolation of gains are needed to preserve a stable transition from one operating point to another.n the contrary, the LPV controller is automatically gain scheduled. It allows design of a nonlinear controller (with the state variables as the scheduling parameters) by using very mature linear control algorithms, such as LQR and H_∞. The resulting controller can guarantee both stability and performance globally.

3.1.1 LPV Modeling

Linear parameter varying (LPV) systems are described by linear differential equations whose parameters depend on some online measured signals (possibly in a nonlinear fashion). A typical LPV model has the following state space form [46]

$$\begin{aligned} \dot{x} &= A(\theta)x + B(\theta)u \\ y &= C(\theta)x + D(\theta)u \end{aligned} \tag{3.1}$$

where the time-varying parameter θ is regarded as an "exogenous" real-time measured signal. Typical assumptions on θ are the bound on magnitude and rate of variation, e.g., $\underline{\theta} \leq \theta \leq \overline{\theta}$ and $\underline{\dot{\theta}} \leq \dot{\theta} \leq \overline{\dot{\theta}}$ for all $t \geq 0$, where the bar below is a lower bound and the bar above is an upper bound. In the subsequent analysis, the notation $(\theta,\ \dot{\theta}) \in \Theta \times \Theta_d$ will be frequently used instead, where Θ and Θ_d are the parameter spaces that contain θ and $\dot{\theta}$ respectively. Hence, the state space form in Eq. (3.1) can be regarded as a collection of linear systems (linear differential inclusion). Later, it will be shown that $\underline{\theta}$, $\overline{\theta}$, $\underline{\dot{\theta}}$ and $\overline{\dot{\theta}}$ provide valuable information in the stability analysis and syndissertation of a gain scheduled controller.

From a linear perspective, θ is treated as a time-varying signal, which is independent of the state variables. Therefore, the state space form in Eq. (3.1) can also be regarded as a linear time varying (LTV) system. However, the following two points make the LPV system different from the traditional LTV system.

1) The parameter θ can only be measured in real time. No future parameter values are available. Hence, the control signal is constrained to be a causal function of the parameter. However, some control algorithms for LTV system explicitly use the future information of this parameter [53] [7].

2) Furthermore, the LPV framework can be extended to represent a nonlinear dynamical model. In this case, it is called a "quasi-LPV" model, where the time-varying parameter θ is a nonlinear function of the measurable state variables [53]. In this case, the parameter becomes "endogenous". In the LPV model, the complex nonlinearity is hidden behind the time-varying parameter which results in a linear but non-stationary dynamical system. For example, the state equation of an input affine nonlinear system can be transferred to a LPV state equation as

$$\dot{x} = f(x) + g(x)u \Longleftrightarrow \dot{x} = A[\theta(x)]x + B[\theta(x)]u \tag{3.2}$$

where $f(x) = A[\theta(x)]x$, $g(x) = B[\theta(x)]$. Here, it is assumed that $\theta(x)$ is a state dependent measurable parameter. An application example will be presented shortly to illustrate this quasi-LPV representation of the nonlinear model.

It is also worth mentioning that the LPV system is strongly connected with the other two modeling formalisms shown below [46].

1. **Hybrid Dynamical Systems:** Hybrid dynamical systems possess both continuous and discrete state variables. A special case related to LPV framework is a model with discrete valued parameters, e.g.

$$\theta(t) \in [\theta_1, \ldots, \theta_n]$$

LPV Systems constitute a specific case of hybrid systems, where the underlying continuous dynamics are linear and the discrete switching dynamics are exogenous.

2. **Jump Linear Systems:** Jump linear systems can be viewed as a case of LPV systems in which parameter trajectories evolve according to a probabilistic rule. In the literature, it is also called "Jump Markov Systems", in which the design of control laws typically exploits the known transition probabilities of the parameters' stochastic evolution.

3.1.2 Stability Analysis of LPV Systems

For stability analysis, the following three different methodologies are proposed to analyze the asymptotic stability of the LPV system in the literature [7].

1. Single quadratic Lyapunov function (SQLF) $V = x^T P x$;

2. Parameter dependent quadratic Lyapunov function (PDQLF) $V = x^T P(\theta) x$ or $V = x^T P(\lambda) x$;

3. Linear fractional representations (LFR) which relies on μ analysis or small gain theorem for performance optimization and robustness analysis;

Here, an example will be presented to illustrate the application of the 1st approach for stability analysis.

For the LPV system $\dot{x} = A(\theta)x$, where the parameter vector $\theta \in R^{m\times 1}$ belongs to a parameter space Θ. The stability analysis resorts to searching for a Lyapunov function $V = x^T P x$ such that the following LMIs are feasible [54].

$$P \succ 0, \quad A^T(\theta)P + PA(\theta) \prec 0, \quad \forall\, \theta \in \Theta \tag{3.3}$$

This is indeed an infinite dimensional LMI feasibility problem due to its continuous dependence on the parameter θ. Fortunately, if the parameter space Θ is a convex hull with finite vertices and $A(\theta)$ depends affinely on θ, there exists a sufficient and necessary finite dimensional LMI relaxation condition as shown in Lemma 7 [7] [53] [54].

Lemma 7 *Suppose the parameter space Θ is a convex hull with finite vertices and $A(\theta)$ depends affinely on $\theta \in R^{m\times 1}$. Then, the LMIs in Eq. (3.3) are feasible if and only if they are feasible on all the vertices of Θ.*

Proof: $A(\theta)$ is an affine matrix function of $\theta \in R^{m\times 1}$ as shown below.

$$A(\theta) = A_0 + \sum_{j=1}^{m} \theta_j A_j \tag{3.4}$$

where θ_j denotes the jth element of θ. $A_0, A_1, \ldots, A_m$ are all constant matrices. Any parameter θ in the convex hull Θ can be represented as a convex combination form shown below.

$$\theta = \sum_{i=1}^{k} \lambda_i \theta^{(i)} \tag{3.5}$$

where $\theta^{(i)}$ denotes one of the k vertices of Θ. λ_i, $i = 1, \ldots, k$ are the normalized scheduling parameters that satisfy the following convex condition.

$$\sum_{i=1}^{k} \lambda_k = 1, \quad \textbf{with} \;\; 0 \le \lambda_i \le 1, \; \forall\, i = 1. \ldots, k$$

Substituting the right side of Eq. (3.5) for θ in Eq. (3.4), the state matrix $A(\theta)$ can be obtained as the similar convex combination form shown below.

$$\begin{aligned} A(\theta) &= A_0 + \sum_{j=1}^{m} \left(\sum_{i=1}^{k} \lambda_i \theta_j^{(i)} \right) A_j \\ &= A_0 + \sum_{i=1}^{k} \lambda_i \left(\sum_{j=1}^{m} \theta_j^{(i)} A_j \right) \\ &= \sum_{i=1}^{k} \lambda_i A(\theta^{(i)}) \end{aligned} \tag{3.6}$$

Furthermore, the parameter dependent matrix $A^T(\theta)P + PA(\theta)$ can be represented as

$$A^T(\theta)P + PA(\theta) = \sum_{i=1}^{k} \lambda_i [A^T(\theta^{(i)})P + PA(\theta^{(i)})] \tag{3.7}$$

If: The nonnegativity of λ_i in Eq. (3.7) guarantees that $A^T(\theta)P + PA(\theta)$ is negative definite if $A^T(\theta^{(i)})P + PA(\theta^{(i)})$ is a negative definite matrix $\forall\, i = 1, \ldots, k$.

Only if: The necessity is quite straightforward. Suppose the negative definite condition of $A^T(\theta^{(i)})P + PA(\theta^{(i)})$ is violated at some vertex. Then, $A^T(\theta)P + PA(\theta)$ cannot be a negative definite matrix $\forall\, \theta \in \Theta$, which leads to a contradiction.

In general, the parameter dependent LMI constraints make the stability analysis for LPV system more complex than the LTI system. Next, Fig. 3.1 and 3.2 are used to illustrate the difference between the LPV model and the LTI model with fixed parameters.

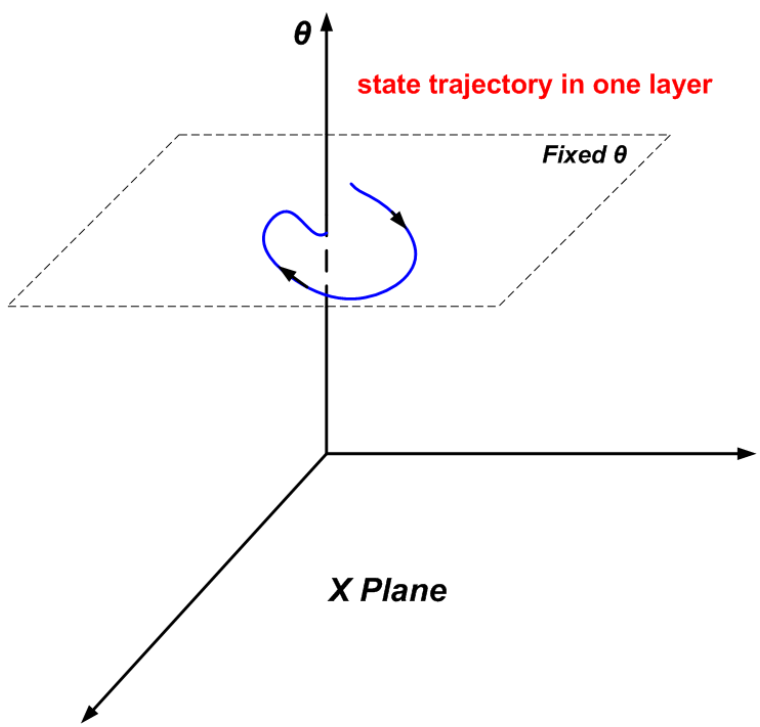

Figure 3.1: The state trajectory with fixed parameters

In Fig. 3.1, the dynamics are linear time invariant in each isolated layer. But, the state trajectory will cross different layers with different LTI dynamics as the the parameter θ varies as shown in Fig. 3.2. For the stability analysis, it is expected that the projection of the state trajectory on the X plane converges to the origin asymptotically irrespective of the variation of θ. This leads to the infinite dimensional LMI feasibility problem in Eq. (3.3).

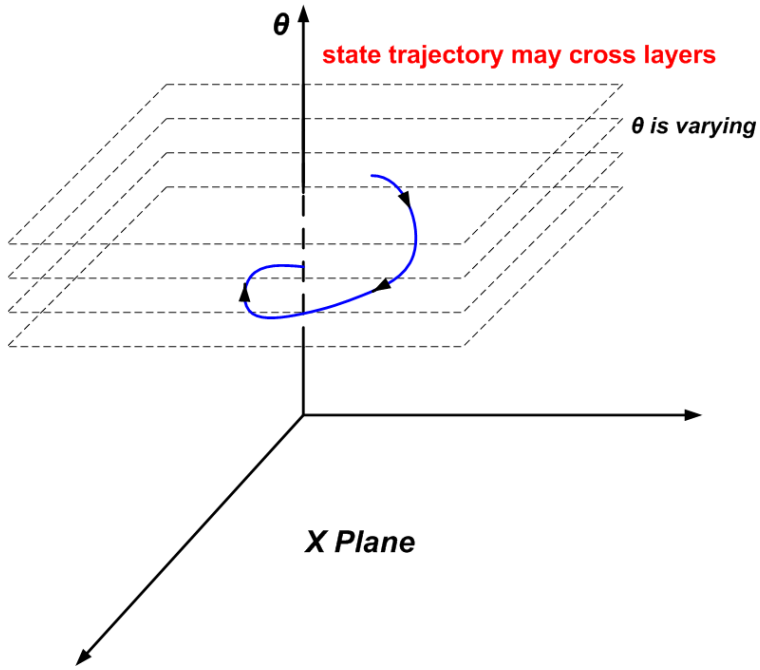

Figure 3.2: The state trajectory with varying parameters

3.1.3 LPV Controller

The exogenous signals or scheduling parameters collected in the vector θ reflect the changes in process dynamics as operating conditions change. Controller parameters should also be adaptive to the variation in the models such that both stability and performance are preserved. However, classical gain scheduling control systems have some eminent drawbacks that are listed below [24] [53].

1. In classical gain scheduling approaches, the controller parameters are tuned only based on local linearized model. Hence, adequate performance and in some cases even stability is not guaranteed at operating conditions other than the design points;

2. Due to the lack of the information of global behavior, searching for the gain scheduling function for multivariable controllers that guarantees the stable transition from one operating point to another is often a tedious and time consuming task;

In general, LPV techniques provide a systematic design procedure for gain-scheduled multivariable controllers. This methodology allows stability, performance and robustness to be

incorporated into a unified framework. Besides θ, the scheduling parameters in the controller can also include $\dot{\theta}$, the derivative of θ, if it is measurable [7] [46]. This provides additional design freedom to improve the performance of the controller. Similar as the LPV process model, the state-space model of the LPV controller depends causally on the history of scheduling parameters $(\theta\ \dot{\theta})$. In what follows, an example will be presented to illustrate the basic design procedure.

Suppose the state space model of the controller has the following form.

$$\begin{aligned} \dot{x}_c &= A_c(\theta,\dot{\theta})x_c + B_c(\theta,\dot{\theta})y \\ u &= C_c(\theta,\dot{\theta})x_c \end{aligned} \qquad (\theta,\ \dot{\theta}) \in \Theta \times \Theta_d \tag{3.8}$$

where Θ and Θ_d represent the parameter spaces for θ and $\dot{\theta}$ respectively. Here, it is assumed that there is no feedthrough term in the controller for simplicity. The goal of the controller is to stabilize the LPV process in Eq. (3.1) back to zero from any initial condition asymptotically. In many applications, the affine parameter dependent controller receives special attention in past research. An example of the state space matrices of this controller are shown below

$$A_c(\theta) = A_{c,0} + \theta_1 A_{c,1} + \ldots + \theta_k A_{c,k}, \quad B_c(\theta) = B_{c,0} + \theta_1 B_{c,1} + \ldots + \theta_k B_{c,k}$$
$$C_c(\theta) = C_{c,0} + \theta_1 C_{c,1} + \ldots + \theta_k C_{c,k}$$

where the matrices $A_{c,i}, B_{c,i}, C_{c,i}, i = 0, 1, \ldots, k$ are decision variables of some SDP algorithm. Here, there is no assumption on the specific gain scheduled controller structure. All the analysis will be discussed from a general perspective. The state equation of the closed-loop system is shown below.

$$\begin{pmatrix} \dot{x} \\ \dot{x}_c \end{pmatrix} = \underbrace{\begin{pmatrix} A(\theta) & B(\theta)C_c(\theta,\dot{\theta}) \\ B_c(\theta,\dot{\theta})C(\theta) & A_c(\theta,\dot{\theta}) + B_c(\theta,\dot{\theta})D(\theta)C_c(\theta,\dot{\theta}) \end{pmatrix}}_{A_{CL}(\theta,\dot{\theta})} \begin{pmatrix} x \\ x_c \end{pmatrix} \tag{3.9}$$

Similar to Eq. (3.3), the semidefinite constraints for the asymptotic stability of the closed-loop system becomes

$$P \succ 0, \quad A_{CL}^T(\theta, \dot{\theta})P + PA_{CL}(\theta, \dot{\theta}) \prec 0, \quad \forall\, (\theta,\ \dot{\theta}) \in \Theta \times \Theta_d \tag{3.10}$$

In most practical applications, this is the feasibility problem of an infinite dimensional bilinear matrix inequality (BMI). In some cases, several mathematical tricks can be applied to transform it to a LMI problem. Alternatively, the positive definite matrix P can be preselected and the BMI is degenerated to a LMI for the controller parameters. But this BMI problem is difficult to solve in general.

Another challenging task is to relax the infinite dimensional semidefinite constraints to a finite dimensional one [46] [22] [21]. If the closed-loop state matrix $A_{CL}(\theta, \dot{\theta})$ depends on θ and $\dot{\theta}$ affinely and both Θ and Θ_d are convex hulls, it is only necessary to guarantee the semidefinite constraints on all the vertices of Θ and Θ_d as proven in Lemma 7. However, the state space model of the closed-loop system usually depends on the parameters θ and $\dot{\theta}$ quadratically or even high-order polynomially. Various relaxation techniques reported in the literature, such as S-Procedure, parameter space gridding, multi-convexity or slack variable method can be applied.

Finally, it is important to remember the following two conclusions.

- If the infinite dimensional semidefinite constraints in Eq. (3.10) are feasible, the closed-loop system is globally asymptotic stable;
- If the scheduling parameter θ or $\dot{\theta}$ is state dependent, the controller in Eq. (3.8) is called a "Quasi-LPV" controller. In this case, the linear control design methods are indeed used to develop a nonlinear controller;

3.1.4 A Numerical Example

In the previous section, the LPV design methodology is discussed in a very abstract level. In the last part of this section, a simple application example is presented to demonstrate the application of this method to develop the controller for a highly nonlinear system.

Suppose the height of the liquid level in a tank is expected to be regulated [24]. By using Bernoulli equation, the following nonlinear ODE can be derived.

$$\dot{h} = \frac{1}{A(h)}(q_i - a\sqrt{2gh}) \tag{3.11}$$

where h is the height of the liquid level; q_i is the incoming liquid flow rate, which is the control signal here; $A(h)$ is the cross-sectional area of a tank at the height h; a and g are the outlet pipe diameter and gravity constant, respectively.

Now, our task is to design a gain-scheduled PI controller that regulates the level height h to any desired height h_d from any positive initial condition. The height h is a measured signal for feedback and gain scheduling.

1. **Step 1: Transform nonlinear ODE to LPV form**

   Let's define the state variable x_1 as

$$x_1 = \sqrt{h_d} - \sqrt{h}$$

   Suppose h_d is a constant. Then, the derivative of x_1 is

$$\dot{x}_1 = -\frac{1}{2\sqrt{h}}\left(\frac{1}{A(h)}(q_i - a\sqrt{2gh})\right)$$

   If the measured time-varying parameter θ is defined as

$$\theta = \frac{1}{2\sqrt{h}A(h)}$$

the derivative of x_1 becomes the following LPV form

$$\dot{x}_1 = a\sqrt{2g}\theta(\sqrt{h_d} - x_1) - \theta q_i$$

2. **Step 2: Gain-Scheduled PI Controller**

   The control signal q_i from the gain-scheduled PI controller is

$$q_i = \theta K_p(\sqrt{h_d} - \sqrt{h}) + \theta K_i \int_0^t (\sqrt{h_d} - \sqrt{h})dt$$

   where θK_p and θK_i represent the linear scheduled gains. Next, the 2nd state variable x_2 is defined as the output of the integrator of the PI controller. Its derivative is

$$\dot{x}_2 = \theta K_i x_1$$

   Then, the state space model of the closed-loop system is

$$\begin{aligned} \dot{x}_1 &= -(a\sqrt{2g}\theta + \theta^2 K_p)x_1 - \theta x_2 + \theta r \\ \dot{x}_2 &= \theta K_i x_1 \end{aligned}$$

   where $r = a\sqrt{2gh_d}$ is regarded as an exogenous constant reference input. The parameter dependent state space matrices $A(\theta)$, $B(\theta)$ are

$$A(\theta) = \begin{pmatrix} -a\sqrt{2g}\theta - \theta^2 K_p & -\theta \\ \theta K_i & 0 \end{pmatrix}, \quad B(\theta) = \begin{pmatrix} \theta \\ 0 \end{pmatrix}$$

3. **Step 3: Search for The Stabilizing Controller Gains K_p, K_i**

   Both x_1 and x_2 are expected to converge to 0 asymptotically. For simplicity, the non-parameter dependent Lyapunov function as $V = x^T P x, P > 0$ can be selected. Its

derivative is

$$\dot{V} = \begin{pmatrix} x \\ r \end{pmatrix}^T \begin{pmatrix} A^T(\theta)P + PA(\theta) & PB(\theta) \\ B^T(\theta)P & 0 \end{pmatrix} \begin{pmatrix} x \\ r \end{pmatrix}$$

If there exists a positive definite matrix P and two gains K_p, K_i such that

$$\begin{pmatrix} A^T(\theta)P + PA(\theta) & PB(\theta) \\ B^T(\theta)P & 0 \end{pmatrix} < 0, \ \ \forall \theta \in [\underline{\theta}, \overline{\theta}]$$

then the level height h will converge to h_d asymptotically. However, there are two obstacles that make the search of P, K_p, K_i satisfying the above matrix inequality problem extremely challenging.

(a) There are infinite numbers for the values of θ. The decision variables P, K_p, K_i should make the semidefinite constraints feasible for each value of θ, which is indeed an infinite dimensional problem;

(b) Even for a fixed value of θ, this matrix inequality is bilinear in the decision variable, which implies the non-convexity of the problem;

4. **Step 4: Finite Dimensional Relaxation**

In this example, the finite dimensional relaxation method that conquers the 1st obstacle will be presented. For the 2nd one, a positive definite matrix P can be pre-selected such that the above semidefinite constraint degenerates to a LMI problem . In what follows, S-Procedure is used to transform infinite dimensional BMI to finite dimensional BMI without any conservatism. First, the θ dependent state space matrices are rewritten in the following form.

$$A(\theta) = \theta \underbrace{\begin{pmatrix} -a\sqrt{2g} & -1 \\ K_i & 0 \end{pmatrix}}_{A_1} + \theta^2 \underbrace{\begin{pmatrix} -K_p & 0 \\ 0 & 0 \end{pmatrix}}_{A_2}, \quad B(\theta) = \theta \underbrace{\begin{pmatrix} 1 \\ 0 \end{pmatrix}}_{B_1}$$

Then, the θ dependent bilinear matrix inequality can be written as

$$\begin{pmatrix} I \\ \theta I \end{pmatrix}^T \underbrace{\left(\begin{array}{cc|cc} 0 & 0 & 0.5(A_1^T P + PA_1) & 0.5PB_1 \\ 0 & 0 & 0.5B_1^T P & 0 \\ \hline 0.5(A_1^T P + PA_1) & 0.5PB_1 & A_2^T P + PA_2 & 0 \\ 0.5B_1^T P & 0 & 0 & 0 \end{array}\right)}_{W} \begin{pmatrix} I \\ \theta I \end{pmatrix} < 0$$

where 0 and I represent the zero and identity matrix with compatible dimensions. It is obvious that this BMI is feasible (independent of θ) if the matrix W is negative definite. However, negative definiteness of W is a very conservative condition, because the constraint $\underline{\theta} \leq \theta \leq \overline{\theta}$ implies that the matrix $(I, \theta I)^T$ is always contained in a polytope with vertices definded by $\underline{\theta}$ and $\overline{\theta}$.

The basic idea of S-Procedure based relaxation is to use a multiplier matrix that captures the semi-algebraic set of θ and apply Lagrangian duality theory to build a matrix whose eigenvalues are the upper bound of the original bilinear matrix. Hence, a sufficient condition for the original infinite dimensional BMI can be derived. The condition is also necessary in the case that only one multiplier exists.

As mentioned before, the time-varying parameter θ is always constrained in the closed set $[\underline{\theta}, \overline{\theta}]$, which implies

$$\underline{\theta} \leq \theta \leq \overline{\theta} \Longleftrightarrow (\theta - \underline{\theta})(\theta - \overline{\theta}) \leq 0$$

The quadratic form of this inequality is

$$\begin{pmatrix} 1 \\ \theta \end{pmatrix}^T \begin{pmatrix} \underline{\theta}\,\overline{\theta} & -0.5(\underline{\theta} + \overline{\theta}) \\ -0.5(\underline{\theta} + \overline{\theta}) & 1 \end{pmatrix} \begin{pmatrix} 1 \\ \theta \end{pmatrix} \leq 0$$

It is trivial to extend the scalar quadratic polynomial inequality to the higher dimensional matrix form.

$$\begin{pmatrix} I \\ \theta I \end{pmatrix}^T \underbrace{\begin{pmatrix} \underline{\theta}\,\overline{\theta} I & -0.5(\underline{\theta}+\overline{\theta})I \\ -0.5(\underline{\theta}+\overline{\theta})I & I \end{pmatrix}}_{M} \begin{pmatrix} I \\ \theta I \end{pmatrix} \leq 0$$

where I represents the identity matrix with appropriate dimensions.

The S-Procedure can then be applied to derive the following sufficient and necessary finite dimensional BMI condition for the original infinite dimensional case

$$W - \tau M < 0, \quad \tau > 0 \tag{3.12}$$

where τ is the Lagrangian multiplier. Finally, if the matrix P is chosen as an identity matrix, the semidefinite constraint in Eq. (3.12) becomes a LMI feasibility problem for K_p, K_i and τ. Therefore, any feasible solution results in a globally convergent gain scheduled PI controller.

5. **Step 5: Simulation Results**

   The simulation results for this tank level control system in the case of two desired level heights can be seen in Fig. 3.3 below. It clearly shows that the tank level converges to the desired height quickly.

3.2 LPV Observer Design for The Bicycle Model

Besides the gain scheduled controller, the LPV design methodology can also be applied to develop a gain scheduled observer. The state-of-the-art LMIs based optimization method will be applied to solve the challenging vehicle state estimation problem in this section. The bicycle model, in which the longitudinal velocity and acceleration are treated as online measured time-varying parameters, will be used for the basis of gain scheduled observer

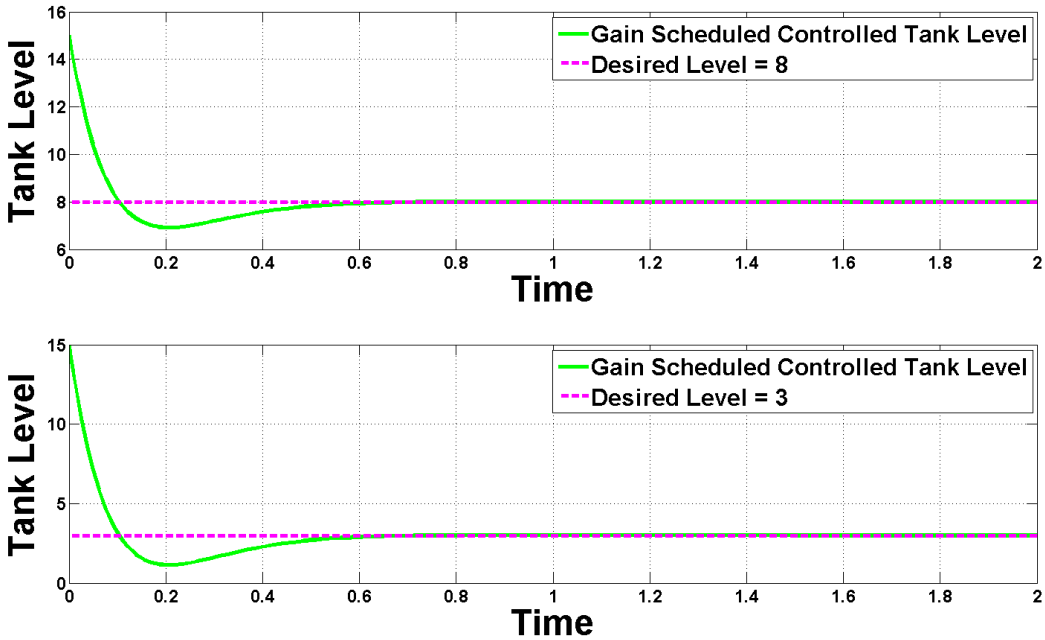

Figure 3.3: Simulation results of the tank lever control system with a gain scheduled PI controller.

development. First, the observer design with perfect measurement of scheduling parameters is presented. Then, the robustness design methodology that improves the performance with respect to the measurement uncertainty will also be discussed.

3.2.1 LPV Representation of The Bicycle Model

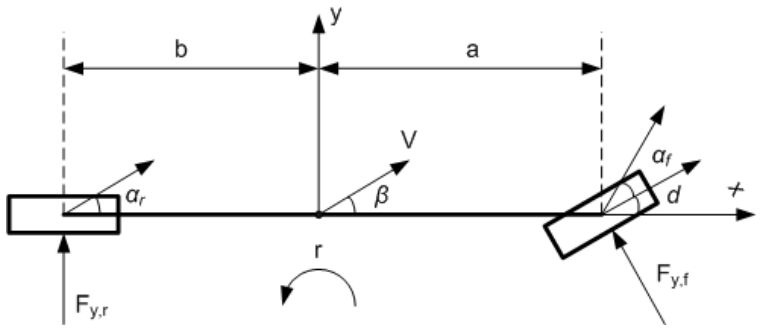

Figure 3.4: Bicycle Model

A 3-DOF bicycle model is widely used to represent lateral vehicle dynamics and study active safety systems in various automotive control literature [16]. In a bicycle model, the

left and right wheels are represented by one wheel each at the front and rear of the vehicle. An illustration of the bicycle model is shown in Fig. 3.4. The definitions of some associated kinematic parameters are also shown in Fig. 3.4. Three basic equations that are used to derive the state space representation of the bicycle model are listed below.

1. Linear Tire-Road Friction Model: The lateral tire forces at front and rear tires are proportional to the front and rear slip angles respectively.

$$F_{y,f} = C_f \alpha_f, \;\; F_{y,r} = C_r \alpha_r \tag{3.13}$$

   where C_f, C_r are the front and rear tire cornering stiffness respectively.

2. Kinematic model for definitions of slip angles:

$$\alpha_f = \delta - \frac{v_y + ar}{v_x}, \;\; \alpha_r = \frac{br - v_y}{v_x}, \;\; \beta = \frac{v_y}{v_x} \tag{3.14}$$

   where α_f, α_r are the slip generated at the front and rear axles and β is the net effect of total slip generated;

3. Newton-Euler Equations for Dynamic Model:

$$\begin{aligned} M(\dot{v}_y + v_x r) &= F_{y,f} + F_{y,r} \\ I_z \dot{r} &= a F_{y,f} - b F_{y,r} \end{aligned} \tag{3.15}$$

where M, I_z, a, b are the mass, yaw inertia, the distance of front and rear wheels from the center of gravity (CG) of the vehicle. C_f, C_r are the cornering stiffness for the front and rear tires. v_x, v_y, a_y are the longitudinal velocity, lateral velocity and lateral acceleration of the CG. r, δ, $\dot{\delta}$ are the yaw rate, steering angle and its derivative, which are treated as the measured input signals.

Note: Different choice of the state variables leads to two difference forms of the linear state-space model.

1) Choosing slip angle β of the CG and yaw rate r as the state variables leads to the following state space model that depends on $1/v_x$ quadratically;

$$\begin{pmatrix} \dot{\beta} \\ \dot{r} \end{pmatrix} = \begin{pmatrix} -\dfrac{C_f + C_r + M\dot{v}_x}{Mv_x} & \dfrac{-aC_f + bC_r}{Mv_x^2} - 1 \\ \dfrac{-aC_f + bC_r}{I_z} & -\dfrac{a^2C_f + b^2C_r}{I_z v_x} \end{pmatrix} \begin{pmatrix} \beta \\ r \end{pmatrix} + \begin{pmatrix} \dfrac{C_f}{Mv_x} \\ \dfrac{aC_f}{I_z} \end{pmatrix} \delta \tag{3.16}$$

2) Choosing lateral velocity v_y of CG and yaw rate r as the state variables leads to the following state space model that depends on $1/v_x$ affinely;

$$\begin{pmatrix} \dot{v_y} \\ \dot{r} \end{pmatrix} = \begin{pmatrix} -\dfrac{C_f + C_r}{Mv_x} & \dfrac{-aC_{\alpha f} + bC_r}{Mv_x} \\ \dfrac{-aC_f + bC_{\alpha r}}{I_z v_x} & -\dfrac{a^2C_f + b^2C_r}{I_z v_x} \end{pmatrix} \begin{pmatrix} v_y \\ r \end{pmatrix} + \begin{pmatrix} \dfrac{C_f}{M}\delta - v_x r \\ \dfrac{aC_f}{I_z}\delta \end{pmatrix} \tag{3.17}$$

3) If the slip angles of the front and rear wheels α_f, α_r are chosen as the state variables [34], this leads to the following state space model that also depends on $1/v_x$ affinely;

$$\begin{aligned} \begin{pmatrix} \dot{\alpha_f} \\ \dot{\alpha_r} \end{pmatrix} &= \begin{pmatrix} -\dfrac{a_x}{v_x} - \dfrac{C_f}{v_x}\left(\dfrac{1}{M} + \dfrac{a^2}{I_z}\right) & \dfrac{C_r}{v_x}\left(\dfrac{ab}{I_z} - \dfrac{1}{M}\right) \\ \dfrac{C_f}{v_x}\left(\dfrac{ab}{I_z} - \dfrac{1}{M}\right) & -\dfrac{a_x}{v_x} - \dfrac{C_r}{v_x}\left(\dfrac{1}{M} + \dfrac{b^2}{I_z}\right) \end{pmatrix} \begin{pmatrix} \alpha_f \\ \alpha_r \end{pmatrix} \\ &+ \begin{pmatrix} \dfrac{a_x}{v_x} & 1 & 1 \\ 0 & 0 & 1 \end{pmatrix} \begin{pmatrix} \delta \\ \dot{\delta} \\ r \end{pmatrix} \end{aligned} \tag{3.18}$$

Most of the prior work of controller/observer design is based on the following two assumptions.

1. Longitudinal velocity v_x is a known constant ($\dot{v}_x = 0$);

2. Cornering Stiffness C_f, C_r are known time-invariant parameters;

Based on these two assumptions, a LTI observer or a Kalman filter can be developed. However, the LTI observer is insufficient to capture the variation of the dynamics. Therefore, a v_x dependent observer has the potential for better performance. Moreover, the variation of cornering stiffness parameters will lead to biased estimation results. In this dissertation, the following two approaches will be used to relax the limitation of the above two assumptions.

1. **LPV based gain-scheduled observer** — using longitudinal velocity v_x and acceleration a_x as the online scheduling parameters;

2. **Interval observer** — producing an envelope to cover all the possible state trajectories resulting from the variation of cornering stiffness C_f, C_r;

The first approach, LPV based gain-scheduled observer design, will be the topic of this chapter. While the interval observer design will be discussed in the next chapter.

Traditional gain-scheduling design methods are inherently *ad hoc* and the resulting scheduled observer provides no stability or performance guarantee for rapid changes in the scheduling variables v_x. LPV model framework directly takes the variation of v_x and its derivative a_x into consideration, if these signals can be measured or estimated online. This design methodology uses a strict mathematical method to develop a gain-scheduled observer based on the measurement of v_x and a_x. Both stability and performance are guaranteed globally. Strictly speaking, the LPV representation in Eq. (3.16), (3.17) and (3.18) is the "Quasi-LPV" model of the nonlinear system, where the longitudinal velocity v_x is also a state variable with its own dynamics. However, the LPV model hides all the nonlinearities behind this parameter. Hence, for the Quasi-LPV case, the LPV observer is indeed a nonlinear observer because the scheduling parameter is a state variable. The LPV based gain-scheduling design methodology allows the user to design a nonlinear observer by using very mature linear observer design methods, such as H_2 and H_∞ filters. In the remaining part of this chapter, the LPV observer design for the bicycle model will be investigated in great detail.

3.2.2 LPV Observer Design with Perfect Knowledge of Scheduling Parameter

Three different state space representations of the bicycle model have been discussed above. Here, the one that uses the front and rear slip angles as the state variables $x = (\alpha_f \;\; \alpha_r)^T$ will be adopted. This affine parameter dependent state space model also significantly simplifies the observer design shown here

$$\begin{aligned} \dot{x} &= (\theta_1 A_1 + \theta_2 A_2)\, x + (B_0 + \theta_2 B_2)\, u \\ y &= Cx \end{aligned} \tag{3.19}$$

where the scheduling parameters θ_1, θ_2 and the state space matrices A_1, A_2, B_0, B_2, C are defined as

$$\theta_1 = \frac{1}{v_x}, \qquad \theta_2 = \frac{a_x}{v_x}$$

$$A_1 = \begin{pmatrix} -C_f\left(\dfrac{1}{M} + \dfrac{a^2}{I_z}\right) & C_r\left(\dfrac{ab}{I_z} - \dfrac{1}{M}\right) \\ C_f\left(\dfrac{ab}{I_z} - \dfrac{1}{M}\right) & -C_r\left(\dfrac{1}{M} + \dfrac{b^2}{I_z}\right) \end{pmatrix}, \quad A_2 = \begin{pmatrix} -1 & 0 \\ 0 & -1 \end{pmatrix}$$

$$B_0 = \begin{pmatrix} 0 & 1 & 1 \\ 0 & 0 & 1 \end{pmatrix}, \quad B_2 = \begin{pmatrix} 1 & 0 & 0 \\ 0 & 0 & 0 \end{pmatrix}, \quad C = \begin{pmatrix} 1 & -1 \end{pmatrix}$$

In this LPV representation, the complex longitudinal dynamics are hidden behind the time-varying parameter sets $\theta = (\theta_1, \theta_2)$. With the information of the variation interval of v_x and a_x, such as $\underline{v}_x \leq v_x \leq \overline{v}_x$, $\underline{a}_x \leq a_x \leq \overline{a}_x$, the four vertices of the polytopic parameter space Θ that contains θ can be derived as

$$\theta^{(1)} = \begin{pmatrix} \dfrac{1}{\underline{v}_x} \\ \\ \dfrac{\overline{a}_x}{\underline{v}_x} \end{pmatrix}, \quad \theta^{(2)} = \begin{pmatrix} \dfrac{1}{\underline{v}_x} \\ \\ \dfrac{\underline{a}_x}{\underline{v}_x} \end{pmatrix}, \quad \theta^{(3)} = \begin{pmatrix} \dfrac{1}{\overline{v}_x} \\ \\ \dfrac{\overline{a}_x}{\overline{v}_x} \end{pmatrix}, \quad \theta^{(4)} = \begin{pmatrix} \dfrac{1}{\overline{v}_x} \\ \\ \dfrac{\underline{a}_x}{\overline{v}_x} \end{pmatrix} \tag{3.20}$$

The output equation $y = Cx$ comes from the kinematic relation between the slip angles and the measured signals shown below.

$$\delta - \frac{a+b}{v_x} r = \alpha_f - \alpha_r \tag{3.21}$$

The corresponding LPV observer has the following state equation

$$\dot{\hat{x}} = (\theta_1 A_1 + \theta_2 A_2)\,\hat{x} + (B_0 + \theta_2 B_2)\,u + L(\theta)\,(y - C\hat{x}) \tag{3.22}$$

where the observer gain $L(\theta)$ depends on the scheduling parameter $\theta = (\theta_1,\ \theta_2)$ affinely.

$$L(\theta) = L_0 + \theta_1 L_1 + \theta_2 L_2 \tag{3.23}$$

The state equation for the observer error $e = x - \hat{x}$ becomes

$$\dot{e} = (\theta_1(A_1 - L_1 C) + \theta_2(A_2 - L_2 C) - L_0 C)\,e \tag{3.24}$$

The tuning parameters L_0, L_1 and L_2 should guarantee the asymptotic stability of this observer error state equation for all the possible values of θ in the domain Θ. The stability analysis method for LPV systems discussed in the previous section can be applied here. The asymptotic convergence of the LPV observer is guaranteed if a Lyapunov function whose derivative is globally negative irrespective of the variation of θ_1 and θ_2 exists. Therefore, the design of a LPV observer resorts to finding a feasible solution for the following semidefinite constraints.

$$P \succ 0 \ \ \textbf{and} \ \ [A(\theta) - L(\theta)C]^T P + P[A(\theta) - L(\theta)C] \prec 0, \quad \forall \theta \in \Theta \tag{3.25}$$

This is indeed an infinite dimensional problem as the parameter θ is defined in continuous space. However, the observer error state matrix $A(\theta) - L(\theta)C$ depends affinely on θ, which

implies that it is sufficient and necessary to guarantee the feasibility of the semidefinite constraints on all the vertices of Θ as proven in Lemma 7.

Therefore, the observer error state equation is asymptotic stable if the observer gains L_0, L_1 and L_2 make the following SDP constraints feasible.

$$\begin{aligned} P &\succ 0 \\ \left(A^T(\theta^{(1)}) - C^T L^T(\theta^{(1)})\right) P + P\left(A(\theta^{(1)}) - L(\theta^{(1)})C\right) &\prec 0 \\ \left(A^T(\theta^{(2)}) - C^T L^T(\theta^{(2)})\right) P + P\left(A(\theta^{(2)}) - L(\theta^{(2)})C\right) &\prec 0 \\ \left(A^T(\theta^{(3)}) - C^T L^T(\theta^{(3)})\right) P + P\left(A(\theta^{(3)}) - L(\theta^{(3)})C\right) &\prec 0 \\ \left(A^T(\theta^{(4)}) - C^T L^T(\theta^{(4)})\right) P + P\left(A(\theta^{(4)}) - L(\theta^{(4)})C\right) &\prec 0 \end{aligned} \tag{3.26}$$

Again, the change of variable method discussed in the last chapter can be applied to transform the BMI problem to the following LMI problem.

$$\begin{aligned} P &\succ 0 \\ \left(A^T(\theta^{(1)})P + PA(\theta^{(1)})\right] - \left[C^T Q^T(\theta^{(1)}) + Q(\theta^{(1)})C\right) &\prec 0 \\ \left(A^T(\theta^{(2)})P + PA(\theta^{(2)})\right] - \left[C^T Q^T(\theta^{(2)}) + Q(\theta^{(2)})C\right) &\prec 0 \\ \left(A^T(\theta^{(3)})P + PA(\theta^{(3)})\right] - \left[C^T Q^T(\theta^{(3)}) + Q(\theta^{(3)})C\right) &\prec 0 \\ \left(A^T(\theta^{(4)})P + PA(\theta^{(4)})\right] - \left[C^T Q^T(\theta^{(4)}) + Q(\theta^{(4)})C\right) &\prec 0 \end{aligned} \tag{3.27}$$

where $Q(\theta) = Q_0 + \theta_1 Q_1 + \theta_2 Q_2$. Once a feasible solution has been found, the observer gains L_0, L_1 and L_2 can be obtained as

$$L_0 = P^{-1}Q_0, \quad L_1 = P^{-1}Q_1, \quad L_2 = P^{-1}Q_2 \tag{3.28}$$

3.2.3 LPV Observer Design with Uncertain Scheduling Parameter

In real-world applications, perfect measurement or estimation of the scheduling parameters becomes unrealistic. The convergence achieved by the above LPV observer based on the nominal model may be destructed by a small amount of measurement or estimation

error. Therefore, it is necessary to develop a design methodology that takes the uncertainty in the scheduling parameters into consideration. In what follows, two types of robust LPV observers will be discussed.

Robust Gain-Scheduled Luenberger Observer

Besides the asymptotic convergence, the observer gains L_0, L_1 and L_2 are also expected to minimize the estimation error in terms of some widely used performance measure in control, such as the H_2 or H_∞ norm [54] [59]. Next, the design methodology will be formulated in a high level systematic way, which allows it to be used in other systems.

Suppose the system under study has the following LPV model

$$\dot{x} = A(\theta)x + B(\theta)u, \quad y = Cx \tag{3.29}$$

where $A(\theta)$, $B(\theta)$ are affine matrix functions of the scheduling parameter $\theta \in R^{k\times 1}$.

$$A(\theta) = A_0 + \theta(1)A_1 + \cdots + \theta(k)A_k, \quad B(\theta) = B_0 + \theta(1)B_1 + \cdots + \theta(k)B_k \tag{3.30}$$

The LPV Luenberger observer is formulated as

$$\dot{\hat{x}} = A(\theta_m)\hat{x} + B(\theta_m)u + L(\theta_m)(y - C\hat{x}) \tag{3.31}$$

where θ_m denotes the measured or estimated scheduling parameter. The deviation of θ_m from θ is represented by θ_Δ as

$$\theta_\Delta = \theta - \theta_m \tag{3.32}$$

The observer gain $L(\theta_m)$ also depends on θ affinely as shown in Eq. (3.23). Then, the observer error state equation becomes

$$\begin{aligned}\dot{x} - \dot{\hat{x}} &= [A(\theta) - L(\theta)C](x - \hat{x}) + B(\theta_m)u + L(\theta_m)(y - C\hat{x}) \\ &= [(A_0 - L_0C) + \textstyle\sum_{i=1}^{k} \theta(i)(A_i - L_iC) + \sum_{i=1}^{k} \theta_\Delta(i)L_iC](x - \hat{x}) \\ &\quad + \textstyle\sum_{i=1}^{k} \theta_\Delta(i)(A_i\hat{x} + B_iu)\end{aligned} \tag{3.33}$$

It can be seen that the measurement or estimation error θ_Δ will induce extra disturbance terms $\sum_{i=1}^{k} \theta_\Delta(A_i\hat{x} + B_iu)$ that keep the observer error from converging to zero even if the state matrix $(A_0 - L_0C) + \sum_{i=1}^{k} \theta(i)(A_i - L_iC) + \sum_{i=1}^{k} \theta_\Delta(i)L_iC$ is asymptotic stable. To reduce the sensitivity of the observer error on this disturbance input, some robust control design techniques, such as H_2 and H_∞ optimization, can be utilized. To facilitate the subsequent analysis, the following observer error state equation will be used.

$$\begin{aligned}\dot{e} &= [(A_0 - L_0C) + \textstyle\sum_{i=1}^{k} \theta(i)(A_i - L_iC) + \sum_{i=1}^{k} \theta_\Delta(i)L_iC]e + \sum_{i=1}^{k} \theta_\Delta(i)(A_i\hat{x} + B_iu) \\ &= A_L(\theta, \theta_\Delta)e + B_L(\theta_\Delta)w\end{aligned} \tag{3.34}$$

The vector input signal $w = (\hat{x}^T \;\; u^T)^T$ is treated as an exogenous disturbance for the observer error. $A_L(\theta, \theta_\Delta)$ and $B_L(\theta_\Delta)$ are the abbreviation of the matrices shown below.

$$\begin{aligned}A_L(\theta, \theta_\Delta) &= (A_0 - L_0C) + \textstyle\sum_{i=1}^{k} \theta(i)(A_i - L_iC) + \sum_{i=1}^{k} \theta_\Delta(i)L_iC \\ B_L(\theta_\Delta) &= [\textstyle\sum_{i=1}^{k} \theta_\Delta(i)A_i \quad \sum_{i=1}^{k} \theta_\Delta(i)B_i]\end{aligned} \tag{3.35}$$

H_2 Observer Design

First, a review of some basic knowledge of the H_2 performance criterion for a MIMO process with a transfer function $T(s)$ is presented. The H_2 norm is defined as [56] [38]

$$\|T\|_2 = \sqrt{\frac{1}{2\pi}\mathbf{trace}\left(\int_{-\infty}^{\infty} T(i\omega)T^*(i\omega)d\omega\right)} \tag{3.36}$$

Suppose the state space realization of $T(s)$ is $\dot{x} = Ax + Bu$, $y = Cx$. Applying Parseval's Theorem [38], the following formula can be obtained.

$$\begin{aligned} \|T\|_2^2 &= \textbf{trace}\left(\int_0^\infty [Ce^{At}B]^T[Ce^{At}B]dt\right) \\ &= \textbf{trace}\left(B^T \underbrace{\int_0^\infty e^{A^Tt}C^TCe^{At}dt}_{Q_0} B\right) \\ &= \textbf{trace}\left(C \underbrace{\int_0^\infty e^{At}BB^Te^{A^Tt}dt}_{P_0} C^T\right) \end{aligned} \tag{3.37}$$

where P_0 and Q_0 are called the controllability and observability Gramians, which are also the solution of the following Lyapunov equations.

Lemma 8 *[38] The H_2 norm of a LTI system $\dot{x} = Ax + Bu$, $y = Cx$ can be computed as*

$$\begin{aligned} \|T\|_2^2 &= \textbf{\textit{trace}}(CP_0C^T), \quad \textbf{\textit{where}}\ AP_0 + P_0A^T + BB^T = 0 \\ \|T\|_2^2 &= \textbf{\textit{trace}}(B^TQ_0B), \quad \textbf{\textit{where}}\ A^TQ_0 + Q_0A + C^TC = 0 \end{aligned} \tag{3.38}$$

H_2 performance criterion is one of the most widely used cost functions in optimal control. Its physical meaning can be interpreted from both a deterministic and stochastic perspective [54] [38] as shown below.

1) **Deterministic Interpretation of H_2 Norm:** Let e_k be the standard unit vector and denote the output of

$$\dot{x} = Ax, \quad y = Cx, \quad x(0) = Be_k$$

Note that this is identical to an impulsive input in channel k. Since $z_k = Ce^{At}Be_k$, its energy can be computed as

$$\int_0^\infty z_k^T(t)z_k(t)dt = e_k^T B^T \left(\int_0^\infty e^{A^T t}C^T Ce^{At}dt\right) Be_k$$

After summing over k, $\|T\|_2^2 = \mathbf{trace}(B^T Q_0 B)$ can be derived. Therefore, the squared H_2 norm is the energy sum of transients of output response.

$$\sum_k \int_0^\infty \|z_k(t)\|^2 \, dt = \|T\|_2^2$$

2) **Stochastic Interpretation of H_2 Norm:** Let w be the white noise input for the LTI system $\dot{x} = Ax + Bw$. Recall that the state-covariance matrix $P(t) = E[x(t)x^T(t)]$ can be computed by solving the following matrix differential equation.

$$\dot{P}(t) = AP(t) + P(t)A^T + BB^T, \quad P(0) = E[x(0)x^T(0)]$$

In the steady-state case ($\dot{P}(t) = 0$), $\lim_{t\to\infty} E[x(t)x^T(t)] = \lim_{t\to\infty} P(t) = P_0$ can be obtained. Furthermore, the following result can be inferred with $z = Cx$.

$$\lim_{t\to\infty} E[z(t)z^T(t)] = \lim_{t\to\infty} \mathbf{trace}(E[Cx(t)x^T(t)C]) = \mathbf{trace}(CP_0C^T)$$

Therefore, the squared H_2 norm is equal to the asymptotic variance of output of the LTI system $\dot{x} = Ax + Bu$, $y = Cx$, where w is the white noise input.

It is also worth mentioning that the state feedback LQR control is equivalent to the optimization of the H_2 norm of the LTI system $\dot{x} = Ax + Bu$, $y = Cx$ [50]. The cost function of the LQR control is shown in Eq. (3.39)

$$J = \int_0^\infty [x^T Qx + u^T Ru]dt \tag{3.39}$$

where $Q = Q^T$, $Q \geq 0$, $R = R^T$, $R \succ 0$. If the state feedback control law $u = -Kx$ is used, the cost function J becomes

$$J = \int_0^\infty [x^T(Q + K^T RK)x]dt \tag{3.40}$$

It is obvious that this cost function is nothing but the energy of the transient output response of the LTI system with the output matrix C satisfying $C^T C = Q + K^T RK$.

As can be seen from Eq. (3.34), the measurement or estimation error θ_Δ acts as a disturbance input for the observer error state equation. If θ_Δ is a zero-mean stochastic measurement or estimation error, the H_2 optimization technique can be applied to minimize the asymptotic variance of the observer error. The search for the optimal observer gains L_0, L_1 and L_2 in terms of the optimal H_2 performance criterion resorts to the following semidefinite programming problem [54] [50]

$$\textbf{minimize } \gamma$$

subject to

$$P \succ 0, \quad \textbf{trace}(Z) < \gamma, \quad \begin{pmatrix} P & I \\ I & Z \end{pmatrix} \succ 0 \tag{3.41}$$

$$\begin{pmatrix} A_L^T(\theta, \theta_\Delta)P + PA_L(\theta, \theta_\Delta) & PB_L(\theta_\Delta) \\ B_L^T(\theta_\Delta)P & -\gamma I \end{pmatrix} \prec 0, \quad \forall(\theta, \theta_\Delta) \in \Theta \times \Theta_\Delta$$

where the matrices $A_L(\theta, \theta_\Delta)$ and $B_L(\theta_\Delta)$ are defined in Eq. (3.35). The semidefinite conditions in Eq. (3.41) come from the result in Lemma 8, but the derivation procedure is omitted here.

H_∞ Observer Design

H_∞ performance criterion is another widely used cost function in control. For the application in the observer design, it can be applied to minimize the upper bound of the

L_2 gain from the disturbance input w to the observer error e as shown in Eq. (3.34). The mathematical formulation of the H_∞ optimization problem is shown below [56] [38].

$$\begin{aligned} &\textbf{minimize } \gamma \\ &\textbf{subject to } \sqrt{\int_0^\infty e^2(t)dt} \leq \gamma \sqrt{\int_0^\infty w^2(t)dt} \end{aligned} \tag{3.42}$$

As mentioned in the previous chapter, the L_2 gain constraint can be transformed to a semidefinite constraint, such as Eq. (2.48), (2.50), (2.51) or (2.52). Similar to the H_2 case, the observer error state equation in Eq. (3.34) is used as the basis for H_∞ observer design. The search for the optimal observer gains L_0, L_1 and L_2 in terms of the optimal H_∞ performance criterion resorts to the following semidefinite programming problem

$$\begin{aligned} &\textbf{minimize } \gamma \\ &\textbf{subject to} \\ &P \succ 0 \\ &\begin{pmatrix} A_L^T(\theta,\theta_\Delta)P + PA_L(\theta,\theta_\Delta) & PB_L(\theta_\Delta) & I \\ B_L^T(\theta_\Delta)P & -\gamma I & 0 \\ I & 0 & -\gamma I \end{pmatrix} \prec 0, \quad \forall(\theta,\theta_\Delta) \in \Theta \times \Theta_\Delta \end{aligned} \tag{3.43}$$

where the matrices $A_L(\theta,\theta_\Delta)$ and $B_L(\theta_\Delta)$ are defined in Eq. (3.35).

Unstructured Robust LPV Observer

As mentioned in the last chapter, structured Luenberger Observer is not the only for state estimation. In this section, the development of an optimal unstructured LPV observer will be discussed. The block diagram of the generalized process model interconnected with the unstructured observer is shown in Fig. 3.5 below.

In this scheme, an observer is designed without any pre-defined structure such that the norm of the observer error $e = x - \hat{x}$ is minimized [55]. The Δ block is a diagonal

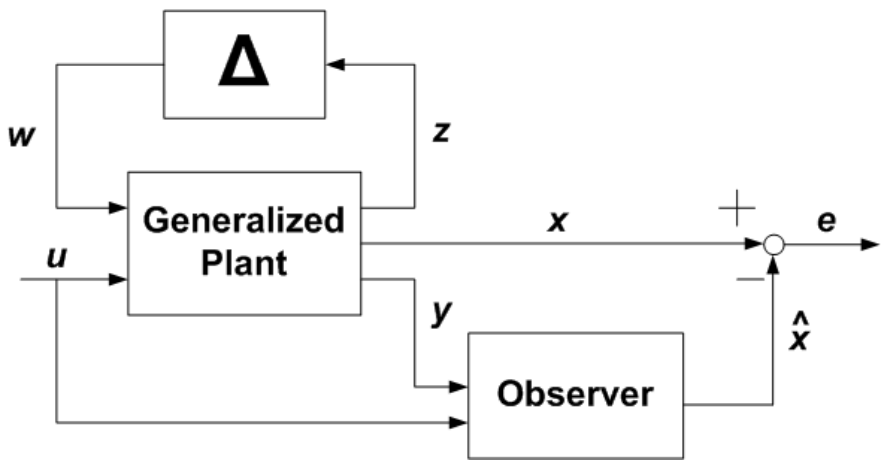

Figure 3.5: The block diagram of the uncertain plant model and the unstructured observer

matrix whose diagonal elements are composed of the measurement or estimation error of the scheduling parameters. Initially, the robust unstructured observer design is discussed in a high-level systematic approach. Later, it will be shown how to transform the bicycle model with uncertain scheduling parameters to this generalized plant representation. First, the state space models of both the generalized process and the unstructured observer will be discussed.

- **The generalized plant with uncertainty:** The state space model of the interconnection of the generalized plant with the Δ block can be seen in what follows

$$\begin{aligned} \dot{x} = A(\theta_m)x + B(\theta_m)u + B_w w, \quad y = Cx \\ z = C_z x + D_z u, \quad w = \Delta z = \Delta C_z x + \Delta D_z u \end{aligned} \tag{3.44}$$

where $\theta_m \in R^{k\times 1}$ denotes the collection of measured or estimated scheduling parameters. The diagonal matrix Δ has the following form

$$\Delta = \begin{pmatrix} \theta(1) - \theta_m(1) & & \\ & \ddots & \\ & & \theta(k) - \theta_m(k) \end{pmatrix} \tag{3.45}$$

where $\theta(i)$, $i = 1, \ldots, k$ denotes the ith real scheduling parameter. In essence, the diagonal terms are the difference of real scheduling parameters and the measured/estimated scheduling parameters. Treating w and z as the state-dependent internal signals, the state equation for the uncertain generalized plant can be rewritten as

$$\dot{x} = [A(\theta_m) + B_w(\theta_m)\Delta C_z]x + [B(\theta_m) + B_w \Delta D_z]u \tag{3.46}$$

- **The unstructured observer:** The unstructured LPV observer has the following state equation

$$\dot{\hat{x}} = A_o(\theta_m)\hat{x} + B_{ou}(\theta_m)u + B_{oy}(\theta_m)y \tag{3.47}$$

where u and y denote the measured input and output signals of the process. $A_o(\theta_m)$, $B_{ou}(\theta_m)$ and $B_{oy}(\theta_m)$ are the affine matrix functions of the measured scheduling parameter $\theta_m \in R^{k\times 1}$.

$$\begin{aligned} A_o(\theta_m) &= A_{o,0} + \theta_m(1)A_{o,1} + \cdots + \theta_m(k)A_{o,k} \\ B_{ou}(\theta_m) &= B_{ou,0} + \theta_m(1)B_{ou,1} + \cdots + \theta_m(k)B_{ou,k} \\ B_{oy}(\theta_m) &= B_{oy,0} + \theta_m(1)B_{oy,1} + \cdots + \theta_m(k)B_{oy,k} \end{aligned} \tag{3.48}$$

The matrices $A_{o,i}$, $B_{ou,i}$, $B_{oy,i}$, $i = 0, 1, \ldots, k$ are the decision variables that the control engineers are looking for such that some performance criteria, such as H_2 and H_∞ norm, are optimized.

When the unstructured observer in Eq. (3.47) is applied, the observer error state equation becomes

$$\begin{aligned} &\dot{x} - \dot{\hat{x}} \\ &= [A(\theta_m) + B_w\Delta C_z - B_{oy}(\theta_m)C]x - A_o(\theta_m)\hat{x} + [B(\theta_m) + B_w\Delta D_z - B_{ou}(\theta_m)]u \\ &= [A(\theta_m) + B_w\Delta C_z - B_{oy}(\theta_m)C](x - \hat{x}) \\ &+[A(\theta_m) + B_w\Delta C_z - B_{oy}(\theta_m)C - A_o(\theta_m)]\hat{x} + [B(\theta_m) + B_w\Delta D_z - B_{ou}(\theta_m)]u \end{aligned} \tag{3.49}$$

Similar to the structured observer, the following observer error state equation will be used to facilitate the subsequent analysis

$$e = A_e(\theta_m, \theta_\Delta)e + B_e(\theta_m, \theta_\Delta)w \tag{3.50}$$

where the vector input signal $w = (\hat{x}^T \ u^T)^T$ is treated as an exogenous disturbance for the observer error. $A_e(\theta_m, \theta_\Delta)$ and $B_e(\theta_m, \theta_\Delta)$ are the abbreviation of the matrices shown in Eq. (3.51).

$$\begin{aligned} &A_e(\theta_m, \theta_\Delta) = A(\theta_m) + B_w \Delta C_z - B_{oy}(\theta_m)C \\ &B_e(\theta_m, \theta_\Delta) \\ &= [A(\theta_m) + B_w \Delta C_z - B_{oy}(\theta_m)C - A_o(\theta_m) \quad B(\theta_m) + B_w \Delta D_z - B_{ou}(\theta_m)] \end{aligned} \tag{3.51}$$

Then, the H_2 or H_∞ optimization technique as discussed for the LPV Luenberger observer can be applied to search for the observer state space matrices $A_{o,i}$, $B_{ou,i}$,$B_{oy,i}$, $i = 0, 1, \ldots, k$ as shown in Eq. (3.48).

- H_2 **Observer Design:** Similar to Eq. (3.41), the search for the optimal observer matrices $A_{o,i}$, $B_{oy,i}$ and $B_{ou,i}$, $i = 0, 1, \ldots, k$ in terms of the optimal H_2 performance criterion resorts to the following semidefinite programming problem

$$\begin{gathered} \textbf{minimize } \gamma \\ \textbf{subject to} \\ P \succ 0, \quad \textbf{trace}(Z) < \gamma, \quad \begin{pmatrix} P & I \\ I & Z \end{pmatrix} \succ 0 \\ \begin{pmatrix} A_e^T(\theta_m, \theta_\Delta)P + PA_e(\theta_m, \theta_\Delta) & PB_e(\theta_m, \theta_\Delta) \\ B_e^T(\theta_m, \theta_\Delta)P & -\gamma I \end{pmatrix} \prec 0, \quad \forall(\theta, \theta_\Delta) \in \Theta \times \Theta_\Delta \end{gathered} \tag{3.52}$$

where the matrices $A_e(\theta_m, \theta_\Delta)$ and $B_e(\theta_m, \theta_\Delta)$ are defined in Eq. (3.51).

- H_∞ **Observer Design:** Similar to Eq. (3.43), the search for the optimal observer matrices $A_{o,i}$, $B_{oy,i}$ and $B_{ou,i}$, $i = 0, 1, \ldots, k$ in terms of the optimal H_∞ performance criterion resorts to the following semidefinite programming problem

$$\textbf{minimize } \gamma$$

subject to

$$P \succ 0$$

$$\begin{pmatrix} A_e^T(\theta_m, \theta_\Delta)P + PA_e(\theta_m, \theta_\Delta) & PB_e(\theta_m, \theta_\Delta) & I \\ B_e^T(\theta_m, \theta_\Delta)P & -\gamma I & 0 \\ I & 0 & -\gamma I \end{pmatrix} \prec 0, \quad \forall(\theta, \theta_\Delta) \in \Theta \times \Theta_\Delta \tag{3.53}$$

where the matrices $A_e(\theta_m, \theta_\Delta)$ and $B_e(\theta_m, \theta_\Delta)$ are defined in Eq. (3.51).

Finite Dimensional Relaxation

The semidefinite conditions in Eq. (3.41), (3.43), (3.52) and (3.53) are indeed infinite dimensional LMI constraints due to their continuous dependence on the parameters θ_m and θ_Δ. To make them numerically tractable, it is necessary to convert them to finite dimensional LMI constraints. It is easy to find that the left side of all these semidefinite constraints are affine matrix functions of the scheduling parameters θ_m and θ_Δ. Therefore, it is sufficient and necessary to guarantee the feasibility of these semidefinite constraints on all the vertices of the polytopic spaces Θ and Θ_Δ as proven in Lemma 7. However, the search for these vertices is not a trivial task, which will be discussed next in detail.

First, a general result for the vertices of the polytopic space for the real vector $(x_1,\ x_1x_2)^T$ is presented.

Lemma 9 *Suppose x_1, $x_2 \in R$ satisfying the lower and upper bounds conditions $\underline{x}_1 \leq x_1 \leq \overline{x}_1$, $\underline{x}_2 \leq x_2 \leq \overline{x}_2$. Then, the vector $(x_1,\ x_1x_2)^T$ lies in a polytopic space with the four vertices*

shown below.

$$\begin{pmatrix} \underline{x}_1 \\ \underline{x}_1\underline{x}_2 \end{pmatrix}, \quad \begin{pmatrix} \underline{x}_1 \\ \underline{x}_1\overline{x}_2 \end{pmatrix}, \quad \begin{pmatrix} \overline{x}_1 \\ \overline{x}_1\underline{x}_2 \end{pmatrix}, \quad \begin{pmatrix} \overline{x}_1 \\ \overline{x}_1\overline{x}_2 \end{pmatrix} \tag{3.54}$$

Proof: The two real variables x_1 and x_2 can be represented as the following convex combination forms

$$x_1 = \lambda_1\underline{x}_1 + \lambda_2\overline{x}_1, \qquad x_2 = \eta_1\underline{x}_2 + \eta_2\overline{x}_2 \tag{3.55}$$

where $\lambda_1 + \lambda_2 = 1$, $\eta_1 + \eta_2 = 1$ with λ_i, $\eta_i \geq 0$, $i = 1, 2$. Then, x_1x_2 can be written as

$$\begin{aligned} x_1x_2 &= (\lambda_1\underline{x}_1 + \lambda_2\overline{x}_1)(\eta_1\underline{x}_2 + \eta_2\overline{x}_2) \\ &= \lambda_1\eta_1\underline{x}_1\underline{x}_2 + \lambda_1\eta_2\underline{x}_1\overline{x}_2 + \lambda_2\eta_1\overline{x}_1\underline{x}_2 + \lambda_2\eta_2\overline{x}_1\overline{x}_2 \end{aligned} \tag{3.56}$$

From Eq. (3.55), the equations shown below can be derived.

$$\begin{gathered} x_1 = \lambda_1(\eta_1 + \eta_2)\underline{x}_1 + \lambda_2(\eta_1 + \eta_2)\overline{x}_1 \\ (\lambda_1 + \lambda_2)(\eta_1 + \eta_2) = \lambda_1\eta_1 + \lambda_1\eta_2 + \lambda_2\eta_1 + \lambda_2\eta_2 = 1 \end{gathered} \tag{3.57}$$

Therefore, the vector $(x_1,\ x_1x_2)^T$ can be represented as the convex combination form shown below

$$\begin{pmatrix} x_1 \\ x_1x_2 \end{pmatrix} = \lambda_1\eta_1 \begin{pmatrix} \underline{x}_1 \\ \underline{x}_1\underline{x}_2 \end{pmatrix} + \lambda_1\eta_2 \begin{pmatrix} \underline{x}_1 \\ \underline{x}_1\overline{x}_2 \end{pmatrix} + \lambda_2\eta_1 \begin{pmatrix} \overline{x}_1 \\ \overline{x}_1\underline{x}_2 \end{pmatrix} + \lambda_2\eta_2 \begin{pmatrix} \overline{x}_1 \\ \overline{x}_1\overline{x}_2 \end{pmatrix} \tag{3.58}$$

with $\sum_i \sum_j \lambda_i\eta_j = 1$ and $\lambda_i\eta_j \geq 0$, i, $j = 1$, 2.

Similarly, the vertices of the polytopic space for a more complex real vector $(x_1,\ x_1x_2,\ x_1x_3,\ x_1x_2x_4)^T$ can also be derived.

Lemma 10 *Suppose x_1, x_2 x_3, $x_4 \in R$ satisfying the lower and upper bounds conditions $\underline{x}_1 \leq x_1 \leq \overline{x}_1$, $\underline{x}_2 \leq x_2 \leq \overline{x}_2$, $\underline{x}_3 \leq x_3 \leq \overline{x}_3$, $\underline{x}_4 \leq x_4 \leq \overline{x}_4$. Then, the vector $(x_1,\ x_1x_2,\ x_1x_3,\ x_1x_2x_4)^T$*

lies in a polytopic space with the sixteen vertices shown below.

$$
\begin{pmatrix} \underline{x}_1 \\ \underline{x}_1\underline{x}_2 \\ \underline{x}_1\underline{x}_3 \\ \underline{x}_1\underline{x}_2\underline{x}_4 \end{pmatrix}, \begin{pmatrix} \underline{x}_1 \\ \underline{x}_1\underline{x}_2 \\ \underline{x}_1\underline{x}_3 \\ \underline{x}_1\underline{x}_2\overline{x}_4 \end{pmatrix}, \begin{pmatrix} \underline{x}_1 \\ \underline{x}_1\underline{x}_2 \\ \underline{x}_1\overline{x}_3 \\ \underline{x}_1\underline{x}_2\underline{x}_4 \end{pmatrix}, \begin{pmatrix} \underline{x}_1 \\ \underline{x}_1\underline{x}_2 \\ \underline{x}_1\overline{x}_3 \\ \underline{x}_1\underline{x}_2\overline{x}_4 \end{pmatrix}
$$

$$
\begin{pmatrix} \underline{x}_1 \\ \underline{x}_1\overline{x}_2 \\ \underline{x}_1\underline{x}_3 \\ \underline{x}_1\overline{x}_2\underline{x}_4 \end{pmatrix}, \begin{pmatrix} \underline{x}_1 \\ \underline{x}_1\overline{x}_2 \\ \underline{x}_1\underline{x}_3 \\ \underline{x}_1\overline{x}_2\overline{x}_4 \end{pmatrix}, \begin{pmatrix} \underline{x}_1 \\ \underline{x}_1\overline{x}_2 \\ \underline{x}_1\overline{x}_3 \\ \underline{x}_1\overline{x}_2\underline{x}_4 \end{pmatrix}, \begin{pmatrix} \underline{x}_1 \\ \underline{x}_1\overline{x}_2 \\ \underline{x}_1\overline{x}_3 \\ \underline{x}_1\overline{x}_2\overline{x}_4 \end{pmatrix}
$$

$$
\begin{pmatrix} \overline{x}_1 \\ \overline{x}_1\underline{x}_2 \\ \overline{x}_1\underline{x}_3 \\ \overline{x}_1\underline{x}_2\underline{x}_4 \end{pmatrix}, \begin{pmatrix} \overline{x}_1 \\ \overline{x}_1\underline{x}_2 \\ \overline{x}_1\underline{x}_3 \\ \overline{x}_1\underline{x}_2\overline{x}_4 \end{pmatrix}, \begin{pmatrix} \overline{x}_1 \\ \overline{x}_1\underline{x}_2 \\ \overline{x}_1\overline{x}_3 \\ \overline{x}_1\underline{x}_2\underline{x}_4 \end{pmatrix}, \begin{pmatrix} \overline{x}_1 \\ \overline{x}_1\underline{x}_2 \\ \overline{x}_1\overline{x}_3 \\ \overline{x}_1\underline{x}_2\overline{x}_4 \end{pmatrix}
$$

$$
\begin{pmatrix} \overline{x}_1 \\ \overline{x}_1\overline{x}_2 \\ \overline{x}_1\underline{x}_3 \\ \overline{x}_1\overline{x}_2\underline{x}_4 \end{pmatrix}, \begin{pmatrix} \overline{x}_1 \\ \overline{x}_1\overline{x}_2 \\ \overline{x}_1\underline{x}_3 \\ \overline{x}_1\overline{x}_2\overline{x}_4 \end{pmatrix}, \begin{pmatrix} \overline{x}_1 \\ \overline{x}_1\overline{x}_2 \\ \overline{x}_1\overline{x}_3 \\ \overline{x}_1\overline{x}_2\underline{x}_4 \end{pmatrix}, \begin{pmatrix} \overline{x}_1 \\ \overline{x}_1\overline{x}_2 \\ \overline{x}_1\overline{x}_3 \\ \overline{x}_1\overline{x}_2\overline{x}_4 \end{pmatrix} \tag{3.59}
$$

Proof: The four real variables x_1, x_2, x_3 and x_4 can be represented as the following convex combination forms

$$
x_1 = \lambda_1\underline{x}_1 + \lambda_2\overline{x}_1, \quad x_2 = \eta_1\underline{x}_2 + \eta_2\overline{x}_2, \quad x_3 = \beta_1\underline{x}_3 + \beta_2\overline{x}_3, \quad x_4 = \rho_1\underline{x}_4 + \rho_2\overline{x}_4 \tag{3.60}
$$

where $\lambda_1 + \lambda_2 = 1$, $\eta_1 + \eta_2 = 1$, $\beta_1 + \beta_2 = 1$, $\rho_1 + \rho_2 = 1$ with λ_i, η_i, β_i, $\rho_i \geq 0$, $i = 1, 2$. Then, x_1x_3 and $x_1x_2x_4$ can be written as

$$\begin{aligned} x_1x_3 &= (\lambda_1\underline{x}_1 + \lambda_2\overline{x}_1)(\beta_1\underline{x}_3 + \beta_2\overline{x}_3) \\ &= \lambda_1\beta_1\underline{x}_1\underline{x}_3 + \lambda_1\beta_2\underline{x}_1\overline{x}_3 + \lambda_2\beta_1\overline{x}_1\underline{x}_3 + \lambda_2\beta_2\overline{x}_1\overline{x}_3 \\ &= \lambda_1\beta_1(\eta_1 + \eta_2)(\rho_1 + \rho_2)\underline{x}_1\underline{x}_3 + \lambda_1\beta_2(\eta_1 + \eta_2)(\rho_1 + \rho_2)\underline{x}_1\overline{x}_3 \\ &+\lambda_2\beta_1(\eta_1 + \eta_2)(\rho_1 + \rho_2)\overline{x}_1\underline{x}_3 + \lambda_2\beta_2(\eta_1 + \eta_2)(\rho_1 + \rho_2)\overline{x}_1\overline{x}_3 \end{aligned} \tag{3.61}$$

$$\begin{aligned} x_1x_2x_4 &= (\lambda_1\underline{x}_1 + \lambda_2\overline{x}_1)(\eta_1\underline{x}_2 + \eta_2\overline{x}_2)(\rho_1\underline{x}_4 + \rho_2\overline{x}_4) \\ &= \lambda_1\eta_1\rho_1\underline{x}_1\underline{x}_2\underline{x}_4 + \lambda_1\eta_1\rho_2\underline{x}_1\underline{x}_2\overline{x}_4 + \lambda_1\eta_2\rho_1\underline{x}_1\overline{x}_2\underline{x}_4 + \lambda_1\eta_2\rho_2\underline{x}_1\overline{x}_2\overline{x}_4 \\ &+\lambda_2\eta_1\rho_1\overline{x}_1\underline{x}_2\underline{x}_4 + \lambda_2\eta_1\rho_2\overline{x}_1\underline{x}_2\overline{x}_4 + \lambda_2\eta_2\rho_1\overline{x}_1\overline{x}_2\underline{x}_4 + \lambda_2\eta_2\rho_2\overline{x}_1\overline{x}_2\overline{x}_4 \\ &= \lambda_1\eta_1\rho_1(\beta_1 + \beta_2)\underline{x}_1\underline{x}_2\underline{x}_4 + \lambda_1\eta_1\rho_2(\beta_1 + \beta_2)\underline{x}_1\underline{x}_2\overline{x}_4 + \lambda_1\eta_2\rho_1(\beta_1 + \beta_2)\underline{x}_1\overline{x}_2\underline{x}_4 \\ &+\lambda_1\eta_2\rho_2(\beta_1 + \beta_2)\underline{x}_1\overline{x}_2\overline{x}_4 + \lambda_2\eta_1\rho_1(\beta_1 + \beta_2)\overline{x}_1\underline{x}_2\underline{x}_4 + \lambda_2\eta_1\rho_2(\beta_1 + \beta_2)\overline{x}_1\underline{x}_2\overline{x}_4 \\ &+\lambda_2\eta_2\rho_1(\beta_1 + \beta_2)\overline{x}_1\overline{x}_2\underline{x}_4 + \lambda_2\eta_2\rho_2(\beta_1 + \beta_2)\overline{x}_1\overline{x}_2\overline{x}_4 \end{aligned} \tag{3.62}$$

From Eq. (3.56), x_1x_2 can be represented as

$$\begin{aligned} x_1x_2 &= \lambda_1\eta_1(\beta_1 + \beta_2)(\rho_1 + \rho_2)\underline{x}_1\underline{x}_2 + \lambda_1\eta_2(\beta_1 + \beta_2)(\rho_1 + \rho_2)\underline{x}_1\overline{x}_2 \\ &+\lambda_2\eta_1(\beta_1 + \beta_2)(\rho_1 + \rho_2)\overline{x}_1\underline{x}_2 + \lambda_2\eta_2(\beta_1 + \beta_2)(\rho_1 + \rho_2)\overline{x}_1\overline{x}_2 \end{aligned} \tag{3.63}$$

Furthermore, the following equality can be derived from Eq. (3.60)

$$(\lambda_1 + \lambda_2)(\eta_1 + \eta_2)(\beta_1 + \beta_2)(\rho_1 + \rho_2) = \sum_i \sum_j \sum_k \sum_m \lambda_i\eta_j\beta_k\rho_m = 1 \tag{3.64}$$

where i, j, k, $m = 1$, 2. Therefore, the vector $(x_1,\ x_1x_2,\ x_1x_3,\ x_1x_2x_4)^T$ can be represented as the convex combination form shown below

$$
\begin{pmatrix} x_1 \\ x_1x_2 \\ x_1x_3 \\ x_1x_2x_4 \end{pmatrix}
$$

$$
= \lambda_1\eta_1\beta_1\rho_1 \begin{pmatrix} \underline{x}_1 \\ \underline{x}_1\underline{x}_2 \\ \underline{x}_1\underline{x}_3 \\ \underline{x}_1\underline{x}_2\underline{x}_4 \end{pmatrix} + \lambda_1\eta_1\beta_1\rho_2 \begin{pmatrix} \underline{x}_1 \\ \underline{x}_1\underline{x}_2 \\ \underline{x}_1\underline{x}_3 \\ \underline{x}_1\underline{x}_2\overline{x}_4 \end{pmatrix} + \lambda_1\eta_1\beta_2\rho_1 \begin{pmatrix} \underline{x}_1 \\ \underline{x}_1\underline{x}_2 \\ \underline{x}_1\overline{x}_3 \\ \underline{x}_1\underline{x}_2\underline{x}_4 \end{pmatrix}
$$

$$
+\lambda_1\eta_1\beta_2\rho_2 \begin{pmatrix} \underline{x}_1 \\ \underline{x}_1\underline{x}_2 \\ \underline{x}_1\overline{x}_3 \\ \underline{x}_1\underline{x}_2\overline{x}_4 \end{pmatrix} + \lambda_1\eta_2\beta_1\rho_1 \begin{pmatrix} \underline{x}_1 \\ \underline{x}_1\overline{x}_2 \\ \underline{x}_1\underline{x}_3 \\ \underline{x}_1\overline{x}_2\underline{x}_4 \end{pmatrix} + \lambda_1\eta_2\beta_1\rho_2 \begin{pmatrix} \underline{x}_1 \\ \underline{x}_1\overline{x}_2 \\ \underline{x}_1\underline{x}_3 \\ \underline{x}_1\overline{x}_2\overline{x}_4 \end{pmatrix}
$$

$$
+\lambda_1\eta_2\beta_2\rho_1 \begin{pmatrix} \underline{x}_1 \\ \underline{x}_1\overline{x}_2 \\ \underline{x}_1\overline{x}_3 \\ \underline{x}_1\overline{x}_2\underline{x}_4 \end{pmatrix} + \lambda_1\eta_2\beta_2\rho_2 \begin{pmatrix} \underline{x}_1 \\ \underline{x}_1\overline{x}_2 \\ \underline{x}_1\overline{x}_3 \\ \underline{x}_1\overline{x}_2\overline{x}_4 \end{pmatrix} + \lambda_2\eta_1\beta_1\rho_1 \begin{pmatrix} \overline{x}_1 \\ \overline{x}_1\underline{x}_2 \\ \overline{x}_1\underline{x}_3 \\ \overline{x}_1\underline{x}_2\underline{x}_4 \end{pmatrix}
$$

$$
+\lambda_2\eta_1\beta_1\rho_2 \begin{pmatrix} \overline{x}_1 \\ \overline{x}_1\underline{x}_2 \\ \overline{x}_1\underline{x}_3 \\ \overline{x}_1\underline{x}_2\overline{x}_4 \end{pmatrix} + \lambda_2\eta_1\beta_2\rho_1 \begin{pmatrix} \overline{x}_1 \\ \overline{x}_1\underline{x}_2 \\ \overline{x}_1\overline{x}_3 \\ \overline{x}_1\underline{x}_2\underline{x}_4 \end{pmatrix} + \lambda_2\eta_1\beta_2\rho_2 \begin{pmatrix} \overline{x}_1 \\ \overline{x}_1\underline{x}_2 \\ \overline{x}_1\overline{x}_3 \\ \overline{x}_1\underline{x}_2\overline{x}_4 \end{pmatrix}
$$

$$
+\lambda_2\eta_2\beta_1\rho_1 \begin{pmatrix} \overline{x}_1 \\ \overline{x}_1\overline{x}_2 \\ \overline{x}_1\underline{x}_3 \\ \overline{x}_1\overline{x}_2\underline{x}_4 \end{pmatrix} + \lambda_2\eta_2\beta_1\rho_2 \begin{pmatrix} \overline{x}_1 \\ \overline{x}_1\overline{x}_2 \\ \overline{x}_1\underline{x}_3 \\ \overline{x}_1\overline{x}_2\overline{x}_4 \end{pmatrix} + \lambda_2\eta_2\beta_2\rho_1 \begin{pmatrix} \overline{x}_1 \\ \overline{x}_1\overline{x}_2 \\ \overline{x}_1\overline{x}_3 \\ \overline{x}_1\overline{x}_2\underline{x}_4 \end{pmatrix}
$$

$$+\lambda_2\eta_2\beta_2\rho_2 \begin{pmatrix} \overline{x}_1 \\ \overline{x}_1\overline{x}_2 \\ \overline{x}_1\overline{x}_3 \\ \overline{x}_1\overline{x}_2\overline{x}_4 \end{pmatrix} \tag{3.65}$$

with $\sum_i \sum_j \sum_k \sum_m \lambda_i\eta_j\beta_k\rho_m = 1$ and $\lambda_i\eta_j\beta_k\rho_m \geq 0$, i, j, k, $m = 1, 2$.

For the case of perfect measurements of the scheduling parameters, the vector $\theta = (\frac{1}{v_x}, \frac{a_x}{v_x})^T$ can be abstracted as the form of $(x_1, x_1x_2)^T$ with $x_1 = \frac{1}{v_x}$ and $x_2 = a_x$. Applying Lemma 9, the four vertices of the polytopic parameter space Θ can be obtained

$$\theta^{(1)} = \begin{pmatrix} \frac{1}{\overline{v}_x} \\ \frac{\underline{a}_x}{\overline{v}_x} \end{pmatrix}, \quad \theta^{(2)} = \begin{pmatrix} \frac{1}{\overline{v}_x} \\ \frac{\overline{a}_x}{\overline{v}_x} \end{pmatrix}, \quad \theta^{(3)} = \begin{pmatrix} \frac{1}{\underline{v}_x} \\ \frac{\underline{a}_x}{\underline{v}_x} \end{pmatrix}, \quad \theta^{(4)} = \begin{pmatrix} \frac{1}{\underline{v}_x} \\ \frac{\overline{a}_x}{\underline{v}_x} \end{pmatrix} \tag{3.66}$$

where the following extreme values are chosen to constitute the above vertices.

$$\underline{v}_x = 15kph, \quad \overline{v}_x = 150kph, \quad \underline{a}_x = -8.0m/s^2, \quad \overline{a}_x = 8.0m/s^2 \tag{3.67}$$

These values are selected based on the of normal operation range of the automotive active safety systems. This polytopic space for the scheduling parameters $\frac{1}{v_x}$ and $\frac{a_x}{v_x}$ is visualized by the shaded region in Fig. 3.6.

For the case of scheduling parameters with uncertain measurement error, the semidefinte constraints in Eq. (3.41), (3.43), (3.52) and (3.53) depend on the parameter vector $(\theta^T, \ \theta_\Delta^T)^T$. It is assumed that the measurement error of the longitudinal velocity and acceleration can be represented as the following multiplicative uncertain form.

$$\Delta v_x = \epsilon_1 v_x, \qquad \Delta a_x = \epsilon_2 a_x \tag{3.68}$$

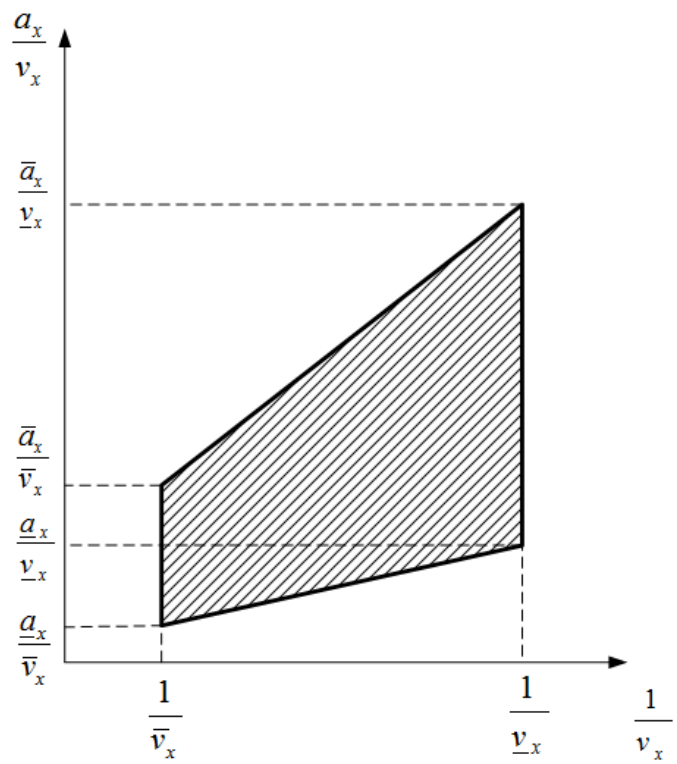

Figure 3.6: The polytopic space for the scheduling parameters $\frac{1}{v_x}$ and $\frac{a_x}{v_x}$.

where the factors ϵ_1 and ϵ_2 are constrained in the intervals $\underline{\epsilon}_1 \leq \epsilon_1 \leq \bar{\epsilon}_1$, $\underline{\epsilon}_2 \leq \epsilon_2 \leq \bar{\epsilon}_2$. Then, the measurement error of the first scheduling parameter $\theta_{\Delta,1}$ becomes

$$\theta_{\Delta,1} = \frac{1}{v_x} - \frac{1}{v_x + \Delta v_x} = \frac{\Delta v_x}{v_x(v_x + \Delta v_x)} = \frac{\epsilon_1}{1+\epsilon_1} \cdot \frac{1}{v_x} \tag{3.69}$$

Similarly, the second scheduling parameter $\theta_{\Delta,2}$ can be derived as

$$\theta_{\Delta,2} = \frac{a_x}{v_x} - \frac{a_x + \Delta a_x}{v_x + \Delta v_x} = \frac{a_x \Delta v_x - v_x \Delta a_x}{v_x(v_x + \Delta v_x)} = \frac{\epsilon_1 - \epsilon_2}{1+\epsilon_1} \cdot \frac{a_x}{v_x} \tag{3.70}$$

The two coefficients $\frac{\epsilon_1}{1+\epsilon_1}$ and $\frac{\epsilon_1-\epsilon_2}{1+\epsilon_1}$ act as the multiplicative uncertain coefficients for the two scheduling parameters $\frac{1}{v_x}$ and $\frac{a_x}{v_x}$. Their variation intervals are shown as

$$\begin{aligned} \frac{1}{1+\frac{1}{\underline{\epsilon}_1}} \leq \frac{\epsilon_1}{1+\epsilon_1} \leq \frac{1}{1+\frac{1}{\overline{\epsilon}_1}} \\ 1-\frac{1+\overline{\epsilon}_2}{1+\underline{\epsilon}_1} \leq \frac{\epsilon_1-\epsilon_2}{1+\epsilon_1} \leq 1-\frac{1+\underline{\epsilon}_2}{1+\overline{\epsilon}_1} \end{aligned} \tag{3.71}$$

Hence, the parameter vector $(\theta^T,\ \theta_\Delta^T)^T = (\frac{1}{v_x},\ \frac{a_x}{v_x},\ \frac{1}{v_x}-\frac{1}{v_x+\Delta v_x},\ \frac{a_x}{v_x}-\frac{a_x+\Delta a_x}{v_x+\Delta v_x})^T$ can be abstracted as the form of $(x_1,\ x_1x_2,\ x_1x_3,\ x_1x_2x_4)^T$ with $x_1=\frac{1}{v_x}$, $x_2=a_x$, $x_3=\frac{\epsilon_1}{1+\epsilon_1}$ and $x_4=\frac{\epsilon_1-\epsilon_2}{1+\epsilon_1}$. Applying Lemma 10, the sixteen vertices of the polytopic spaces for the vector $(\theta^T,\ \theta_\Delta^T)^T$ can be obtained.

$$\begin{pmatrix} \theta \\ \theta_\Delta \end{pmatrix}^{(1)} = \begin{pmatrix} \frac{1}{\overline{v}_x} \\ \frac{\underline{a}_x}{\overline{v}_x} \\ \frac{1}{\overline{v}_x}\cdot\frac{1}{1+\frac{1}{\underline{\epsilon}_1}} \\ \frac{\underline{a}_x}{\overline{v}_x}\cdot\left(1-\frac{1+\overline{\epsilon}_2}{1+\underline{\epsilon}_1}\right) \end{pmatrix}, \quad \begin{pmatrix} \theta \\ \theta_\Delta \end{pmatrix}^{(2)} = \begin{pmatrix} \frac{1}{\overline{v}_x} \\ \frac{\underline{a}_x}{\overline{v}_x} \\ \frac{1}{\overline{v}_x}\cdot\frac{1}{1+\frac{1}{\underline{\epsilon}_1}} \\ \frac{\underline{a}_x}{\overline{v}_x}\cdot\left(1-\frac{1+\underline{\epsilon}_2}{1+\overline{\epsilon}_1}\right) \end{pmatrix}$$

$$\begin{pmatrix} \theta \\ \theta_\Delta \end{pmatrix}^{(3)} = \begin{pmatrix} \frac{1}{\overline{v}_x} \\ \frac{\underline{a}_x}{\overline{v}_x} \\ \frac{1}{\overline{v}_x}\cdot\frac{1}{1+\frac{1}{\overline{\epsilon}_1}} \\ \frac{\underline{a}_x}{\overline{v}_x}\cdot\left(1-\frac{1+\overline{\epsilon}_2}{1+\underline{\epsilon}_1}\right) \end{pmatrix}, \quad \begin{pmatrix} \theta \\ \theta_\Delta \end{pmatrix}^{(4)} = \begin{pmatrix} \frac{1}{\overline{v}_x} \\ \frac{\underline{a}_x}{\overline{v}_x} \\ \frac{1}{\overline{v}_x}\cdot\frac{1}{1+\frac{1}{\overline{\epsilon}_1}} \\ \frac{\underline{a}_x}{\overline{v}_x}\cdot\left(1-\frac{1+\underline{\epsilon}_2}{1+\overline{\epsilon}_1}\right) \end{pmatrix}$$

$$\begin{pmatrix} \theta \\ \theta_\Delta \end{pmatrix}^{(5)} = \begin{pmatrix} \dfrac{1}{\overline{v}_x} \\ \dfrac{\overline{a}_x}{\overline{v}_x} \\ \dfrac{1}{\overline{v}_x} \cdot \dfrac{1}{1+\frac{1}{\underline{\epsilon}_1}} \\ \dfrac{\overline{a}_x}{\overline{v}_x} \cdot \left(1 - \dfrac{1+\overline{\epsilon}_2}{1+\underline{\epsilon}_1}\right) \end{pmatrix}, \quad \begin{pmatrix} \theta \\ \theta_\Delta \end{pmatrix}^{(6)} = \begin{pmatrix} \dfrac{1}{\overline{v}_x} \\ \dfrac{\overline{a}_x}{\overline{v}_x} \\ \dfrac{1}{\overline{v}_x} \cdot \dfrac{1}{1+\frac{1}{\underline{\epsilon}_1}} \\ \dfrac{\overline{a}_x}{\overline{v}_x} \cdot \left(1 - \dfrac{1+\underline{\epsilon}_2}{1+\overline{\epsilon}_1}\right) \end{pmatrix}$$

$$\begin{pmatrix} \theta \\ \theta_\Delta \end{pmatrix}^{(7)} = \begin{pmatrix} \dfrac{1}{\overline{v}_x} \\ \dfrac{\overline{a}_x}{\overline{v}_x} \\ \dfrac{1}{\overline{v}_x} \cdot \dfrac{1}{1+\frac{1}{\overline{\epsilon}_1}} \\ \dfrac{\overline{a}_x}{\overline{v}_x} \cdot \left(1 - \dfrac{1+\overline{\epsilon}_2}{1+\underline{\epsilon}_1}\right) \end{pmatrix}, \quad \begin{pmatrix} \theta \\ \theta_\Delta \end{pmatrix}^{(8)} = \begin{pmatrix} \dfrac{1}{\overline{v}_x} \\ \dfrac{\overline{a}_x}{\overline{v}_x} \\ \dfrac{1}{\overline{v}_x} \cdot \dfrac{1}{1+\frac{1}{\overline{\epsilon}_1}} \\ \dfrac{\overline{a}_x}{\overline{v}_x} \cdot \left(1 - \dfrac{1+\underline{\epsilon}_2}{1+\overline{\epsilon}_1}\right) \end{pmatrix}$$

$$\begin{pmatrix} \theta \\ \theta_\Delta \end{pmatrix}^{(9)} = \begin{pmatrix} \dfrac{1}{\underline{v}_x} \\ \dfrac{\underline{a}_x}{\underline{v}_x} \\ \dfrac{1}{\underline{v}_x} \cdot \dfrac{1}{1+\frac{1}{\underline{\epsilon}_1}} \\ \dfrac{\underline{a}_x}{\underline{v}_x} \cdot \left(1 - \dfrac{1+\overline{\epsilon}_2}{1+\underline{\epsilon}_1}\right) \end{pmatrix}, \quad \begin{pmatrix} \theta \\ \theta_\Delta \end{pmatrix}^{(10)} = \begin{pmatrix} \dfrac{1}{\underline{v}_x} \\ \dfrac{\underline{a}_x}{\underline{v}_x} \\ \dfrac{1}{\underline{v}_x} \cdot \dfrac{1}{1+\frac{1}{\underline{\epsilon}_1}} \\ \dfrac{\underline{a}_x}{\underline{v}_x} \cdot \left(1 - \dfrac{1+\underline{\epsilon}_2}{1+\overline{\epsilon}_1}\right) \end{pmatrix}$$

$$\begin{pmatrix} \theta \\ \theta_\Delta \end{pmatrix}^{(11)} = \begin{pmatrix} \dfrac{1}{\underline{v}_x} \\ \dfrac{\underline{a}_x}{\underline{v}_x} \\ \dfrac{1}{\underline{v}_x} \cdot \dfrac{1}{1+\frac{1}{\overline{\epsilon}_1}} \\ \dfrac{\underline{a}_x}{\underline{v}_x} \cdot \left(1 - \dfrac{1+\overline{\epsilon}_2}{1+\underline{\epsilon}_1}\right) \end{pmatrix}, \quad \begin{pmatrix} \theta \\ \theta_\Delta \end{pmatrix}^{(12)} = \begin{pmatrix} \dfrac{1}{\underline{v}_x} \\ \dfrac{\underline{a}_x}{\underline{v}_x} \\ \dfrac{1}{\underline{v}_x} \cdot \dfrac{1}{1+\frac{1}{\overline{\epsilon}_1}} \\ \dfrac{\underline{a}_x}{\underline{v}_x} \cdot \left(1 - \dfrac{1+\underline{\epsilon}_2}{1+\overline{\epsilon}_1}\right) \end{pmatrix}$$

$$\begin{pmatrix} \theta \\ \theta_\Delta \end{pmatrix}^{(13)} = \begin{pmatrix} \frac{1}{\underline{v}_x} \\ \frac{\overline{a}_x}{\underline{v}_x} \\ \frac{1}{\underline{v}_x} \cdot \frac{1}{1+\frac{1}{\underline{\epsilon}_1}} \\ \frac{\overline{a}_x}{\underline{v}_x} \cdot \left(1 - \frac{1+\overline{\epsilon}_2}{1+\underline{\epsilon}_1}\right) \end{pmatrix}, \quad \begin{pmatrix} \theta \\ \theta_\Delta \end{pmatrix}^{(14)} = \begin{pmatrix} \frac{1}{\underline{v}_x} \\ \frac{\overline{a}_x}{\underline{v}_x} \\ \frac{1}{\underline{v}_x} \cdot \frac{1}{1+\frac{1}{\underline{\epsilon}_1}} \\ \frac{\overline{a}_x}{\underline{v}_x} \cdot \left(1 - \frac{1+\underline{\epsilon}_2}{1+\overline{\epsilon}_1}\right) \end{pmatrix}$$

$$\begin{pmatrix} \theta \\ \theta_\Delta \end{pmatrix}^{(15)} = \begin{pmatrix} \frac{1}{\underline{v}_x} \\ \frac{\overline{a}_x}{\underline{v}_x} \\ \frac{1}{\underline{v}_x} \cdot \frac{1}{1+\frac{1}{\overline{\epsilon}_1}} \\ \frac{\overline{a}_x}{\underline{v}_x} \cdot \left(1 - \frac{1+\overline{\epsilon}_2}{1+\underline{\epsilon}_1}\right) \end{pmatrix}, \quad \begin{pmatrix} \theta \\ \theta_\Delta \end{pmatrix}^{(16)} = \begin{pmatrix} \frac{1}{\underline{v}_x} \\ \frac{\overline{a}_x}{\underline{v}_x} \\ \frac{1}{\underline{v}_x} \cdot \frac{1}{1+\frac{1}{\overline{\epsilon}_1}} \\ \frac{\overline{a}_x}{\underline{v}_x} \cdot \left(1 - \frac{1+\underline{\epsilon}_2}{1+\overline{\epsilon}_1}\right) \end{pmatrix} \tag{3.72}$$

where the following extreme values $\underline{v}_x$, $\overline{v}_x$, $\underline{a}_x$ and $\overline{a}_x$ are already defined in Eq. (3.67). The variation interval for the multiplicative factors ϵ_1 and ϵ_2 are shown below.

$$\underline{\epsilon}_1 = -0.1, \quad \overline{\epsilon}_1 = 0.1, \quad \underline{\epsilon}_2 = -0.2, \quad \overline{\epsilon}_2 = 0.2 \tag{3.73}$$

General Plant Representation

Finally, the derivation of the general plant representation shown in Fig. 3.5 of the bicycle model with uncertain scheduling parameters is presented. Generally, the procedure that is presented in the brief introduction for linear fractional representation in previous chapter will be followed. The affine parameter dependent state space model is shown below again

$$\begin{aligned} \dot{x} &= ((\theta_{m,1} + \theta_{\Delta,1})A_1 + (\theta_{m,2} + \theta_{\Delta,2})A_2)\, x + (B_0 + (\theta_{m,2} + \theta_{\Delta,2})B_2)\, u \\ y &= Cx \end{aligned} \tag{3.74}$$

where $\theta_{m,1}$, $\theta_{m,2}$ denote the measured scheduling parameters and $\theta_{\Delta,1}$, $\theta_{\Delta,2}$ are the uncertain measurement error for each parameter. The state space matrices A_1, A_2, B_0, B_2, C are defined as

$$A_1 = \begin{pmatrix} -C_f\left(\frac{1}{M}+\frac{a^2}{I_z}\right) & C_r\left(\frac{ab}{I_z}-\frac{1}{M}\right) \\ C_f\left(\frac{ab}{I_z}-\frac{1}{M}\right) & -C_r\left(\frac{1}{M}+\frac{b^2}{I_z}\right) \end{pmatrix}, \quad A_2 = \begin{pmatrix} -1 & 0 \\ 0 & -1 \end{pmatrix}$$

$$B_0 = \begin{pmatrix} 0 & 1 & 1 \\ 0 & 0 & 1 \end{pmatrix}, \quad B_2 = \begin{pmatrix} 1 & 0 & 0 \\ 0 & 0 & 0 \end{pmatrix}, \quad C = \begin{pmatrix} 1 & -1 \end{pmatrix}$$

$\theta_{\Delta,1}A_1$, $\theta_{\Delta,2}A_2$ and $\theta_{\Delta,2}B_2$ can be factorized as the following forms

$$\theta_{\Delta,1}A_1 = \underbrace{\begin{pmatrix} -\left(\frac{1}{M}+\frac{a^2}{I_z}\right) & \left(\frac{ab}{I_z}-\frac{1}{M}\right) \\ \left(\frac{ab}{I_z}-\frac{1}{M}\right) & -\left(\frac{1}{M}+\frac{b^2}{I_z}\right) \end{pmatrix}}_{L_{1,1}} \underbrace{\begin{pmatrix} \theta_{\Delta,1} & 0 \\ 0 & \theta_{\Delta,1} \end{pmatrix}}_{\theta_{\Delta,1}I_2} \underbrace{\begin{pmatrix} C_f & 0 \\ 0 & C_r \end{pmatrix}}_{R_{1,1}}$$

$$\theta_{\Delta,2}A_2 = \underbrace{\begin{pmatrix} 1 & 0 \\ 0 & 1 \end{pmatrix}}_{L_{2,1}} \underbrace{\begin{pmatrix} \theta_{\Delta,2} & 0 \\ 0 & \theta_{\Delta,2} \end{pmatrix}}_{\theta_{\Delta,2}I_2} \underbrace{\begin{pmatrix} -1 & 0 \\ 0 & -1 \end{pmatrix}}_{R_{2,1}}$$

$$\theta_{\Delta,2}B_2 = \underbrace{\begin{pmatrix} 1 & 0 \\ 0 & 1 \end{pmatrix}}_{L_{2,1}} \underbrace{\begin{pmatrix} \theta_{\Delta,2} & 0 \\ 0 & \theta_{\Delta,2} \end{pmatrix}}_{\theta_{\Delta,2}I_2} \underbrace{\begin{pmatrix} 1 & 0 & 0 \\ 0 & 0 & 0 \end{pmatrix}}_{R_{2,2}}$$

where I_2 denotes a 2×2 identity matrix. To conform with the procedure presented in the last chapter, the factorization of the lumped state space matrices can be obtained as

$$\begin{pmatrix} A_1 & 0 \\ 0 & 0 \end{pmatrix} = \begin{pmatrix} L_{1,1} \\ 0 \end{pmatrix} \begin{pmatrix} R_{1,1} & 0 \end{pmatrix}$$

$$\begin{pmatrix} A_2 & B_2 \\ 0 & 0 \end{pmatrix} = \begin{pmatrix} L_{2,1} \\ 0 \end{pmatrix} \begin{pmatrix} R_{2,1} & R_{2,2} \end{pmatrix}$$

By applying Eq. (2.7), the bicycle model can be rewritten as

$$\begin{aligned} \begin{pmatrix} \dot{x} \\ y \end{pmatrix} &= \begin{pmatrix} A(\theta_m) & B(\theta_m) \\ C(\theta_m) & 0 \end{pmatrix} \begin{pmatrix} x \\ u \end{pmatrix} + \begin{pmatrix} L_{1,1} & L_{2,1} \\ 0 & 0 \end{pmatrix} \begin{pmatrix} w_1 \\ w_2 \end{pmatrix} \\ \begin{pmatrix} z_1 \\ z_2 \end{pmatrix} &= \begin{pmatrix} R_{1,1} & 0 \\ R_{2,1} & R_{2,2} \end{pmatrix} \begin{pmatrix} x \\ u \end{pmatrix} \end{aligned} \tag{3.75}$$

where the nominal θ_m scheduled state space matrices $A(\theta_m)$, $B(\theta_m)$ and $C(\theta_m)$ are defined as

$$A(\theta_m) = \theta_{m,1}A_1 + \theta_{m,2}A_2, \quad B(\theta_m) = B_0 + \theta_{m,2}B_2, \quad C(\theta_m) = C$$

To match the generalized plant model in Eq. (3.44), the matrices B_w, C_z and D_z are

$$B_w = \begin{pmatrix} L_{1,1} & L_{2,1} \end{pmatrix}, \quad C_z = \begin{pmatrix} R_{1,1} \\ R_{2,1} \end{pmatrix}, \quad D_z = \begin{pmatrix} 0 \\ R_{2,2} \end{pmatrix}$$

The vectors $(w_1 \;\; w_2)^T$ and $(z_1 \;\; z_2)^T$ are related by

$$\begin{pmatrix} w_1 \\ w_2 \end{pmatrix} = \begin{pmatrix} \theta_{\Delta,1} I_2 & 0 \\ 0 & \theta_{\Delta,2} I_2 \end{pmatrix} \begin{pmatrix} z_1 \\ z_2 \end{pmatrix}$$

3.3 Simulation Results

In this section, some simulation examples are presented to demonstrate the application of the SDP based LPV observer design methodology by using CarSim data. In the simulation test, a sedan is used to follow the trajectory of the standard "Double Lane Change" maneuver. A screen shot of the simulation can be seen in Fig. 3.7. Its longitudinal velocity profile, which decreases from 78kph to 23kph gradually, is shown in Fig. 3.8. The basic

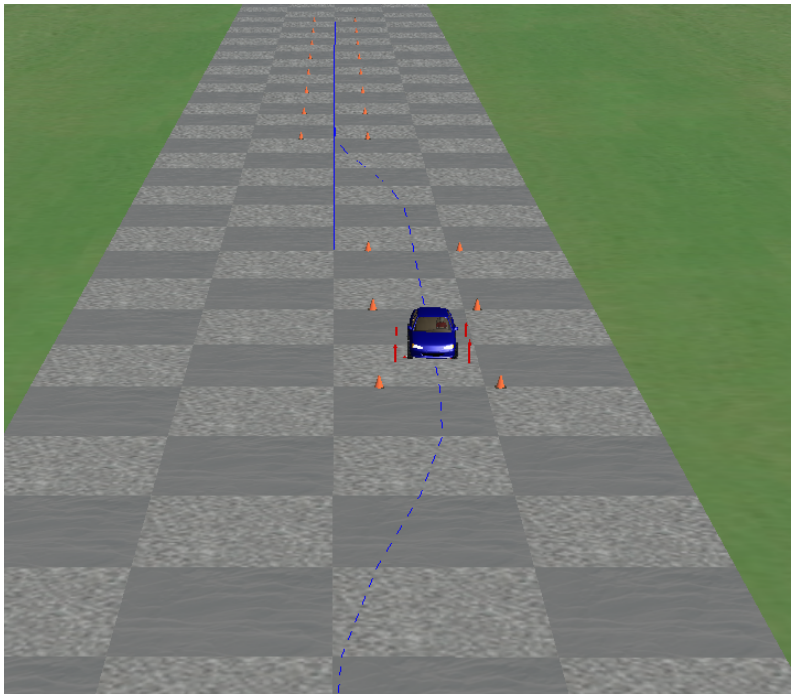

Figure 3.7: The screen shot of the simulation.

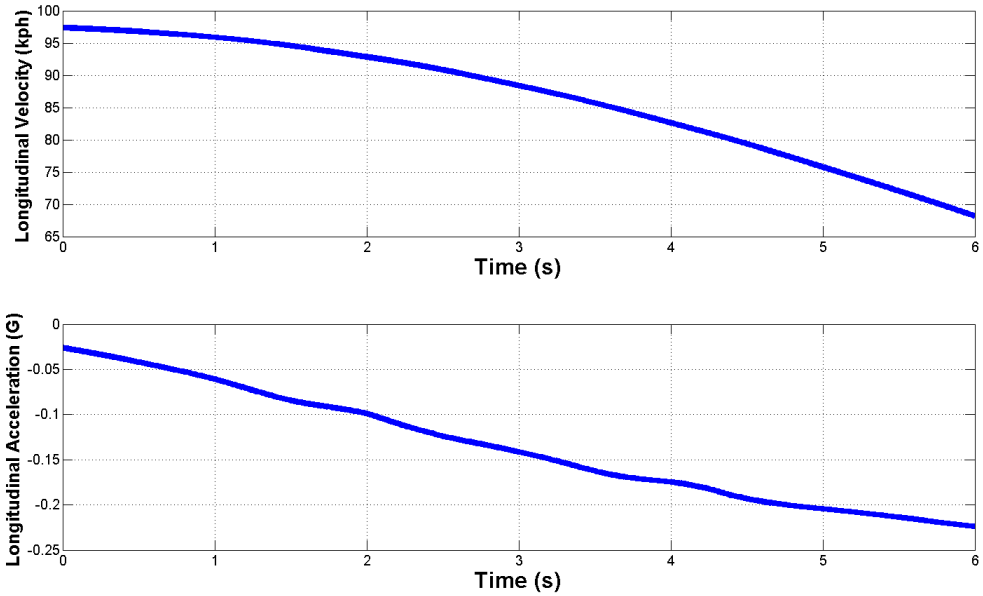

Figure 3.8: Longitudinal velocity and acceleration profile in the simulation.

vehicle inertial parameters and location of CG are shown below.

$$M = 800\,(\mathbf{kg}), \quad I_z = 1152\,(\mathbf{kg}{\cdot}m^2)$$

$$a = 0.948\,(\mathbf{m}), \quad b = 1.422\,(\mathbf{m})$$

The cornering stiffness parameters are

$$C_f = 76500\,(\mathbf{N/rad}), \quad C_r = 51000\,(\mathbf{N/rad})$$

First, the convergent LPV observer gains obtained by solving the LMI feasibility problem in Eq. 3.27 with perfect measurement of longitudinal velocity and acceleration is simulated.

$$L_0 = \begin{pmatrix} 0.0477 \\ 0.0477 \end{pmatrix}, \quad L_1 = \begin{pmatrix} -65.7731 \\ -63.7411 \end{pmatrix}, \quad L_2 = \begin{pmatrix} -0.4363 \\ -0.4363 \end{pmatrix}$$

The simulated estimation results are presented in Fig. 3.9. To illustrate the convergence of the observer, it is initialized 1 second later than the maneuver at a different initial condition. Fig. 3.9 shows that the two estimated slip angles converge to the true value.

Next, the measurement errors in the scheduling parameters are taken into consideration. The optimal H_2 and H_∞ gain parameters can be derived by solving the LMI optimization problems in Eq. (3.41) and (3.43).

- Optimal H_2 gains for Luenberger observer

$$L_0 = \begin{pmatrix} 7250.9 \\ 6962.8 \end{pmatrix}, \quad L_1 = \begin{pmatrix} 35776 \\ 34423 \end{pmatrix}, \quad L_2 = \begin{pmatrix} 831.9374 \\ 773.2087 \end{pmatrix}$$

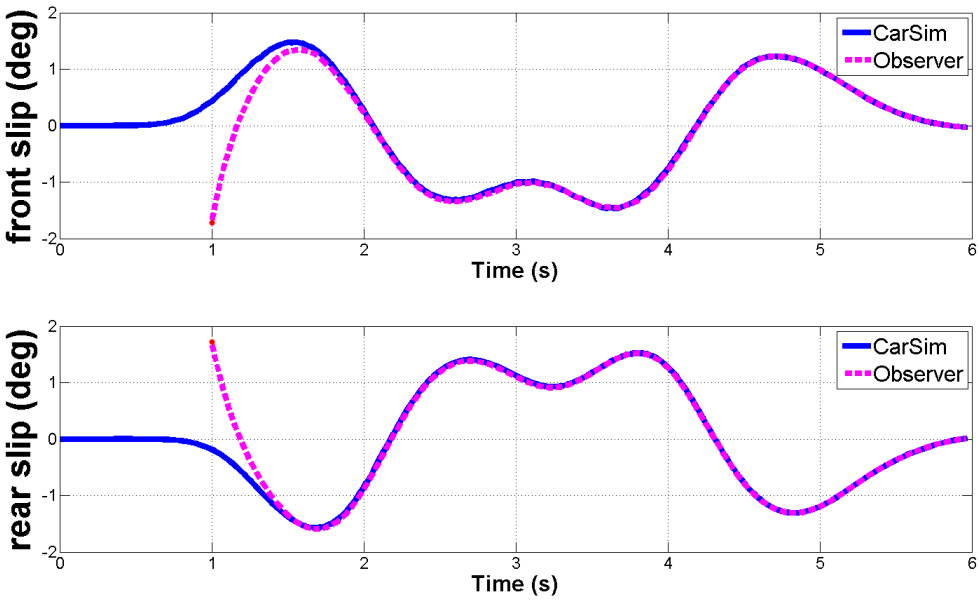

Figure 3.9: The simulation results of gain scheduled observer in tire side angle estimation.

- Optimal H_∞ gains for Luenberger observer

$$L_0 = \begin{pmatrix} 390.3628 \\ 376.0443 \end{pmatrix}, \quad L_1 = \begin{pmatrix} 941.1064 \\ 908.2782 \end{pmatrix}, \quad L_2 = \begin{pmatrix} 104.0730 \\ 100.1726 \end{pmatrix}$$

The unstructured H_2 and H_∞ optimal LPV observer state space matrices defined in Eq. (3.48) can be derived by solving the LMI optimization problems in Eq. (3.52) and (3.52).

- Unstructured optimal H_2 observer

$$A_{o,0} = \begin{pmatrix} -2319.1 & -2321.0 \\ -2531.0 & -2532.7 \end{pmatrix}, \quad A_{o,1} = \begin{pmatrix} -2982.7 & -2818.1 \\ -1432.1 & -1581.4 \end{pmatrix}$$

$$A_{o,2} = \begin{pmatrix} 125.4695 & 126.4443 \\ 121.1414 & 120.1646 \end{pmatrix}, \quad B_{ou,0} = \begin{pmatrix} 0.3352 & 1 & 1 \\ 0.3364 & 0 & -1 \end{pmatrix}$$

$$B_{ou,1} = \begin{pmatrix} -1.5886 & 0 & 0 \\ -1.4224 & 0 & 0 \end{pmatrix}, \quad B_{ou,2} = \begin{pmatrix} 0.9821 & 0 & 0 \\ 0.0147 & 0 & 0 \end{pmatrix}$$

$$B_{oy,0} = \begin{pmatrix} 2320.3 \\ 2532.2 \end{pmatrix}, \quad B_{oy,1} = \begin{pmatrix} 2824.4 \\ 1432.6 \end{pmatrix}, \quad B_{oy,2} = \begin{pmatrix} -126.4374 \\ -121.1343 \end{pmatrix}$$

- Unstructured optimal H_∞ observer

$$A_{o,0} = \begin{pmatrix} -324.2065 & -324.4028 \\ -311.0927 & -310.6798 \end{pmatrix}, \quad A_{o,1} = \begin{pmatrix} -360.3333 & -202.7391 \\ -194.5750 & -352.6795 \end{pmatrix}$$

$$A_{o,2} = \begin{pmatrix} -1.0852 & -0.1374 \\ -0.1474 & -1.1605 \end{pmatrix}, \quad B_{ou,0} = \begin{pmatrix} -0.9175 & 1 & 1 \\ -0.8422 & 0 & -1 \end{pmatrix}$$

$$B_{ou,1} = \begin{pmatrix} 2.1202 & 0 & 0 \\ 2.0056 & 0 & 0 \end{pmatrix}, \quad B_{ou,2} = \begin{pmatrix} 1.2391 & 0 & 0 \\ 0.2549 & 0 & 0 \end{pmatrix}$$

$$B_{oy,0} = \begin{pmatrix} 324.2891 \\ 310.8739 \end{pmatrix}, \quad B_{oy,1} = \begin{pmatrix} 206.7304 \\ 200.8320 \end{pmatrix}, \quad B_{oy,2} = \begin{pmatrix} 0.1406 \\ 0.1824 \end{pmatrix}$$

In the next simulation results, artificial errors are added in the longitudinal velocity and acceleration signals. The simulation results in the two cases for the uncertain multiplicative factors ϵ_1 and ϵ_2 are presented. In the 1st case, ϵ_1 and ϵ_2 are perturbed to -0.04 and 0.06 respectively. The simulation results from the gain scheduled Luenberger observer with optimal H_2 and H_∞ gain parameters can be seen in Fig. 3.10 and 3.11 below. While the simulation results from the unstructured LPV observer with optimal H_2 and H_∞ parameters can be seen in Fig. 3.12 and 3.13.

In the 2nd case, the two uncertain multiplicative factors ϵ_1 and ϵ_2 are perturbed to -0.10 and 0.15 respectively. The simulation results from the gain scheduled Luenberger

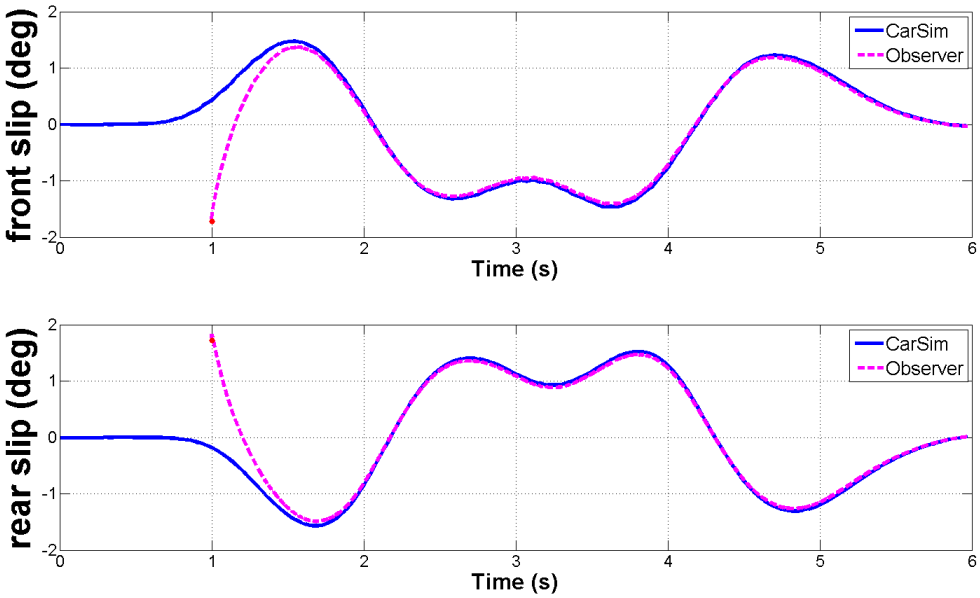

Figure 3.10: The simulation results of the optimal H_2 LPV Luenberger observer with $\epsilon_1 = -0.04$, $\epsilon_2 = 0.06$.

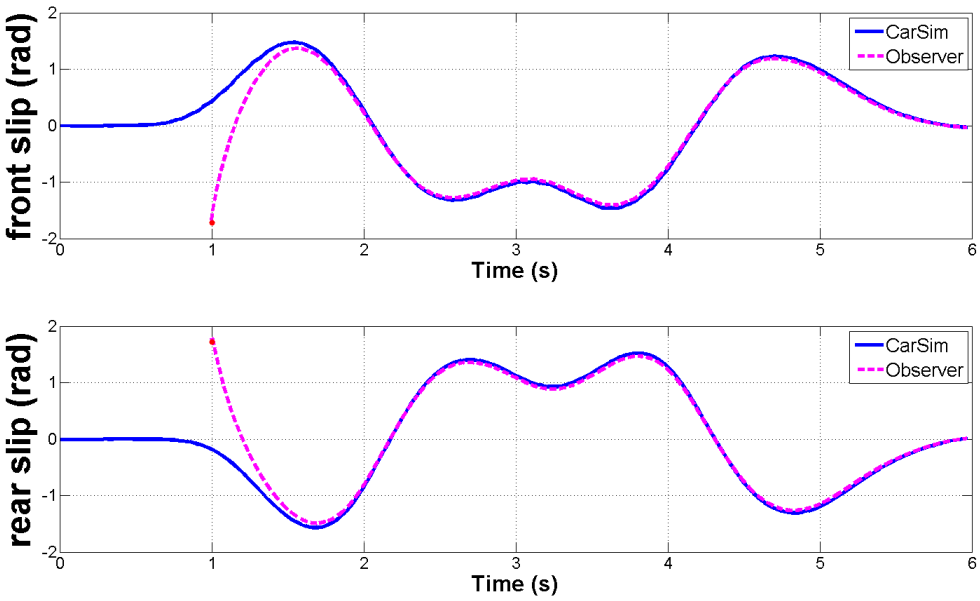

Figure 3.11: The simulation results of the optimal H_∞ LPV Luenberger observer with $\epsilon_1 = -0.04$, $\epsilon_2 = 0.06$.

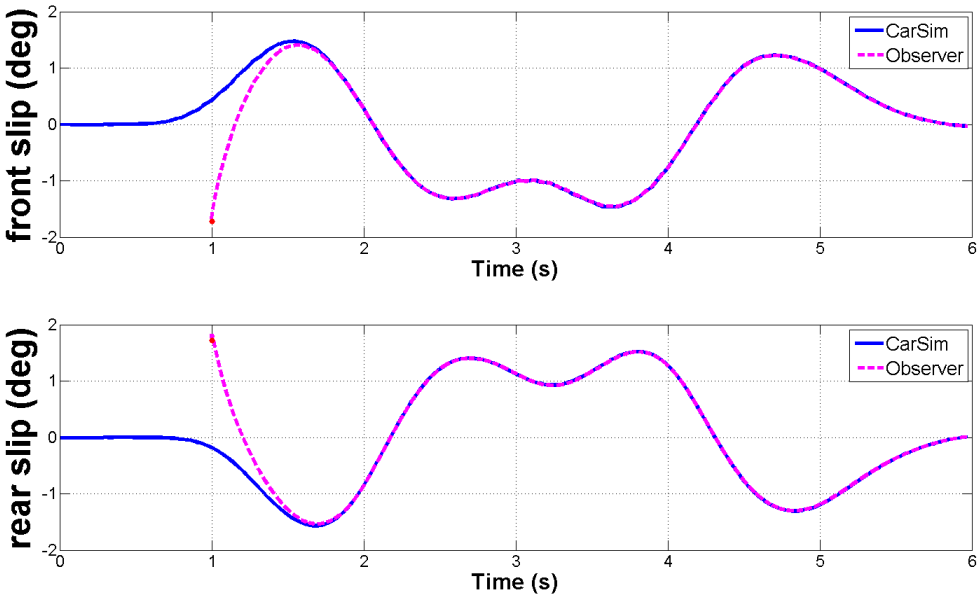

Figure 3.12: The simulation results of the optimal H_2 LPV unstructured observer with $\epsilon_1 = -0.04$, $\epsilon_2 = 0.06$.

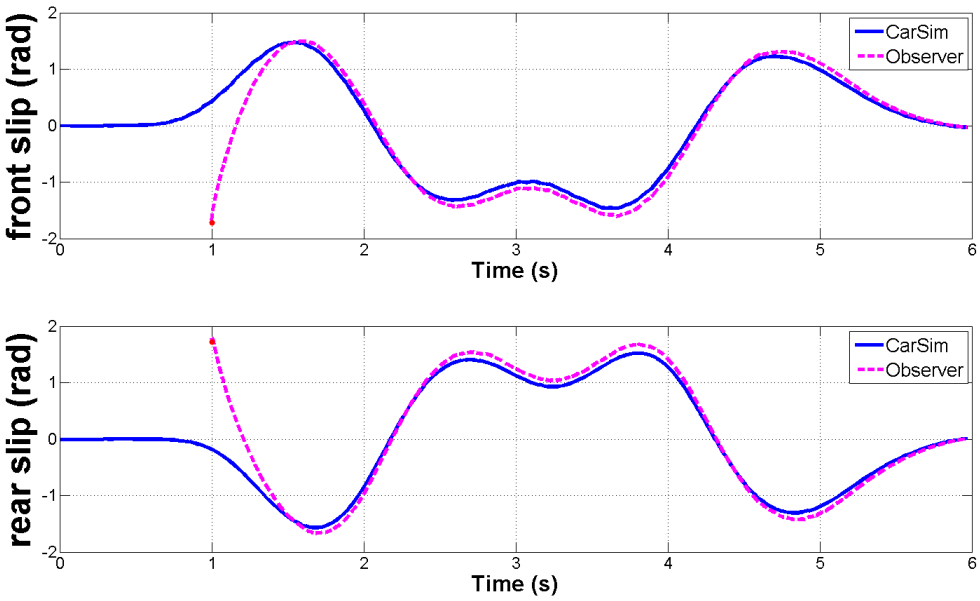

Figure 3.13: The simulation results of the optimal H_∞ LPV unstructured observer with $\epsilon_1 = -0.04$, $\epsilon_2 = 0.06$.

observer with optimal H_2 and H_∞ gain parameters can be seen in Fig. 3.14 and 3.15 below. While those from the unstructured LPV observer are shown in Fig. 3.16 and 3.17 below.

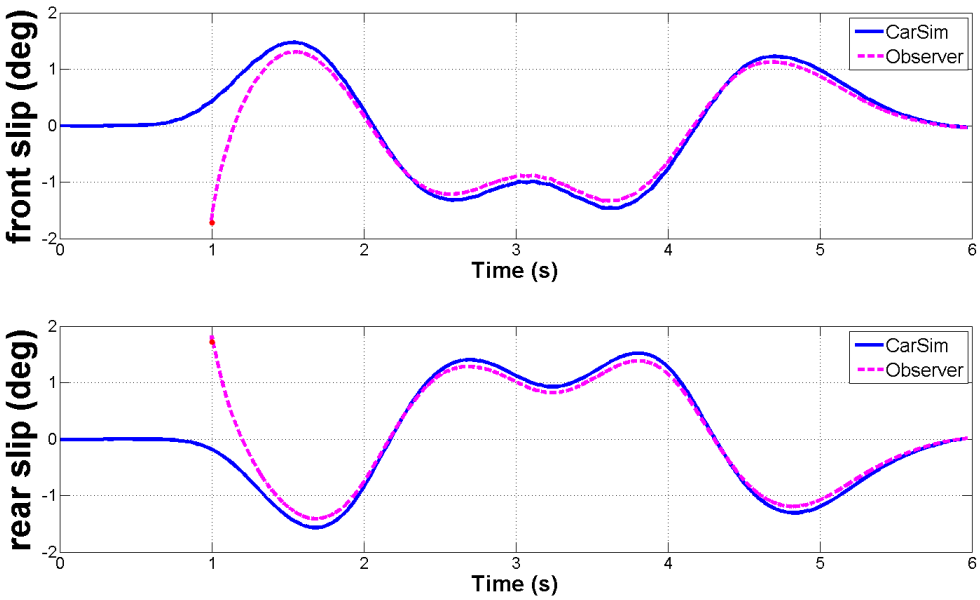

Figure 3.14: The simulation results of the optimal H_2 LPV Luenberger observer with $\epsilon_1 = -0.10$, $\epsilon_2 = 0.15$.

The simulation results show that the estimated tire slip angles from the LPV observer converge quickly to those from the more complex CarSim model. However, the estimation error become biased when the artificial measurement error is added in the longitudinal velocity and acceleration. Furthermore, the H_2/H_∞ optimized Luenberger observer show better estimation results than the unstructured observers, when the uncertain multiplicative factors ϵ_1 and ϵ_2 are constrained in an interval closed to zero. On the other hand, the unstructured observers result in a smaller estimation error, in case that the factors ϵ_1 and ϵ_2 are perturbed to their extreme values. Unsurprisingly, the state space model of the unstructured observer is not restricted by the nominal model of the system. The semidefinite programming problems in Eq. 3.52 and 3.53 emphasize on optimizing the H_2 and H_∞ norms in the worst case. Hence, the performance in nominal case has be be sacrificed.

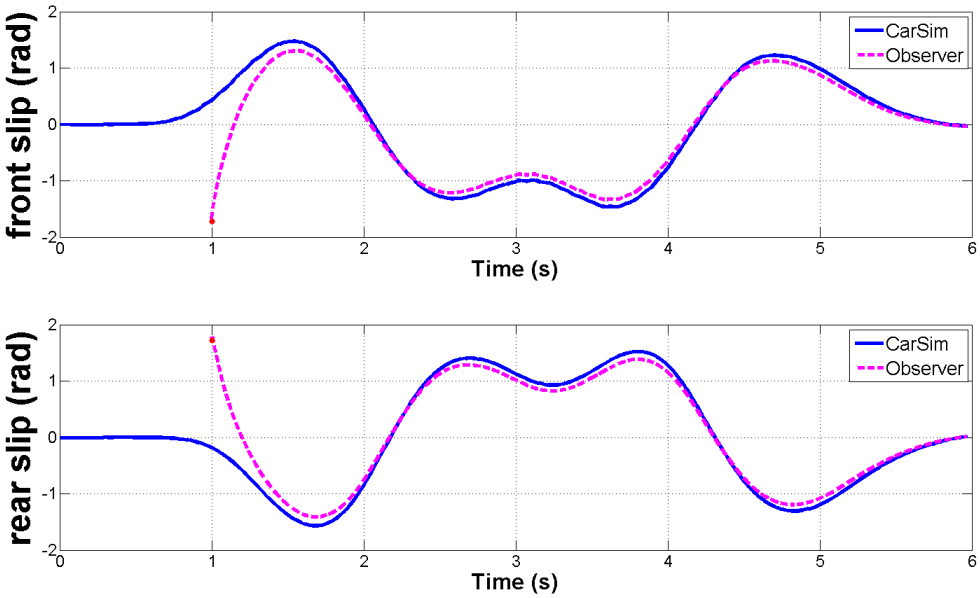

Figure 3.15: The simulation results of the optimal H_∞ LPV Luenberger observer with $\epsilon_1 = -0.10$, $\epsilon_2 = 0.15$.

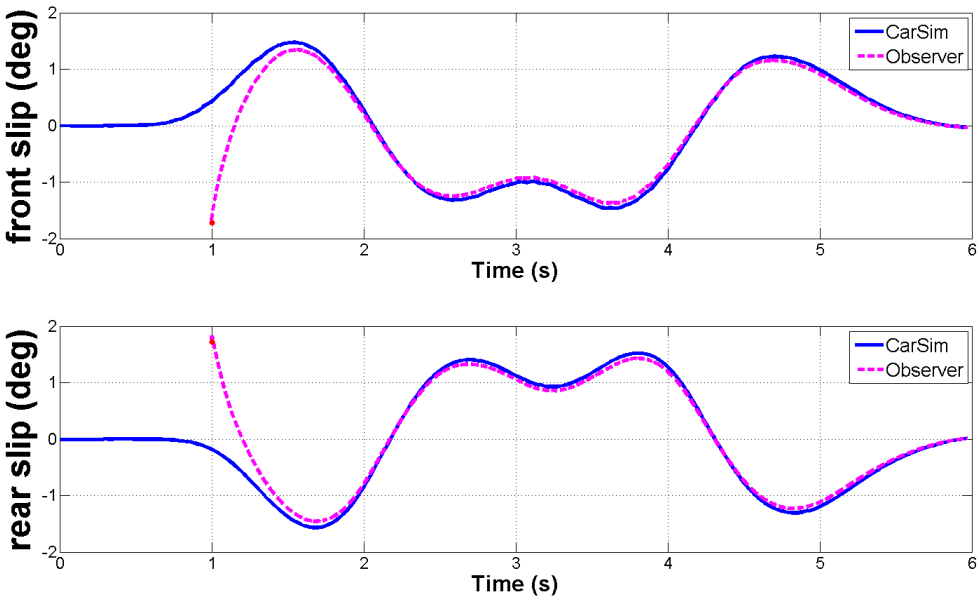

Figure 3.16: The simulation results of the optimal H_2 LPV unstructured observer with $\epsilon_1 = -0.10$, $\epsilon_2 = 0.15$.

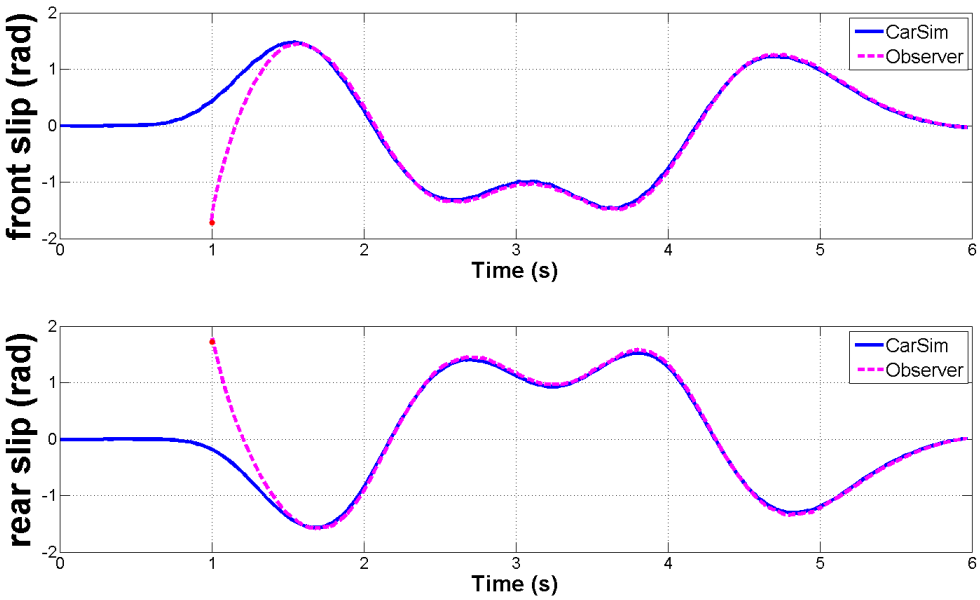

Figure 3.17: The simulation results of the optimal H_∞ LPV unstructured observer with $\epsilon_1 = -0.10$, $\epsilon_2 = 0.15$.

3.4 Conclusions

The linear parameter varying (LPV) modeling and observer design methodology for the three DOF bicycle model were presented in this chapter. Both gain-scheduled Luenberger observer and unstructured observer approaches were discussed and compared. The search of convergent parameters resorts to LMIs based optimization problems. Besides the asymptotic convergence, the robust design technique that aims at increasing the estimation accuracy in the presence of measurement error of the scheduling parameters was also discussed. Both structured and unstructured observer design methodologies were presented. Although the unstructured observer can achieve a more optimal value for the cost function than the Luenberger observer, the lack of physical interpretations makes this design methodology very difficult to debug and impractical in real-world applications.

Chapter 4

LPV Interval Observer Design with Uncertain cornering Stiffness

4.1 Introduction

In the last chapter, the gain-scheduled observer design methodology for the three DOF bicycle model is discussed. Although the time-varying longitudinal velocity and acceleration have been treated as scheduling parameters for updating the observer gains, the uncertain tire cornering stiffness parameters still remain as a severe handicap in developing a high performance observer. However, the accurate estimation of state variables is a fundamental requirement in many safety critical systems, such as in autonomous driving, automotive active safety systems and fault tolerant flight control systems. These challenging applications necessitate a robust observer design methodology that explicitly takes the model uncertainty into consideration.

The sliding mode observer is one such an approach that treats model uncertainty as a disturbance signal preventing the observer error from converging to a pre-defined stable sliding surface. Then, non-smooth functions with large amplitude are used to dominate the uncertainties [30] [27]. However, practical constraints in real-time embedded systems, such as slow sampling rate, degrade the effect of the non-smooth functions which will result in an undesirable chattering phenomenon. Another popular method is to apply classical robust control theory to observer design, such as robust H_∞ observer which aims at attenuating the $L2$ gain from the disturbance input to the observer error [35] [55]. On the other hand, a parameter adaptation algorithm can be developed to cope with the parameter uncertainty [33] [66] in the adaptive observer. However, this technique suffers an important disadvantage that many real-world application systems cannot satisfy the strict assumptions required for a successful solution to exist for the observer design problem.

The interval observer has become a popular observer design method in the presence of input uncertainty in the control community during the last decade [37]. Unlike the Kalman filter, which treats the external disturbance as a stochastic signal with known statistical property [13], the interval observer ignores any probability distribution of the unmeasured disturbance input signals but assumes that they are always constrained in a known time-invariant or time-varying interval. Instead of a single estimation curve for each state variable, the interval observer computes the lower and upper bounds of all the admissible values of the states in the presence of bounded input uncertainty. For safety critical systems, this envelope provides an estimation of the worst case values. In existing literature, there are two ways to achieve such an interval estimation. The first one is the so-called set membership approach. In this method, the disturbance input vector is assumed to be constrained in a convex set. The optimization algorithm together with the model of the system and available measurement data, is used to compute another convex outer approximation, such as an ellipsoid [26] [43] or zonotopes [60] [61], to cover all the admissible state vectors.

Another technique for interval observer design is the cooperative observer error approach, which requires that the observer error state matrix is not only a Hurwitz matrix but also a Metzler matrix (i.e. all its off-diagonal elements are nonnegative for continuous-time case). This property preserves the order of the state variables at any instant of time the same with their initial conditions [42] [47] [44]. However, searching for a qualified observer gain is not a trivial task. Hence, the existing methods to obtain an interval observer gain in an analytical way become unsuitable for more complex high order systems and are difficult to be generalized to parameter varying systems [51]. To overcome this difficulty, some methods that release the cooperative constraint for the observer error through a coordinate transformation have been proposed [28] [62]. In spite of the elegant theoretical proof, these coordinate transformation methods only consider the uncertainty in the input channel rather than the model uncertainty, which puts a question mark on the applicability to systems with large variational parameters.

In this chapter, a systematic interval observer design method for both linear-time-invariant (LTI) and linear-parameter-varying (LPV) systems with parametric uncertainty by using the cooperative observer error approach will be presented. It will be shown that the uncertain parameters can be treated as a disturbance signal for the observer error. Unlike previous the methods discussed above, the well-developed semidefinite programming (SDP) approach [58] [54] is proposed to search for the qualified observer gains, which result in a robustly stable and cooperative observer error dynamical system. Then, the proposed design methodology will be applied to the development of the interval observer for a vehicle state estimation problem with the cornering stiffness values as the uncertain parameters with known variation ranges.

The remainder of this chapter is organized as follows. First, some background knowledge is reviewed in Section 4.2. Next, the design of the interval observer for LTI systems with parametric uncertainty is presented in Section 4.3. Then, this approach is extended to the gain-scheduled interval observer development for the LPV systems in Section 4.4. Finally, this design methodology is applied to a vehicle state estimation problem in Section 4.5. Section 4.6 contains the final conclusions for this chapter.

4.2 Notation and Background

This section presents some theoretical background related to the interval observer design from the literature. The symbol R represents the set of real numbers. $R^{m\times n}$ denotes the set of $m \times n$ matrices whose elements all belong to R. For matrices $X, Y \in R^{m\times n}$, $X \geq Y$ or $Y \leq X$ indicates that each element in X is no smaller than its counterpart in Y. For symmetric matrices $A, B \in R^{n\times n}$, $A \succ B$ or $B \prec A$ means that $A - B$ is a positive definite matrix.

4.2.1 Metzler Matrix

A matrix $A \in R^{n\times n}$ is called a Metzler matrix or a cooperative matrix if all its off-diagonal elements are nonnegative [37] [68].

4.2.2 Positive Linear Systems

Suppose a matrix $A \in R^{n\times n}$ is Hurwitz and Metzler. The solutions to a pair of linear systems

$$\begin{aligned} \dot{x}^+ &= Ax^+ + w^+ \\ \dot{x}^- &= Ax^- + w^- \end{aligned} \tag{4.1}$$

always satisfy the inequality $0 \leq x^-(t) \leq x^+(t)$, $\forall\, t \geq 0$ if the following conditions are satisfied [68]:

$$0 \leq x^-(0) \leq x^+(0) \;\; and \;\; 0 \leq w^-(t) \leq w^+(t), \;\; \forall\, t \geq 0 \tag{4.2}$$

4.2.3 Interval Observer for A LTI System with Uncertain Input

The interval observer is an application of the positive linear system theory to observer design for disturbance affected or uncertain linear systems. Consider the following state space model,

$$\dot{x} = Ax + Bu + w, \quad y = Cx \tag{4.3}$$

where w is the unmeasured disturbance input that satisfies the element-wise interval condition $w^- \leq w \leq w^+$, $\forall\, t \geq 0$. The interval observer constitutes a pair of subsystems shown below [37]

$$\begin{aligned} \dot{x}^+ &= Ax^+ + Bu + L(y - Cx^+) + w^+ \\ \dot{x}^- &= Ax^- + Bu + L(y - Cx^-) + w^- \end{aligned} \tag{4.4}$$

where the observer gain L is tuned to guarantee that $A - LC$ is a Hurwitz and Metzler matrix. Then, $x^-(t)$ and $x^+(t)$ are the lower and upper bounds of the state x as shown in

Eq. (4.5) if the initial condition satisfies $x^-(0) \leq x(0) \leq x^+(0)$.

$$x^-(t) \leq x(t) \leq x^+(t) \quad \forall\, t \geq 0 \tag{4.5}$$

4.2.4 Lyapunov Stability for The Positive Linear Systems

Similar to other linear systems, the stability analysis of the positive linear systems can resort to searching for a candidate Lyapunov function.

Theorem 2 *[68] The positive linear system in Eq. (4.1) is asymptotically stable if and only if there exists a diagonal matrix $P = diag(p_{11}, \ldots, p_{nn})$, such that*

$$P \succ 0 \quad and \quad A^T P + PA \prec 0 \tag{4.6}$$

As will be shown later, restricting the Lyapunov matrix P to a diagonal form will significantly facilitate the design of the interval observer.

4.3 Interval Observer Design for LTI Systems with Parametric Uncertainty

Observer design for the uncertain LTI system is a very challenging task that control engineers face. As discussed in Section 4.2, the system must satisfy very strict conditions to create an observer that is robust to the model uncertainty. If it is impossible to observe the state trajectory accurately, it would be particularly useful to estimate an envelope that covers all the possible state trajectories from the admissible uncertain dynamical systems. In the application of process monitoring, this estimated interval indicates the worst case range of the states. In the next section, it is shown that the parametric uncertainty is equivalent to an input uncertainty as shown in Eq. (4.4) for the observer error dynamics.

4.3.1 LTI Interval Observer Design

Consider the following linear system,

$$\dot{x} = A(\xi)x + B(\xi)u, \quad y = Cx \tag{4.7}$$

where $x \in R^n$, $y \in R^m$, $A \in R^{n\times n}$, $B \in R^{n\times l}$, $C \in R^{m\times n}$ and (A, C) is observable. $\xi = [\xi_1, \ldots, \xi_s]^T$ denotes the collections of time-invariant and time-varying uncertain parameters. They are assumed to be in a polytopic set Ξ with $\xi^{(j)}$, $j = 1, \ldots, h$ as the vertices.

Unlike the traditional Luenberger Observer design method, which only requires the observer error to be asymptotically stable, the state matrix $A - LC$ for the observer error should also be a Metzler matrix in the interval observer such that $\hat{x}^-(t)$ and $\hat{x}^+(t)$ will not cross the true state $x(t)$ even in the transient response. Next, the search for a qualified interval observer gain through a LMI approach will be presented.

Lemma 11 *Suppose $P \in R^{n\times n}$ is a diagonal positive definite matrix. The matrix $R \in R^{n\times n}$ is a Metzler matrix if and only if PR is a Metzler matrix.*

Proof: Since both P and P^{-1} are diagonal positive definite matrices, the sign of each element in the matrix PR is always the same with that in the matrix R. Therefore, if either PR or R is a Metzler matrix, the both are Metzler matrices.

The design of the interval observer for the parametric uncertain LTI system is summarized in Theorem 3.

Theorem 3 *For the parametric uncertain linear system in Eq. (4.7), the interval observer is composed of two subsystems shown below.*

$$\begin{aligned} \dot{\hat{x}}^+ &= A(\xi_0)\hat{x}^+ + B(\xi_0)u + L(y - C\hat{x}^+) + w^+(\hat{x}^+, \xi, u) \\ \dot{\hat{x}}^- &= A(\xi_0)\hat{x}^- + B(\xi_0)u + L(y - C\hat{x}^-) + w^-(\hat{x}^-, \xi, u) \end{aligned} \tag{4.8}$$

where $L \in R^{n\times m}$ is the observer gain. ξ_0 is the nominal value of the uncertain parameter ξ, $\xi \in \Xi$. $w^+(\hat{x}^+, \xi, u)$ and $w^-(\hat{x}^-, \xi, u)$ denote the following upper and lower limit functions in the domain of operation.

$$\begin{aligned} w^+(\hat{x}^+, \xi, u) &\geq [A(\xi) - A(\xi_0)]\hat{x}^+ + [B(\xi) - B(\xi_0)]u \\ w^-(\hat{x}^-, \xi, u) &\leq [A(\xi) - A(\xi_0)]\hat{x}^- + [B(\xi) - B(\xi_0)]u \end{aligned} \tag{4.9}$$

Suppose there exist two matrices P and Q that satisfy the three conditions listed below.

1. *$P \in R^{n\times n}$ is a diagonal positive definite matrix;*

2. *The LMI condition shown in Eq. (4.10) is feasible.*

$$A^T(\xi)P + PA(\xi) - (C^TQ^T + QC) \prec 0, \ \ \forall\, \xi \in \Xi \tag{4.10}$$

   where $Q \in R^{n\times m}$;

3. *$PA(\xi) - QC$ is a Metzler matrix $\forall\, \xi \in \Xi$;*

Then, if the observer gains L are obtained as $L = P^{-1}Q$, Eq. (4.8) constitutes an interval observer for system in Eq. (4.7).

Proof: The observer error for $\hat{x}^+$ can be derived as

$$\begin{aligned} &\dot{\hat{x}}^+ - \dot{x} \\ &= [A(\xi_0) - A(\xi)]\hat{x}^+ + A(\xi)(\hat{x}^+ - x) - LC(\hat{x}^+ - x) \\ &\quad + w^+(\hat{x}^+, \xi, u) - [B(\xi) - B(\xi_0)]u \\ &= [A(\xi) - LC](\hat{x}^+ - x) + w^+(\hat{x}^+, \xi, u) \\ &\quad - [A(\xi) - A(\xi_0)]\hat{x}^+ - [B(\xi) - B(\xi_0)]u \end{aligned} \tag{4.11}$$

Substituting PL for Q in the LMI in Eq. (4.10), it is easy to see that the feasibility of this LMI guarantees that $A(\xi) - LC$ is a Hurwitz matrix. While, Lemma 11 implies that $A(\xi) - LC$ is a Metzler matrix if and only if $PA(\xi) - QC$ is a Metzler matrix $\forall\, \xi \in \Xi$.

Besides a copy of the nominal model and a linear correction term as in the Luenberger Observer, an additional signal $w^+(\hat{x}^+, \xi, u)$ is introduced to subdue $[A(\xi)-A(\xi_0)]\hat{x}^+ + [B(\xi)-B(\xi_0)]u$. This term can be regarded as the unmeasured disturbance input resulting from the mismatch between the nominal model and true process for the observer error, in the interval observer. Therefore, the observer error $\hat{x}^+ - x$ in Eq. (4.11) is indeed a positive linear system which implies that $\hat{x}^+$ constitutes the upper limit for the real state x.

Similarly, the positivity for the observer error $x - \hat{x}^-$ can be proven, which is omitted for brevity. In summary, $\hat{x}+^(t)$ and $\hat{x}^-(t)$ constitute the interval estimation for $x(t)$, if the initial condition satisfies $\hat{x}^-(0) \leq x(0) \leq \hat{x}^+(0)$.

$$\hat{x}^-(t) \leq x(t) \leq \hat{x}^+(t), \quad \forall\, t \geq 0 \tag{4.12}$$

$w^+(\hat{x}^+, \xi, u)$ and $w^-(\hat{x}^-, \xi, u)$ are indeed the worst-case input uncertainty resulting from the uncertain parameters. To realize the interval observer in Eq. (4.8), it is necessary to estimate the element-wise upper and lower bounds of the deviation matrices $[A(\xi) - A(\xi_0)]\hat{x}^+ + [B(\xi) - B(\xi_0)]u$ and $[A(\xi) - A(\xi_0)]\hat{x}^- + [B(\xi) - B(\xi_0)]u$. If the matrices $A(\xi)$ and $B(\xi)$ are nonlinear matrix functions of ξ, this problem can be solved by a constrained numerical optimization algorithm. However, if both matrices depend on ξ affinely, the following result in Lemma 12 can be applied to estimate $w^+(\hat{x}^+, \xi, u)$ and $w^-(\hat{x}^-, \xi, u)$ analytically.

Lemma 12 *[28] Given a matrix $T \in R^{m\times n}$, define $T^+ = \max\{0, T\}$, $T^- = T^+ - T$, with $\max\{\cdot,\cdot\}$ being an element-wise maximum operator. Let $v \in R^n$ be a vector variable, $v^- \leq v \leq v^+$ for some $v^-, v^+ \in R^n$, then*

$$T^+v^- - T^-v^+ \leq Tv \leq T^+v^+ - T^-v^- \tag{4.13}$$

For the affine parameter dependent matrices $A(\xi)$, $B(\xi)$ shown in Eq. (4.14),

$$\begin{aligned} A(\xi) &= A_0 + \xi_1 A_1 + \cdots + \xi_s A_s \\ B(\xi) &= B_0 + \xi_1 B_1 + \cdots + \xi_s B_s \end{aligned} \tag{4.14}$$

$[A(\xi) - A(\xi_0)]\hat{x}^+ + [B(\xi) - B(\xi_0)]u$ can be written in the following linear transformation form.

$$\begin{aligned} &[A(\xi) - A(\xi_0)]\hat{x}^+ + [B(\xi) - B(\xi_0)]u \\ &= \underbrace{\begin{pmatrix} A_1\hat{x}^+ + B_1 u & \ldots & A_s\hat{x}^+ + B_s u \end{pmatrix}}_{T_1} \underbrace{\begin{pmatrix} \xi - \xi_0 \end{pmatrix}}_{v} \end{aligned} \tag{4.15}$$

Similarly, $[A(\xi) - A(\xi_0)]\hat{x}^- + [B(\xi) - B(\xi_0)]u$ is shown as

$$\begin{aligned} &[A(\xi) - A(\xi_0)]\hat{x}^- + [B(\xi) - B(\xi_0)]u \\ &= \underbrace{\begin{pmatrix} A_1\hat{x}^- + B_1 u & \ldots & A_s\hat{x}^- + B_s u \end{pmatrix}}_{T_2} \underbrace{\begin{pmatrix} \xi - \xi_0 \end{pmatrix}}_{v} \end{aligned} \tag{4.16}$$

According to Lemma 12, $w^+(\hat{x}^+, \xi, u)$ and $w^-(\hat{x}^-, \xi, u)$ can be calculated as

$$\begin{aligned} w^+(\hat{x}^+, \xi, u) &= T_1^+ v^+ - T_1^- v^- \\ w^-(\hat{x}^-, \xi, u) &= T_2^+ v^- - T_2^- v^+ \end{aligned} \tag{4.17}$$

where the matrices T_1, T_2 and v are defined in Eq. (4.15) and (4.16). Note that T_1^+, T_1^-, T_2^+ and T_1^- are time varying matrices dependent on the state estimate $\hat{x}^+$, $\hat{x}^-$ and input u, while v^+ and v^- are bounds on the parameters.

Another challenging task is to search for the observer gain L that results in a robustly stable and cooperative observer error dynamics. As can be seen in Eq. (4.10), the robust stabilization of the observer error is an infinite dimensional LMI problem. However, the affine dependence of the state space matrices on ξ make it only necessary to guarantee the semidefinite condition on all the vertices of the polytopic parameter space Ξ [35] [54] [11].

In what follows, it will be proven that this guarantee is also true for the third condition that requires the state matrix of the observer error is a Metzler matrix $\forall\, \xi \in \Xi$.

Lemma 13 *Suppose the matrix $A(\xi) \in R^{n\times n}$ is an affine matrix function of $\xi \in R^{s\times 1}$ shown in Eq. (4.14). The uncertain parameter vector ξ is always contained in a polytope Ξ with vertices $\xi^{(j)}, j = 1, \ldots, h$. Then, $A(\xi)$ is a Metzler matrix $\forall\, \xi \in \Xi$ if and only if $A(\xi^{(j)}), \forall\, j = 1, \ldots, h$ is a Metzler matrix.*

Proof: If: The affine dependence of $A(\xi)$ on ξ implies that $A(\xi)$ can be constructed as the convex combination of $A(\xi^{(j)}), \forall\, j = 1, \ldots, h$.

$$A(\xi) = \sum_{j=1}^{h} \theta_j A(\xi^{(j)}) \tag{4.18}$$

where $\theta_1 + \cdots + \theta_h = 1$, $0 \leq \theta_j \leq 1$. The non negativity of θ_j guarantees that the non negativity of all the off-diagonal elements of $A(\xi^j)$ are preserved on those of $A(\xi)$.

Only if: The necessity is quite straightforward. Suppose some $A(\xi^{(j)})$ violates the condition of a Metzler matrix. Then, $A(\xi)$ cannot be a Metzler matrix $\forall\, \xi \in \Xi$, which leads to a contradiction.

4.4 Interval Observer Design for LPV Systems

In many real-world applications, the dynamical model of the process contains some time-varying uncertain parameters that can be measured online, such as the vehicle speed in automotive active safety systems. Hence, the controller and observer gains can be updated accordingly to achieve robust stability and performance. This is the so-called gain-scheduling design technique. The linear-parameter-varying (LPV) modeling and design methodology is widely accepted as a robust way to develop a gain-scheduled controller and observer [53] [46]. In this section, the interval observer design developed for uncertain LTI systems will be extended to LPV systems which contain both measured and unmeasured uncertain parameters.

4.4.1 Gain-Scheduled Interval Observer

Consider the following LPV plant,

$$\dot{x} = A(\eta, \xi)x + B(\eta, \xi)u, \quad y = Cx \tag{4.19}$$

where ξ is the same unmeasured uncertain parameter vector as the LTI case, which is assumed to be in a polytope Ξ. $\eta = [\eta_1, \ldots, \eta_r]^T$ denotes the collections of measured time-varying parameters, which is constrained in a polytope E with $\eta^{(i)}, i = 1, \ldots, g$ as the vertices.

The design of gain-scheduled interval observer is summarized in Theorem 4.

Theorem 4 *For the parametric uncertain LPV system in Eq. (4.19), where both $A(\eta, \xi)$ and $B(\eta, \xi)$ depend on η affinely, the gain-scheduled interval observer is composed of two subsystems shown below*

$$\begin{aligned}
\dot{\hat{x}}^+ &= A(\eta, \xi_0)\hat{x}^+ + B(\eta, \xi_0)u + w^+(\hat{x}^+, \eta, \xi, u) \\
&\quad + L(\eta)(y - C\hat{x}^+) \\
\dot{\hat{x}}^- &= A(\eta, \xi_0)\hat{x}^- + B(\eta, \xi_0)u + w^-(\hat{x}^-, \eta, \xi, u) \\
&\quad + L(\eta)(y - C\hat{x}^-)
\end{aligned} \tag{4.20}$$

where ξ_0 is the nominal value of the uncertain parameter ξ, $\xi \in \Xi$. $w^+(\hat{x}^+, \eta, \xi, u)$ and $w^-(\hat{x}^-, \eta, \xi, u)$ denote the following upper and lower limit functions in the domain of operation.

$$\begin{aligned}
& w^+(\hat{x}^+, \eta, \xi, u) \\
& \geq [A(\eta, \xi) - A(\eta, \xi_0)]\hat{x}^+ + [B(\eta, \xi) - B(\eta, \xi_0)]u \\
& w^-(\hat{x}^-, \eta, \xi, u) \\
& \leq [A(\eta, \xi) - A(\eta, \xi_0)]\hat{x}^- + [B(\eta, \xi) - B(\eta, \xi_0)]u
\end{aligned} \tag{4.21}$$

The η-scheduled observer gain $L(\eta)$ has an affine form shown below

$$L(\eta) = L_0 + \eta_1 L_1 + \cdots + \eta_r L_r \tag{4.22}$$

where $L_i \in R^{n\times m}$, $i = 0, 1, \ldots, r$. Suppose there exist matrices P and $Q_0, \ldots, Q_r$ that satisfy the three conditions listed below.

1. *$P \in R^{n\times n}$ is a diagonal positive definite matrix;*

2. *The LMI conditions shown in Eq. (4.23) are feasible $\forall\, \eta \in E$, $\forall\, \xi \in \Xi$;*

$$A^T(\eta,\xi)P + PA(\eta,\xi) - [C^T Q^T(\eta) + Q(\eta)C] \prec 0 \tag{4.23}$$

   $Q(\eta)$ is an affine matrix function of η.

$$Q(\eta) = Q_1 + \eta_1 Q_1 + \cdots + \eta_r Q_r \tag{4.24}$$

   where $Q_i \in R^{n\times m}$, $i = 0, 1, \ldots, r$.

3. *$PA(\eta,\xi) - Q(\eta)C$ is a Metzler matrix $\forall\, \eta \in E$, $\forall\, \xi \in \Xi$;*

Then, the observer gains L_i, $i = 0, 1, \ldots, r$ can be obtained as

$$L_i = P^{-1} Q_i \tag{4.25}$$

so as to ensure that Eq. (4.20) constitutes a gain scheduled interval observer for systems in Eq. (4.19).

Proof: The state equation for the observer error $e = \hat{x}^+ - x$ is shown as

$$\begin{aligned}
&\dot{\hat{x}}^+ - \dot{x} \\
&= [A(\eta,\xi_0) - A(\eta,\xi)]\hat{x}^+ + A(\eta,\xi)(\hat{x}^+ - x) \\
&\quad -L(\eta)C(\hat{x}^+ - x) + w^+(\hat{x}^+,\eta,\xi,u) \\
&\quad -[B(\eta,\xi) - B(\eta,\xi_0)]u \\
&= [A(\eta,\xi) - L(\eta,)C](\hat{x}^+ - x) + w^+(\hat{x}^+,\eta,\xi,u) \\
&\quad -[A(\eta,\xi) - A(\eta,\xi_0)]\hat{x}^+ - [B(\eta,\xi) - B(\eta,\xi_0)]u
\end{aligned} \tag{4.26}$$

Substituting $PL(\eta)$ for $Q(\eta)$ in the LMI in Eq. (4.23), it is easy to see that the feasibility of this LMI guarantees the robust asymptotic convergence of the observer error state matrix $A(\eta,\xi) - L(\eta)C$. While Lemma 11 proves that $A(\eta,\xi) - L(\eta)C$ is a Metzler matrix if and only if $PA(\eta,\xi) - Q(\eta)C$ is a Metzler matrix $\forall\, \eta \in E$, $\forall\, \xi \in \Xi$. Moreover, the observer error state equation in Eq. (4.26) shows that $w^+(\hat{x}^+,\eta,\xi,u) - [A(\eta,\xi) - A(\eta,\xi_0)]\hat{x}^+ - [B(\eta,\xi) - B(\eta,\xi_0)]u$ acts as a positive input signal for the observer error according to the definition of $w^+(\hat{x}^+,\eta,\xi,u)$ in Eq. (4.21). Therefore, the observer error $\hat{x} - x$ in Eq. (4.26) is a positive time-varying linear system, which implies that $\hat{x}^+$ is an upper limit for the true state x. Similarly, the positivity of the observer error $x - \hat{x}^-$ can be proven, which is omitted for brevity.

The interval estimation result of a linear mapping stated in Lemma 12 can be used to derive the upper and lower limit functions $w^+(\hat{x}^+,\eta,\xi,u)$, $w^-(\hat{x}^-,\eta,\xi,u)$ as shown in Eq. (4.15) and (4.16), if $A(\eta,\xi)$ and $B(\eta,\xi)$ are affine matrix functions of ξ.

From Theorem 4, it can be seen that ensuring that $PA(\eta,\xi) - Q(\eta)C$ is a Metzler matrix and ensuring that the LMI in Eq. (4.23) is satisfied are more challenging than the LTI case due to the presence of two sets of parameters η and ξ in the LMI condition and cooperative constraint for the observer error. Fortunately, there still exists a finite dimensional relaxation for this infinite dimensional problem, which is presented in Lemma 14.

Lemma 14 *Suppose the matrix $A(\eta,\xi) \in R^{n\times n}$ is a bilinear matrix function of $\eta \in R^{r\times 1}$ and $\xi \in R^{s\times 1}$, which are assumed to be contained in the polytopes E and Ξ with $\eta^{(i)}, i = 1,\ldots,g$ and $\xi^{(j)}, j = 1,\ldots,h$ as the vertices for each one. Then, $A(\eta,\xi)$ is a Hurwitz and Metzler matrix $\forall\, \eta \in E$, $\forall\, \xi \in \Xi$ if and only if there exists a matrix P satisfying the three conditions listed below.*

1. *$P \in R^{n\times n}$ is a diagonal positive definite matrix;*

2. *The following LMI condition is feasible $\forall\, i = 1,\ldots,g,\ \forall\, j = 1,\ldots,h$;*

$$P \succ 0, \quad A^T(\eta^{(i)},\xi^{(j)})P + PA(\eta^{(i)},\xi^{(j)}) \prec 0 \tag{4.27}$$

3. $A(\eta^{(i)}, \xi^{(j)})$ is a Metzler matrix $\forall\, i = 1, \ldots, g,\ \forall\, j = 1, \ldots, h$;

Proof: If: $A(\eta, \xi)$ depends on η and ξ bilinearly implies that it can be written in the following convex combination form [54]

$$\begin{aligned} A(\eta, \xi) &= \lambda_1 A(\eta^{(1)}, \xi) + \cdots + \lambda_g A(\eta^{(g)}, \xi) \\ &= \sum_{i=1}^{g} \lambda_i A(\eta^{(i)}, \xi) \end{aligned} \tag{4.28}$$

where $\lambda_i \geq 0$, and $\lambda_1 + \cdots + \lambda_g = 1$. Next, $A(\eta^{(i)}, \xi)$ has a similar convex combination form

$$\begin{aligned} A(\eta^{(i)}, \xi) &= \theta_{i,1} A(\eta^{(i)}, \xi^{(1)}) + \cdots + \theta_h A(\eta^{(i)}, \xi^{(h)}) \\ &= \sum_{j=1}^{h} \theta_{i,j} A(\eta^{(i)}, \xi^{(j)}) \end{aligned} \tag{4.29}$$

where $\theta_{i,j} \geq 0$, and $\theta_{i,1} + \cdots + \theta_{i,h} = 1$. Substituting the result in Eq. (4.29) for $A(\eta^{(i)}, \xi)$ in Eq. (4.28), $A(\eta, \xi)$ can be written as the following form.

$$A(\eta, \xi) = \sum_{i=1}^{g} \sum_{j=1}^{h} \lambda_i \theta_{i,j} A(\eta^{(i)}, \xi^{(j)}) \tag{4.30}$$

Then, the middle matrix in the quadratic form of the derivative of the Lyapunov function $V = x^T P x$ becomes

$$\begin{aligned} &A^T(\eta, \xi) P + P A(\eta, \xi) \\ &= \sum_{i=1}^{g} \sum_{j=1}^{h} \lambda_i \theta_{i,j} [A^T(\eta^{(i)}, \xi^{(j)}) P + P A(\eta^{(i)}, \xi^{(j)})] \end{aligned} \tag{4.31}$$

The non negativity of λ_i and $\theta_{i,j}$ guarantees that $A^T(\eta, \xi) P + P A(\eta, \xi) \prec 0$, $\forall\, \eta \in E$, $\forall\, \xi \in \Xi$ if the LMIs $P \succ 0$ and $A^T(\eta^{(i)}, \xi^{(j)}) P + P A(\eta^{(i)}, \xi^{(j)}) \prec 0$ are feasible $\forall\, i = 1, \ldots, g,\ \forall\, j = 1, \ldots, h$.

Only if: The necessity is quite straightforward. Suppose some $A(\eta^{(i)}, \xi^{(j)})$ violates the LMIs condition in Eq. (4.27) or it is not a Metzler matrix. Then, $A(\eta, \xi)$ cannot be a Metzler matrix $\forall\, \eta \in E$, $\forall\, \xi \in \Xi$, which leads to a contradiction.

4.4.2 Gain-Scheduled Interval Observer with L2 Gain Minimization

Besides the asymptotic convergence of the upper and lower bounds of $\hat{x}^+$ and $\hat{x}^-$, the width of the estimation interval $\hat{x}^+ - \hat{x}^-$ is also expected to be as small as possible so that the interval observer is more robust to the model uncertainty. To achieve this goal, the $L2$ gain from the disturbance resulting from model uncertainty to the width of the estimation interval can be minimized.

Theorem 5 *For the gain-scheduled interval observer in Eq. (4.20), the optimal L2 observer design can be formulated as the following semidefinite programming (SDP) problem*

$$\begin{aligned} &\min \ \ \gamma \\ &\textit{subject to} \\ &\qquad P = diag(p_{11}, \ldots, p_{nn}) \succ 0, \\ &\begin{pmatrix} A_L(\eta,\xi)^T P + P A_L(\eta,\xi) & P & I \\ P & -\gamma I & 0 \\ I & 0 & -\gamma I \end{pmatrix} \prec 0, \\ &PA_L(\eta,\xi) \textit{ is a Metzler matrix}, \ \forall\, \eta \in E, \forall\, \xi \in \Xi; \end{aligned} \tag{4.32}$$

where $A_L(\eta, \xi) = A(\eta, \xi) - L(\eta)C$. Then the L2 gain from model uncertainty to estimation width $\hat{x}^+ - \hat{x}^-$ is no larger than γ.

$$\sqrt{\int_0^\infty (\hat{x}^+ - \hat{x}^-)^T (\hat{x}^+ - \hat{x}^-) dt} \leq \gamma \sqrt{\int_0^\infty w^T w dt} \tag{4.33}$$

where w denotes the input from the model uncertainty.

Proof: The dynamic model for the observer error can be simplified as

$$\begin{aligned} \dot{\hat{x}}^+ - \dot{x} &= [A(\eta,\xi) - L(\eta)C](\hat{x}^+ - x) + w^+ \\ \dot{x} - \dot{\hat{x}}^- &= [A(\eta,\xi) - L(\eta)C](x - \hat{x}^-) + w^- \end{aligned} \tag{4.34}$$

where w^+, w^- represent the disturbance resulting from the mismatch between the model and true process. Adding these two state equations together, the estimation interval can be obtained

$$\begin{aligned} \dot{\hat{x}}^+ - \dot{\hat{x}}^- &= [A(\eta,\xi) - L(\eta)C](\hat{x}^+ - \hat{x}^-) + (w^+ + w^-) \\ y &= \hat{x}^+ - \hat{x}^- \end{aligned} \tag{4.35}$$

where the input signal is $w^+ + w^-$ and the output y is equal to the state vector $\hat{x}^+ - \hat{x}^-$. Then, the SDP condition in Eq. (4.32) is just the application of bounded real lemma [58] [54] for the state space model in Eq. (4.35) except that the Lyapunov matrix P is constrained to be a diagonal form for positive linear systems. Moreover, it is also necessary to make $A_L(\eta,\xi)$ a Metzler matrix such that the resulting observer is qualified for interval estimation. Since the positive definite matrix P has a diagonal form, it is equivalent to the cooperative constraint for the matrix $PA_L(\eta,\xi)$.

Remark 1 *To solve the above SDP problem, anther matrix variable $Q(\eta)$ defined in Eq. (4.24) is still needed in order to transform it to a LMI problem. The observer gains can be obtained by applying Eq. (4.25). If $A(\eta,\xi)$ is a bilinear matrix function of η, ξ and $L(\eta)$ depends on η affinely as shown in Eq. (4.22), the infinite dimensional LMI can be relaxed to a finite dimensional one on all the vertices of the polytopes E and Ξ according to Lemma 14.*

4.5 Robust Slip Angle Estimation

In this section, a slip angle estimation problem will be used to illustrate the application of the gain-scheduled interval observer design methodology. The side slip angle is a vital signal that affects the stability of a vehicle under cornering. Unfortunately, no commercial

vehicles are equipped with sensors which can directly measure this signal, which is both due to cost concerns and technical challenges. This motivates the need for an efficient and accurate algorithm for estimating slip angles.

4.5.1 3 DOF Bicycle Model

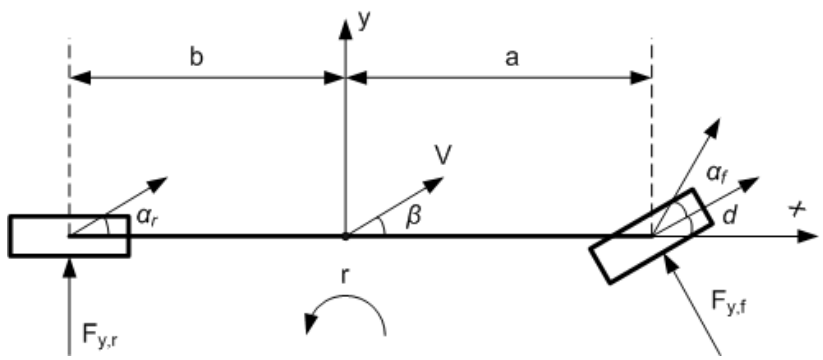

Figure 4.1: Bicycle Model

The state space form of the 3-DOF bicycle model that is shown in last chapter is still used here to represent lateral vehicle dynamics. As before, the slip angles of the front and rear wheels α_f, α_r are chosen as the state variables [34]. The matrices $A(\eta, \xi)$, $B(\eta, \xi)$ and input vector u in the state equation are shown below.

$$A(\eta, \xi) = \begin{pmatrix} -\frac{a_x}{v_x} - \frac{C_f}{v_x}\left(\frac{1}{M} + \frac{a^2}{I_z}\right) & \frac{C_r}{v_x}\left(\frac{ab}{I_z} - \frac{1}{M}\right) \\ \\ \frac{C_f}{v_x}\left(\frac{ab}{I_z} - \frac{1}{M}\right) & -\frac{a_x}{v_x} - \frac{C_r}{v_x}\left(\frac{1}{M} + \frac{b^2}{I_z}\right) \end{pmatrix} \tag{4.36}$$

$$B(\eta, \xi) = \begin{pmatrix} \frac{a_x}{v_x} & 1 & 1 \\ 0 & 0 & 1 \end{pmatrix} \tag{4.37}$$

where a_x is the longitudinal acceleration, which is assumed to be measured together with v_x. The control input vector u is

$$u = \begin{pmatrix} \delta \\ \dot{\delta} \\ r \end{pmatrix} \tag{4.38}$$

where M, I_z, a, b are the mass, yaw inertia, the distance of front and rear wheels from the CG of the vehicle. C_f, C_r are the cornering stiffness for the front and real tires. v_x, a_x are the longitudinal velocity and acceleration of the CG. r, δ, $\dot{\delta}$ are the yaw rate, steering angle and its derivative, which are treated as the measured input signals. Here, it is assumed that the cornering stiffness C_f and C_r are the critical uncertain parameters that affect the performance of the slip angle estimation algorithm. The uncertain parameter vector ξ together with the measured time-varying parameter vector η can be seen in Eq. (4.39) below.

$$\eta = \begin{pmatrix} \dfrac{1}{v_x} \\ \\ \dfrac{a_x}{v_x} \end{pmatrix}, \quad \xi = \begin{pmatrix} C_f \\ C_r \end{pmatrix} \tag{4.39}$$

It is obvious that the state matrix $A(\eta, \xi)$ depends on η and ξ bilinearly. With the information of the variation interval of v_x and a_x, such as $\underline{v}_x \leq v_x \leq \overline{v}_x$, $\underline{a}_x \leq a_x \leq \overline{a}_x$, the four vertices of the polytopic parameter space E can be derived as.

$$\eta^{(1)} = \begin{pmatrix} \dfrac{1}{\underline{v}_x} \\ \\ \dfrac{\overline{a}_x}{\underline{v}_x} \end{pmatrix}, \quad \eta^{(2)} = \begin{pmatrix} \dfrac{1}{\underline{v}_x} \\ \\ \dfrac{\underline{a}_x}{\underline{v}_x} \end{pmatrix}, \quad \eta^{(3)} = \begin{pmatrix} \dfrac{1}{\overline{v}_x} \\ \\ \dfrac{\overline{a}_x}{\overline{v}_x} \end{pmatrix}, \quad \eta^{(4)} = \begin{pmatrix} \dfrac{1}{\overline{v}_x} \\ \\ \dfrac{\underline{a}_x}{\overline{v}_x} \end{pmatrix} \tag{4.40}$$

Similarly, the four vertices of the polytopic parameter space Ξ shown below result from $\underline{C}_f \leq C_f \leq \overline{C}_f$, $\underline{C}_r \leq C_r \leq \overline{C}_r$.

$$\xi^{(1)} = \begin{pmatrix} \overline{C}_f \\ \overline{C}_r \end{pmatrix}, \quad \xi^{(2)} = \begin{pmatrix} \overline{C}_f \\ \underline{C}_r \end{pmatrix}, \quad \xi^{(3)} = \begin{pmatrix} \underline{C}_f \\ \overline{C}_r \end{pmatrix}, \quad \xi^{(4)} = \begin{pmatrix} \underline{C}_f \\ \underline{C}_r \end{pmatrix} \tag{4.41}$$

Besides the above state equations, there also exists a kinematic relation between slip angles and the measured signals shown below.

$$\delta - \frac{a+b}{v_x} r = \alpha_f - \alpha_r \tag{4.42}$$

This kinematic model can regarded as the output equation, which can be abstracted as

$$y = \begin{pmatrix} 1 & -1 \end{pmatrix} \begin{pmatrix} \alpha_f \\ \alpha_r \end{pmatrix} \tag{4.43}$$

4.5.2 LPV Interval Observer Design

The gain-scheduled interval observer in Eq. (4.20) contains a copy of the nominal model. In this example, the nominal cornering stiffness are chosen as

$$C_{f,0} = 76500(N/rad), \quad C_{r,0} = 51000(N/rad) \tag{4.44}$$

Their variation range is assumed to be constrained in the following interval

$$\begin{aligned} 60000(N/rad) \leq C_f \leq 90000(N/rad) \\ 35000(N/rad) \leq C_r \leq 65000(N/rad) \end{aligned} \tag{4.45}$$

Since the state space matrices $A(\eta, \xi)$ and $B(\eta, \xi)$ in Eq. (4.36) depends on C_f and C_r affinely, Lemma 12 can be directly applied to estimate the upper and lower limit functions $w^+(\hat{x}^+, \eta, \xi, u)$ and $w^-(\hat{x}^-, \eta, \xi, u)$.

Another important step is to search for the velocity-acceleration scheduled observer gain parameters in Eq. (4.22). In this example, Theorem 5 is applied to achieve a minimal width of the estimation interval $\hat{x}^+ - \hat{x}^-$. Because $A(\eta, \xi)$ in Eq. (4.36) is a bilinear matrix function of η and ξ, it is sufficient and necessary to guarantee the LMI feasibility and cooperative constraint for the observer error on all the vertices of the polytopes E and Ξ as shown in Lemma 14. For the uncertain parameter ξ, its variation range shown in Eq. (4.45) can be substituted in Eq. (4.41) to obtain the vertices of polytope Ξ. For the scheduling parameter η defined in Eq. (4.39), all four vertices of the polytope E shown in Eq. (4.40) can be derived

from the following physical constraints in the real applications.

$$15kph \leq v_x \leq 150kph, \quad -8.0m/s^2 \leq a_x \leq 8.0m/s^2 \tag{4.46}$$

Applying the SDP solver SeDuMi 1.3 with the toolbox YALMIP [9] as the interface, the following observer gain is obtained.

$$L(\eta) = \begin{pmatrix} 1.7127 \\ 1.3431 \end{pmatrix} + \eta_1 \begin{pmatrix} -58.5902 \\ -42.9510 \end{pmatrix} + \eta_2 \begin{pmatrix} -0.5579 \\ -0.4398 \end{pmatrix} \tag{4.47}$$

4.5.3 Simulation Results

The gain-scheduled interval observer is validated by using the data from CarSim, a commercial simulation software. In the simulation test, a sedan is simulated to follow the trajectory of the standard "Double Lane Change" maneuver. However, in this section the two lanes have different cornering stiffness along the trajectory as shown in Fig. 4.2. The variation of the cornering stiffness along the simulation time and the corresponding nonlinear tire curves for the front and rear tires can be seen in Fig. 4.3 and 4.4 respectively.

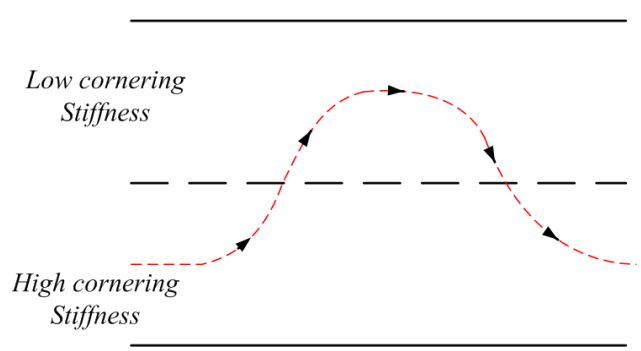

Figure 4.2: Trajectory of double lane change maneuver

A nominal observer is utilized which is only based on the nominal model for the lane with high cornering stiffness, for comparison with the interval observer. The simulation results can be seen in Fig. 4.5 below. It is clear that the estimated slip angles of the nominal observer start to deviate from true states at $1.5secs$ when the vehicle enters the lane with

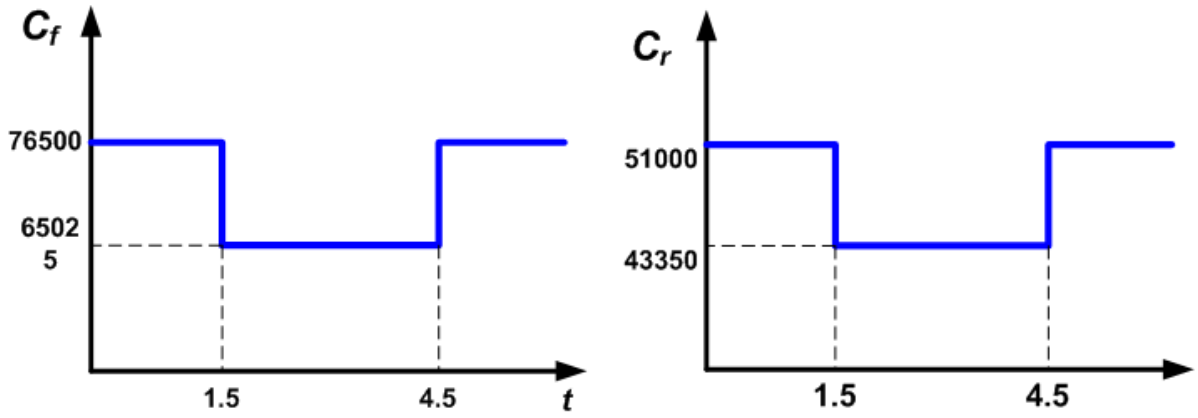

Figure 4.3: Cornering stiffness curves for the front and rear tires

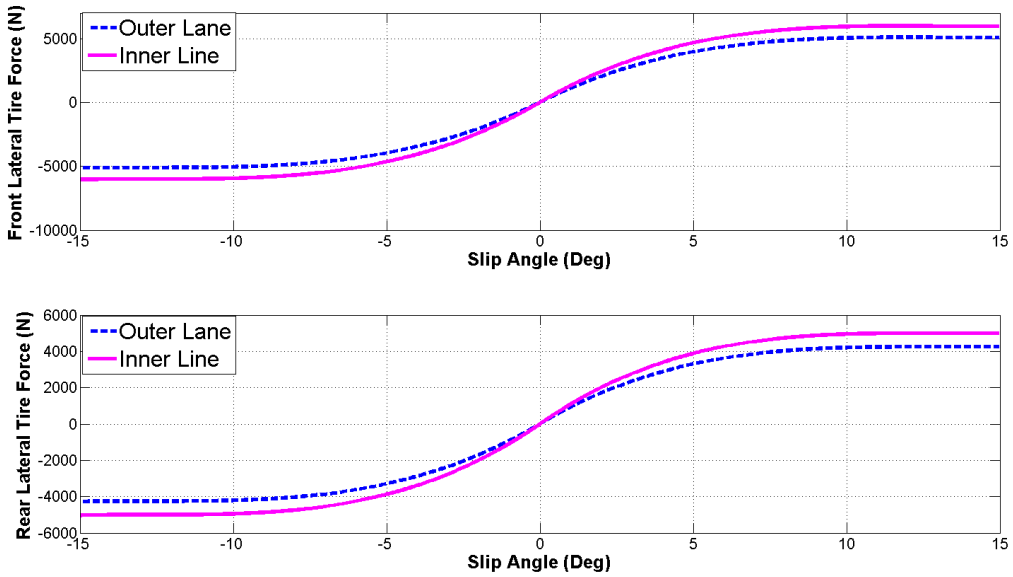

Figure 4.4: Relationship between slip angles and lateral tire forces

low cornering stiffness and then converge back at 4.5$secs$ when the vehicle reenters the lane with high cornering stiffness. However, the interval observer simulation result in Fig. 4.6 shows that the envelope from the interval observer can still cover true state trajectory in the presence of uncertain cornering stiffness.

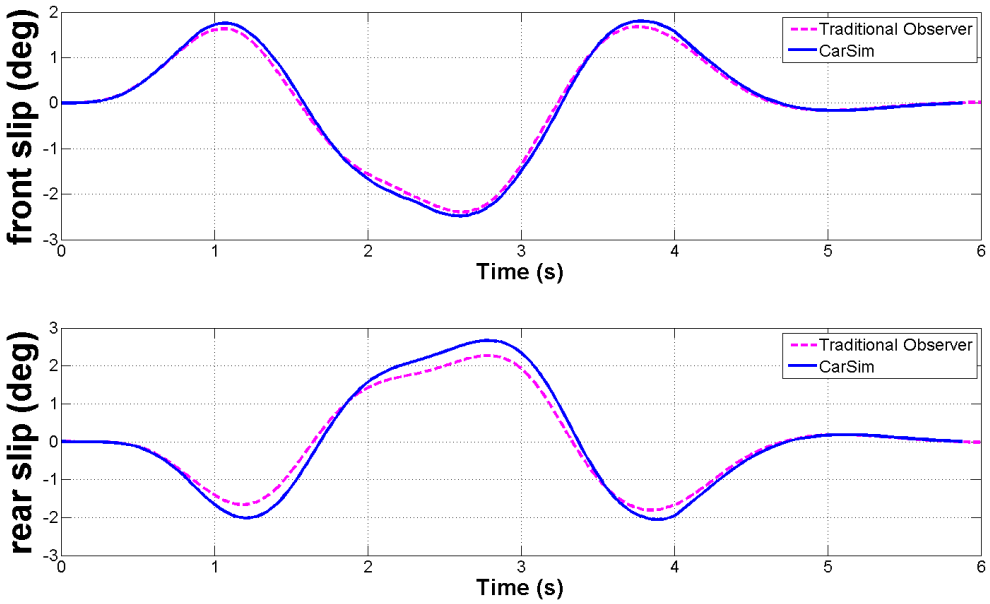

Figure 4.5: Simulation results of the nominal observer

4.6 Conclusions

In this chapter, an interval observer design methodology for LTI and LPV systems with parametric uncertainty is presented. It has been shown that uncertain parameters can be treated as a disturbance input for the observer error. Then, a simple analytical method to estimate the variation interval of this input uncertainty is developed. The search for the qualified observer gain, such that the observer error is robustly stable and cooperative, is cast as a convex semidefinite programming problem. A simulation example for slip angle estimation in the presence of uncertain cornering stiffness is used to illustrate the validity of the theoretical results.

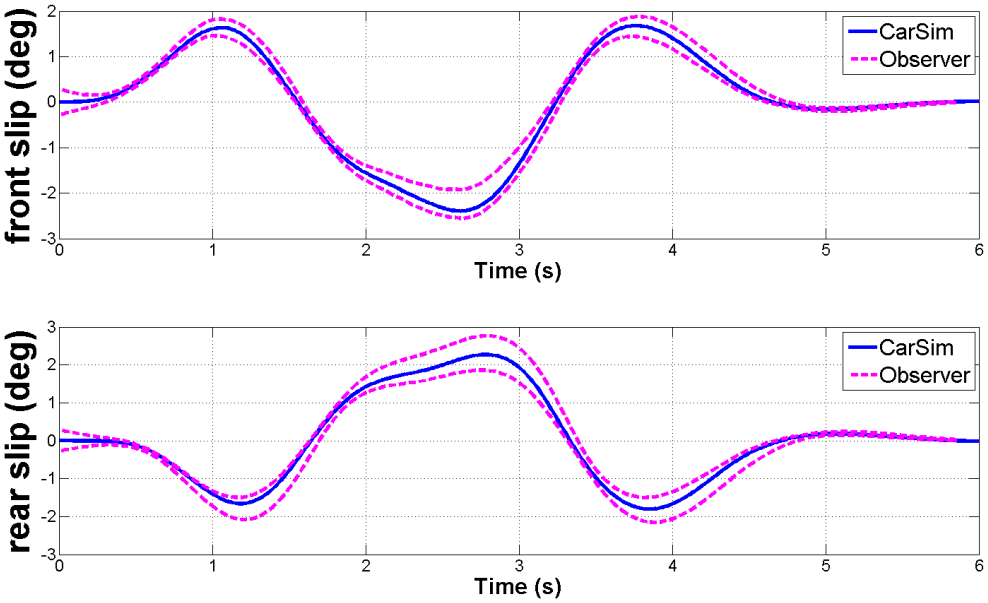

Figure 4.6: Simulation results of the interval observer

Chapter 5

Gain Scheduled Nonlinear Observer Design

5.1 Introduction

Although it has been shown that the uncertain linear cornering stiffness parameters can be considered in the interval observer framework, the linear relationship between the friction force and slip angle is still insufficient to model the vehicle dynamics in some extreme maneuver, such as fishhook or other high dynamic evasive maneuver. In fact, the tire-road friction is a very complex physical phenomenon, which is represented by various complicated mathematical models, such as Magic Formula and Dugoff tire model [34], which makes the design of the controller or estimator extremely challenging. In this chapter, a gain-scheduled nonlinear observer design methodology will be developed and applied to the tire slip angle estimation.

Observer designs for nonlinear dynamical systems has been a very active research field since the 1980s due to its importance in both nonlinear feedback controller design and process monitoring for complex systems. Many research results can be found in the literature. One popular method has been proposed by Krener and Isidori (1983) [40], Krener and Respondek (1985) [41] and Xiaohua Xia (1989) [67]. The core idea of the method is to find a nonlinear coordinate transformation, which requires solving a set of partial differential equations, such that all the nonlinearities are incorporated in the output injection terms. These terms are restricted to be functions of the input u and output y only. Then, a nonlinear observer, which contains a copy of the transformed state equation and a correction term, can be used to perform an exact error linearization in order that the stability and convergence speed of the observer error dynamics can be guaranteed by using very mature linear observer design methods. However, the existence of such a coordinate transformation imposes a very

strict condition on the vector field of the original system, which is difficult to satisfy in many real-world applications. Moreover, it is also widely realized that this linearization based method is vulnerable to model uncertainty, which severely limits its application in real-world engineering problems.

To deal with model uncertainty, high-gain observers [8] [20] and sliding mode observers [27] [30] have been developed. In these two methods, the uncertain nonlinear terms in the vector field are treated as a source of disturbance signals that prevent the observer error from becoming small or converging to a predefined stable sliding surface. High gains or the non-smooth functions are designed to make the observer more robust to the uncertainties. However, the size of the gains can be limited in real embedded systems due to finite word length in micro computers as well as higher order model uncertainties. A slow sampling rate also degrades the effect of the non-smooth function in the sliding mode observer which will result in undesirable chattering phenomenon. These practical constraints limit the application of these two types of observers.

The extended Luenberger nonlinear observer is a natural extension of the Luenberger observer for linear systems. It contains a copy of the model of the nonlinear process and a linear measurement correction term. The search of the convergent observer gains in an analytical way for this observer has been extensively studied since the early 1970s, such as F. E. Thau (1973) [1], S. Raghavan (1992) [2], R. Rajamani (1998) [4]. However, the results reported in those papers are often applicable only to nonlinear systems with small Lipschitz constants.

In the last two decades, semi-definite programming (SDP) has gained popularity in the control systems community [58] [54]. There are also a vast amount of applications of this numerical method to search for the convergent extended Luenberger observer gain. Phanomchoeng and Rajamani (2010) [49] transformed the Lipschitz conditions to a quadratic polynomial constraint and derived a sufficient stability condition in terms of LMIs by using the S-Procedure Lemma. It is pointed out that the small Lipschitz constant problem has been

significantly improved. A. Zemouche, M. Boutayeb and G. I. Bara [72] [70] [71] proposed a method that incorporates the derivative bounds of the nonlinear functions to represent the observer error model as a LPV system which the observer gain aims to asymptotically stabilize. Phanomchoeng and Rajamani (2011) [34] developed a similar method that uses the bounded Jacobian matrix of the nonlinear function to transform the observer error model to a polytopic uncertain linear system, which is asymptotically stabilized by the observer gain. Many other papers, such as A. Howel and K. Hedrick (2002) [36], M. Abbaszadeh and H. J. Marquez (2006) [17], Y. Wang and D. M. Bevly (2012) [66] and so on, used the methods more or less similar to these approaches.

Based on the structure of the extended Luenberger observer, M. Arcak and P. Kokotovic (2001) [23], X. Fan and M. Arcak (2003) [32] proposed a two DOF observer structure. Besides the linear measurement correction term on the observer state equation, another correction term is added to the input of the nonlinear function. For a class of systems with monotonic non-decreasing nonlinearities, the search of the two observer gains becomes a LMI problem. S. Ibrir (2007) [14] extended Arcak's two DOF observer structure to a discrete time version and showed that the monotonic non-decreasing requirement can be relaxed by reshaping the slope of the nonlinear functions. A. Zemouche and M. Boutayeb (2009) [69] showed that their LPV approach in the extended Luenberger observer can also be applied to Arcak's two DOF observer structure. However, some conservatism exists in the derived LMI conditions in the author's opinion. A more general result is presented by B. Acikmese, M. Corless [19] which uses incremental quadratic constraints to cover the algebraic conditions of the difference between the state vectors of the plant model and the observer and the difference between their corresponding nonlinear vector fields. Then, the convergence condition of the proposed observer is derived from the S procedure. One innovation in [19] is that the use of a third observer gain is proposed to cancel non convex terms in the semidefinite condition. But this method also limits the tuning of this additional gain, which results in some conservatism.

The construction of the incremental quadratic constraints for several types of nonlinearities is also discussed in [19].

Besides the methods discussed above, the well-known extended Kalman filter (EKF) and unscented Kalman filter (UKF) are also popular in literature [13]. Although there exist many successful applications of these methods especially in the field of navigation [29], the convergence of the observer error is generally only guaranteed locally [72]. For complex nonlinear dynamical systems, the convergence and robustness to model uncertainty is far from satisfactory.

The research result presented in this chapter will follow the direction in [34] [72] [69] [71] and [19]. The convergence and performance analysis is studied in the framework of the *Lure* system, where the algebraic condition on the input and output of the nonlinear memoryless block in the feedback loop is covered by the multivariable sector conditions from the bounded Jacobian matrices of the nonlinear functions. As will be shown, the convergence condition for the extended Luenberger observer can be represented as a semidefinite programming problem with much less LMI constraints than that in [72] [71] [34]. Moreover, the LMI conditions for both convergence and *L2* performance optimization of the two DOF observer in [69] [19] are just the convex inner approximation of the more general quadratic matrix inequalities. It will be shown that a much less conservative and simpler LMI conditions can be derived for searching for the two convergent observer gains. Also, different from the result in [19], the Differential Mean Value Theorem (DMVT) is applied to construct the multiplier matrix for the incremental quadratic constraints in an analytical way rather than treating the multiplier matrix as a decision variable. This further reduces the size of the optimization problem without introducing any conservatism. The search of optimal observer gains in terms of *L2* performance is also discussd. Finally, this observer design methodology is further applied to Lipschitz nonlinear systems with affine dependence on measured time-varying parameters. It will be shown that Arcak's two-DOF nonlinear observer can be augmented to a gain-scheduling framework for parameter varying systems.

The remainder of this chapter is organized as follows. The method that searches for the convergent observer gains for the extended Luenberger observer and Arcak's two-DOF nonlinear observer is proposed in Section 5.2. Then, this method is augmented to the gain scheduled observer design for a class of parameter dependent nonlinear systems in Section 5.3. The theoretical results are applied to two detailed simulation examples in Section 5.4. Section 5.5 contains the final conclusions.

5.2 Observer Design for Nonlinear Time Invariant Systems

5.2.1 Problem Statement

Consider the nonlinear system represented by Eq. (5.1)

$$\dot{x} = Ax + B_f f(x) + \Psi(y, u), \quad y = Cx \tag{5.1}$$

where $x \in R^n$, $y \in R^l$, $A \in R^{n\times n}$, $B_f \in R^{n\times m}$, $C \in R^{l\times n}$ and (A, C) is observable. $f(x) \in R^n \to R^m$ is a vector of differentiable Lipschitz continuous nonlinear functions and $\Psi(y, u)$ is an output injection function. In this chapter, the following two types of nonlinear observers will be discussed.

- Extended Luenberger Observer [71]:

$$\dot{\hat{x}} = A\hat{x} + B_f f(\hat{x}) + \Psi(y, u) + L_1(y - C\hat{x}) \tag{5.2}$$

  where L_1 is the observer gain;

- Arcak's Two DOF Nonlinear Observer [23] [32]:

$$\dot{\hat{x}} = A\hat{x} + B_f f[\hat{x} + L_2(y - C\hat{x})] + \Psi(y, u) + L_1(y - C\hat{x}) \tag{5.3}$$

  where L_1 and L_2 are two observer gains;

It is clear that both observers contain a copy of the model of the original system and a linear correction term $L_1(y - C\hat{x})$. Arcak's two DOF observer framework provides another linear correction term $L_2(y - C\hat{x})$ which is embedded in the argument of the nonlinear function $f(\cdot)$. The corresponding observer error ($e = x - \hat{x}$) dynamical equations for these two observers are shown below.

- Extended Luenberger Observer:

$$\dot{e} = (A - L_1 C)e + B_f[f(x) - f(\hat{x})] \tag{5.4}$$

- Arcak's Two DOF Nonlinear Observer:

$$\dot{e} = (A - L_1 C)e + B_f[f(x) - f(\hat{x} + L_2(y - C\hat{x}))] \tag{5.5}$$

From the Differential Mean Value Theorem (DMVT), it is known that the two difference functions $f(x) - f(\hat{x})$ and $f(x) - f(\hat{x} + L_2(y - C\hat{x}))$ are equal to $K(x - \hat{x})$ and $\bar{K}(x - \hat{x})$ respectively. The proportional factors K and $\overline{K}$ are time-varying matrices but always constrained in the closed sets defined by the lower and upper bounds of the Jacobian matrix of $f(x)$ in the domain of interest [72] [34]. Therefore, the observer error models in Eq. (5.4) and (5.5) can be represented as the *Lure* system shown in Fig. 5.1 below.

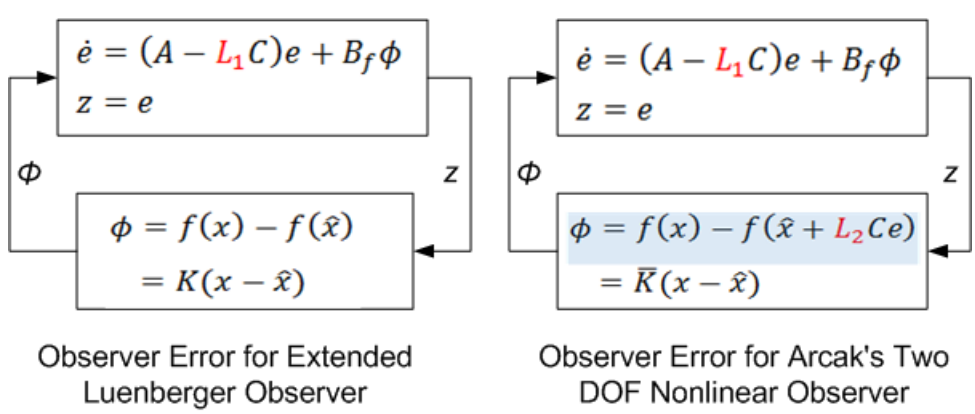

Figure 5.1: Lure-System Representation of the Observer Error System

Here, the two difference functions $f(x) - f(\hat{x})$ and $f(x) - f(\hat{x} + L_2(y - C\hat{x}))$ construct the memoryless nonlinearities in the feedback loops, where the input is the observer error e and the output is denoted as $\phi(t, e)$ that is proportional to e with a time-varying factor. Next, development of the algorithm that searches for the two gains L_1 and L_2 to make the observer error models in Eq. (5.4) and (5.5) asymptotically stable will be provided..

5.2.2 Sector Condition for e and $\phi(t, e)$

Several conditions of the semi-algebraic set of e and $\phi(t, e)$ can be found in the literature. For the monotonic non-decreasing function $f(x)$, Arcak and Kokotovic prove that e and $\phi(t, e)$ satisfy the passivity condition [23]. For the Lipschitz continuous nonlinearity, Phanomchoeng and Rajamani derived a sector condition based on the local Lipschitz constant of $f(x)$ [49]. In [19], Acikmese and Corless present a more general incremental quadratic constraint as the semi-algebraic set of e and $\phi(t, e)$. In this section, a sector condition based on bounded Jacobian matrices of the nonlinear function $f(x)$ is presented.

Lemma 15 *Consider the Lipschitz continuous function $f(x) \in R^n \to R^m$. Suppose the two matrices $K_1, K_2 \in R^{m \times n}$ are lower and upper bound Jacobian matrices of $f(x)$ in the domain of interest*

$$K_1(i, j) \leq \frac{\partial f_i(x)}{\partial x_j} \leq K_2(i, j) \tag{5.6}$$

where $f_i(x)$ is the ith element of the vector function $f(x)$ and x_j is the jth element of the vector x. Then, $e = x - \hat{x}$ and $\phi(t, e) = f(x) - f(\hat{x})$ satisfy the following sector condition.

$$[\phi(t, e) - K_1 e]^T [\phi(t, e) - K_2 e] \leq 0 \tag{5.7}$$

Proof: The Differential Mean Value Theorem (DMVT) gives us the following inequality.

$$K_1(x - \hat{x}) \leq f(x) - f(\hat{x}) \leq K_2(x - \hat{x}) \tag{5.8}$$

Here, the symbol $\leq$ means the element-wise inequality for two matrices with the same dimension. Eq. (5.8) is also equivalent to a pair of inequalities shown below.

$$\begin{aligned} f(x) - f(\hat{x}) - K_1(x - \hat{x}) \geq 0 \\ f(x) - f(\hat{x}) - K_2(x - \hat{x}) \leq 0 \end{aligned} \tag{5.9}$$

Therefore, the sector condition in Eq. (5.7) is quite straightforward.

Remark 1 *The conditions in Eq. (5.6) and (5.7) are rather general. For the monotonic non-decreasing function $f(x)$ in [23], K_1, K_2 can be chosen as*

$$K_1(i,j) = 0 \ \textit{and} \ K_2(i,j) = \gamma_{i,j} \tag{5.10}$$

where $\gamma_{i,j}$ is the local Lipschitz constants satisfying

$$\|f_i(x) - f_i(\hat{x})\|_2 \leq \gamma_{i,j} \|x_j - \hat{x}_j\|_2$$

For another example, the local Lipschitz property discussed in [49] is just a special case of Eq. (5.7) setting the elements of K_1, K_2 as the local Lipschitz constants

$$K_1(i,j) = -\gamma_{i,j} \ \textit{and} \ K_2(i,j) = \gamma_{i,j} \tag{5.11}$$

Note, a Lipschitz constant is just the maximal absolute value of the partial derivative of the function $f(x)$. This implies that the sector conditions in Eq. (5.6) and (5.7) represent a smaller semi-algebraic set than that defined by the matrices K_1, K_2 in Eq. (5.11). Therefore, the conservatism is reduced.

The quadratic form of Eq. (5.7) is

$$\begin{pmatrix} e \\ \phi \end{pmatrix}^T \underbrace{\begin{pmatrix} \frac{K_1^T K_2 + K_2^T K_1}{2} & -\frac{K_1^T + K_2^T}{2} \\ -\frac{K_1 + K_2}{2} & I \end{pmatrix}}_{M} \begin{pmatrix} e \\ \phi \end{pmatrix} \leq 0 \tag{5.12}$$

Based on the result in Lemma 2, the derivation of the sector condition of $e = x - \hat{x}$ and $\phi(t, e) = f(x) - f(\hat{x} + L_2(y - Cx))$ for Arcak's two DOF observer is shown as follows in Lemma 16.

Lemma 16 *Consider the Lipschitz continuous function $f(x) \in R^n \to R^m$. Suppose $e = x - \hat{x}$ and $f(x) - f(\hat{x})$ satisfy the sector condition in Eq. (5.7) in the domain of interest. Then, the semi-algebraic set of e and $\phi(t, e) = f(x) - f(\hat{x} + L_2(y - Cx))$ is covered by the following sector condition.*

$$[\phi(t, e) - K_1(I + L_2 C)e]^T [\phi(t, e) - K_2(I + L_2 C)e] \leq 0 \tag{5.13}$$

where I is an identity matrix with compatible dimension.

Proof: Suppose $\overline{e}$ is defined as

$$\overline{e} = x - [\hat{x} + L_2(y - C\hat{x})] = (I - L_2 C)e \tag{5.14}$$

Substituting $(I - L_2 C)e$ for $\overline{e}$ in the sector condition for $\overline{e}$ and $\phi(t, e)$ in the form of Eq. (5.7), the quadratic inequality in Eq. (5.13) can be derived

$$\begin{pmatrix} e \\ \phi \end{pmatrix}^T \begin{pmatrix} I - L_2 C & 0 \\ 0 & I \end{pmatrix}^T M \begin{pmatrix} I - L_2 C & 0 \\ 0 & I \end{pmatrix} \begin{pmatrix} e \\ \phi \end{pmatrix} \leq 0 \tag{5.15}$$

where M is defined in Eq. (5.12).

5.2.3 Sufficient Stability Condition for *Lure* System

Before discussing the search of the convergent observer gains, a brief review of the stability condition is presented for the *Lure* system whose state space model is shown as

$$\begin{aligned} \dot{x} &= Ax + Bw \\ z &= Cx + Dw \\ w &= \Delta(z) \end{aligned} \tag{5.16}$$

where $\Delta(\cdot)$ is a nonlinear Lipschitz continuous time-varying function. The relationship of its input and output signals z and w is covered by a homogeneous quadratic polynomial inequality in the form of Eq. (5.17)

$$\begin{pmatrix} z \\ w \end{pmatrix}^T \begin{pmatrix} Q & S \\ S^T & R \end{pmatrix} \begin{pmatrix} z \\ w \end{pmatrix} \leq 0 \tag{5.17}$$

where Q, R are real symmetric matrices. The inequality of Eq. (5.17) can be used to represent many important semi-algebraic sets, such as the sector condition and *L2* gain of a Lipschitz continuous function. Then, the following result in Theorem 6 shows the sufficient conditions for the asymptotic stability of this *Lure* system.

Theorem 6 (B.Acikmese, M.Corless (2008)[18]) *The feedback interconnected system in Eq. (5.16), where the input-output relationship of the operator $\Delta(\cdot)$ satisfies the homogeneous quadratic polynomial inequality in the form of Eq. (5.17), is asymptotically stable if the following linear matrix inequalities (LMIs) are feasible.*

$$\begin{gathered} P \succ 0 \\ \begin{pmatrix} A^TP + PA & PB \\ B^TP & 0 \end{pmatrix} - (*)^T \begin{pmatrix} Q & S \\ S^T & R \end{pmatrix} \begin{pmatrix} C & D \\ 0 & I \end{pmatrix} \prec 0 \end{gathered} \tag{5.18}$$

where $*$ can be deduced from symmetry.

5.2.4 Search for The Observer Gains L_1, L_2

Similar to the stability analysis result in Theorem 2, the semidefinite programming approach is used to search for the convergent observer gains L_1, L_2 in this chapter. The LMI feasibility problem for the extended Luenberger observer is formulated in Lemma 17.

Lemma 17 *Consider the nonlinear system in Eq. (5.1) with the matrices K_1 and K_2 being the lower and upper bounds of the Jacobian matrix of the Lipschitz continuous nonlinear function $f(x)$ in the domain of interest. Applying the extended Luenberger observer in Eq. (5.2), the observer error $e = x - \hat{x}$ is asymptotically stable if there exist a matrix P, and an observer gain L_1 such that*

$$\begin{gathered} P \succ 0, \\ \begin{pmatrix} (A - L_1C)^T P + P(A - L_1C) & PB_f \\ B_f^T P & 0 \end{pmatrix} - M \prec 0 \end{gathered} \tag{5.19}$$

where M is defined in Eq. (5.12).

Proof: As discussed above, the observer error model in Eq. (5.4) can be represented as a *Lure* system where the sector condition for the state difference $x - \hat{x}$ and the difference function $f(x) - f(\hat{x})$ is shown in Eq. (5.12). The semidefinite constraints in Eq. (5.19) can be derived from Theorem 2 by matching the state space matrices for the general *Lure* system in Eq. (5.16) to the observer error model of Eq. (5.4).

Remark 2 *Although Eq. (5.19) is a bilinear matrix inequality (BMI) constraint for the decision variables P and L_1, it can be transformed to an equivalent LMI constraint by using a common trick which defines the new matrix variable Y as $Y = PL_1$. If the resulting LMI is feasible, the observer gain is $L_1 = P^{-1}Y$ [58].*

Remark 3 *Compared with the method discussed in [34][72][71], which transfers the observer error model in Eq. (5.4) into a LPV framework, the LMI in Eq. (5.19) has a much lower dimension. Therefore, the computation effort is significantly reduced.*

For Arcak's two DOF nonlinear observer, a similar matrix inequality condition can be derived and shown in Lemma 18.

Lemma 18 *Consider the system in Eq. (5.1) with the matrices K_1 and K_2 being the lower and upper bounds of the Jacobian matrix of the Lipschitz continuous nonlinear function $f(x)$ in the domain of interest. Applying Arcak's two DOF nonlinear observer in Eq. (5.3), the observer error $e = x - \hat{x}$ is asymptotically stable if there exist a matrix P, and two observer gains L_1, L_2 such that*

$$\begin{gathered} P \succ 0, \\ \begin{pmatrix} (A - L_1C)^T P + P(A - L_1C) & PB_f \\ B_f^T P & 0 \end{pmatrix} \\ - \begin{pmatrix} I - L_2C & 0 \\ 0 & I \end{pmatrix}^T M \begin{pmatrix} I - L_2C & 0 \\ 0 & I \end{pmatrix} \prec 0 \end{gathered} \tag{5.20}$$

where M is defined in Eq. (5.12).

Proof: This proof is similar to that for Lemma 13. The only difference is that the input and output of the nonlinear block in the feedback loop of the *Lure* system becomes the state difference $x - \hat{x}$ and the difference functions $f(x) - f(\hat{x} + L_2(y - C\hat{x}))$ whose sector condition is shown in Eq. (5.15).

However, the matrix inequality condition in Eq. (5.20) depends on the observer gain L_2 quadratically, except the case in which either K_1 or K_2 is a zero matrix. This prohibits the application of the efficient interior-point algorithm to search for the feasible decision variables. Fortunately, it is shown in Theorem 7 that the search of the asymptotically

convergent observer gains L_1, L_2 becomes a LMI problem by representing the nonlinear state space model of the process in Eq. (5.1) as a slightly different but equivalent form.

Theorem 7 *Consider the nonlinear system in Eq. (5.1) and the following two DOF observer*

$$\begin{aligned} \dot{\hat{x}} = \; & A\hat{x} + B_f f[\hat{x} + L_2(y - C\hat{x})] + \Psi(y,u) \\ & +(L_1 - B_f K_1 L_2)(y - C\hat{x}) \end{aligned} \tag{5.21}$$

where the matrices K_1 and K_2 are the lower and upper bounds of the Jacobian matrix of the Lipschitz continuous nonlinear function $f(x)$ in the domain of interest. The existence of a matrix P and two observer gains L_1, L_2, such that the following semidefinite conditions in Eq. (5.22) are feasible, implies the asymptotic stability of the observer error $e = x - \hat{x}$.

$$\begin{gathered} P \succ 0 \\ \begin{pmatrix} \overline{A}^T P + P\overline{A} & PB_f \\ B_f^T P & 0 \end{pmatrix} - (*)^T M_1 \begin{pmatrix} I - L_2 C & 0 \\ 0 & I \end{pmatrix} \prec 0 \end{gathered} \tag{5.22}$$

where $*$ can be deduced from symmetry. The matrix $\overline{A}$ denotes $\overline{A} = A + B_f K_1 - L_1 C$. The multiplier matrix M_1 is

$$M_1 = \begin{pmatrix} 0 & -\frac{K_2^T - K_1^T}{2} \\ -\frac{K_2 - K_1}{2} & I \end{pmatrix} \tag{5.23}$$

where 0 denotes a zero matrix with compatible dimension.

Proof: The nonlinear state space model in Eq. (5.1) can be rewritten as the following equivalent form

$$\begin{aligned} \dot{x} &= (A + B_f K_1)x + B_f[-K_1 x + f(x)] + \Psi(y,u) \\ y &= Cx \end{aligned} \tag{5.24}$$

where the matrix K_1 is the lower bound of the Jacobian matrix $(\partial f / \partial x)$. The observer state equation in Eq. (5.21) is just Arcak's two DOF nonlinear observer for this equivalent state

space representation. The augmented nonlinear function $\overline{f}(x)$ is defined as

$$\overline{f}(x) = -K_1 x + f(x) \tag{5.25}$$

The Jacobian matrix of $\overline{f}(x)$ becomes

$$\left(\frac{\partial \overline{f}}{\partial x}\right) = -K_1 + \left(\frac{\partial f}{\partial x}\right) \tag{5.26}$$

It is obvious that $\left(\partial \overline{f}/\partial x\right)$ satisfies the following element-wise inequality.

$$0_{m\times n} \leq \left(\frac{\partial \overline{f}}{\partial x}\right) \leq K_2 - K_1$$

Therefore, the lower and upper bounds of $\left(\partial \overline{f}/\partial x\right)$ are

$$\overline{K}_1 = 0_{m\times n}, \quad \overline{K}_2 = K_2 - K_1 \tag{5.27}$$

After replacing K_1, K_2 in the matrix M and $A - L_1 C$ in Eq. (5.20) with $\overline{K}_1$, $\overline{K}_2$ in Eq. (5.27) and $\overline{A}$, the semidefinite condition in Eq. (5.22) is obtained.

The matrix inequality condition in Eq. (5.22) depends on the observer gain L_2 linearly. By applying the variable change method discussed in Remark 2, the efficient interior-point algorithm can be applied to solve this LMI feasibility problem.

Remark 4 *The LMI condition stated in Theorem 1 in [69] for the design of two DOF nonlinear observer is a conservative condition for the search of L_1, L_2 because the elements of the vectors ϵ and ζ are not independent. The semidefinite condition for the matrix in the quadratic form of the derivative of the Lyapunov function with vector $\begin{pmatrix}\epsilon^T & \zeta^T\end{pmatrix}^T$ will result in conservatism. Also, the dimension of those LMIs in [69] is much higher than Eq. (5.22), which requires more computation effort.*

Remark 5 *Also different from the result in [19], it is proposed to use the differential mean value theorem to construct the multiplier matrix for the incremental quadratic constraints in an explicit way rather than treating the multiplier matrix as a decision variable. This significantly reduces the size of the optimization problem in the case of a high-dimension nonlinear function $f(x)$. Furthermore, the approach in [19] may return a conservative multiplier for an enlarged semi-algebraic set, which is always undesirable.*

5.2.5 Nonlinear Optimal *L2* Observer Design

Besides asymptotic convergence, it is also possible to design the observer to satisfy a performance criterion, such as minimization of the *L2* gain from an unmeasured disturbance to the observer error. This is also called an H_∞ observer design problem that has been discussed in some previous papers [72] [69]. The remaining portion of this chapter will focus on Arcak's two DOF observer due to its greater generality than the extended Luenberger observer.

Suppose the model of the nonlinear process in Eq. (5.1) is augmented as

$$\begin{aligned} \dot{x} &= Ax + B_f f(x) + \Psi(y,u) + B_w w \\ y &= Cx \\ y_p &= C_p x \end{aligned} \tag{5.28}$$

where w is the unmeasured disturbance input. y is the measurement signal. y_p denotes the unmeasured signal needs to be estimated. If Arcak's two DOF nonlinear observer in Eq. (5.21) is used, the estimation error $z_p = y_p - \hat{y}_p$ is

$$\begin{aligned} \dot{e} &= \overline{A}e + B_f[\overline{f}(x) - \overline{f}(\hat{x} + L_2(y - C\hat{x}))] \\ &\quad + B_w w \\ z_p &= C_p e \end{aligned} \tag{5.29}$$

where the matrix $\overline{A}$ and function $\overline{f}(\cdot)$ are defined in Theorem 3 and Eq. (5.25) respectively. The observer gains should be designed to make the estimation error z_p insensitive to the disturbance w. The following result presents a semidefinite condition for the optimal *L2* observer design for this problem.

Theorem 8 *Consider the observer error dynamic model in Eq. (5.29) with the matrices K_1 and K_2 being the lower and upper bounds of the Jacobian matrix of the Lipschitz continuous nonlinear function $f(x)$ in the domain of interest. The optimal L2 observer design can be formulated as the following semidefinite programming problem*

$$
\begin{aligned}
&min\ \gamma \\
&subject\ to \\
&P \succ 0, \quad \tau > 0 \\
&\begin{pmatrix} \overline{A}^T P + P\overline{A} + C_p^T C_p & PB_f & PB_w \\ B_f^T P & 0 & 0 \\ B_w^T P & 0 & -\gamma^2 I \end{pmatrix} \\
&-\tau \begin{pmatrix} I - L_2 C & 0 & 0 \\ 0 & I & 0 \\ 0 & 0 & 0 \end{pmatrix}^T \begin{pmatrix} 0 & -\frac{K_2^T - K_1^T}{2} & 0 \\ -\frac{K_2 - K_1}{2} & I & 0 \\ 0 & 0 & 0 \end{pmatrix} \begin{pmatrix} I - L_2 C & 0 & 0 \\ 0 & I & 0 \\ 0 & 0 & 0 \end{pmatrix} \prec 0
\end{aligned}
\tag{5.30}
$$

where τ is a scalar S-Procedure multiplier. $\overline{A}$ is the same as that in Theorem 3.

Proof: Suppose $V = e^T P e$ is the storage function and $\phi(t, e)$ is defined as $\phi(t, e) = \overline{f}(x) - \overline{f}(\hat{x} + L_2(y - C\hat{x}))$. The dissipativity inequality for *L2* performance has the following form [58] [54] [35] [64].

$$\dot{V}(e, \phi, w) - (\gamma^2 w^T w - z_p^T z_p) < 0 \tag{5.31}$$

where $\dot{V}(e, \phi, w)$ is the derivative of the storage function along the trajectory. γ is the upper bound of the *L2* gain from w to z_p. As discussed above, e and $\phi(t, e)$ are constrained in

a sector condition defined by the lower and upper bounded Jacobian matrices $0_{m\times n}$ and $K_2 - K_1$, such as $\phi^T[\phi - (K_2 - K_1)e] < 0$. By applying S-Procedure, the robust dissipativity condition shown below [54] can be derived

$$\dot{V}(e, \phi, w) - (\gamma^2 w^T w - z_p^T z_p) - \tau\phi^T[\phi - (K_2 - K_1)e] < 0 \tag{5.32}$$

where τ is a positive scalar factor. The LMI condition in Eq. (5.30) is just the quadratic form of this dissipativity inequality with e, ϕ and w as the free variables.

Remark 6 *The semidefinite condition in Eq. (5.30) depends on the decision variables τ and L_2 bilinearly. Again, the change variable method that defines the new variable $\overline{L}_2$ as $\overline{L}_2 = \tau L_2$ to linearize this matrix inequality can be used. Once the resulting LMI condition is feasible, the observer gain L_2 can be derived as $L_2 = \overline{L}_2/\tau$.*

One disadvantage of this LMI based observer design method is that the SDP solver may return observer gains with a large norm [19], which is undesirable in most real-world applications, where the range of the controller or observer gains are limited by finite word length of the micro-controllers. But it is difficult to restrict the observer gains L_1, L_2 directly because they are not decision variables in the LMI constraints. Although B. Acikmese and M. Corless (2011) provide a remedy on this issue, it is based on the assumption that no non-zero constant terms exist in the LMI constraints, which Eq. (5.30) does not satisfy. In what follows, some additional LMI constraints that limit the norm of the two observer gains based on some mild assumptions are presented.

Suppose ϵ_1, ϵ_2 are the maximum allowed norm for the two observer gains L_1, L_2. This implies the inequalities shown below.

$$Y^T P^{-2} Y \leq \epsilon_1 I \ \ and \ \ \tau^{-2}\overline{L}_2^T \overline{L}_2 \leq \epsilon_2 I \tag{5.33}$$

From Schur Complement, the equivalent SDP constraints can be obtained.

$$\begin{pmatrix} \epsilon_1 I & Y^T \\ Y & P^2 \end{pmatrix} \geq 0, \quad \begin{pmatrix} \epsilon_2 I & \overline{L}_2^T \\ \overline{L}_2 & \tau^2 I \end{pmatrix} \geq 0 \tag{5.34}$$

These additional matrix inequalities depend on the decision variables P and τ quadratically. A LMI relaxation can be achieved by adding following mild constraints

$$P \geq \alpha I \ \ and \ \ \tau \geq \beta \tag{5.35}$$

where $0 < \alpha, \beta << 1$ are small positive numbers assigned by the user. Then, the sufficient conditions for Eq. (5.33) and (5.34) are the following LMIs that depend on the decision variables Y and $\overline{L}_2$ linearly.

$$\begin{pmatrix} \epsilon_1 I & Y^T \\ Y & \alpha^2 I \end{pmatrix} \geq 0, \quad \begin{pmatrix} \epsilon_2 I & \overline{L}_2^T \\ \overline{L}_2 & \beta^2 I \end{pmatrix} \geq 0 \tag{5.36}$$

Because the calculation of L_1, L_2 needs the inverse of P and τ, the additional constraint in Eq. (5.35) also improves the numerical reliability of the algorithm.

5.3 Observer Design for Parameter Varying Nonlinear (PVNL) Systems

In the previous section, the observer design for time invariant Lipschitz nonlinear systems has been discussed. However, the systems under control in real world applications often have time varying components. In some cases, the change of the dynamics of the controlled system is reflected in the continuous variation of some model parameters. If the state space model is linear with measured time-varying or state dependent parameters being virtually fixed, this type of system is called a linear-parameter-varying (LPV) system, which has been extensively studied since the early 1990s [53] [46]. If the model contains additional nonlinearities besides those hidden behind the time-varying parameters, it can be called a

parameter varying nonlinear (PVNL) system. However, there is very little research results on observers for these kinds of systems.

5.3.1 Convergent Gain-Scheduled Nonlinear Observer Design

In this section, the nonlinear observer design method is extended to parameter varying nonlinear systems, whose state space model can be abstracted as

$$\begin{aligned} \dot{x} &= A(\lambda)x + B_f(\lambda)f(x) + \Psi(y,u) \\ y &= C(\lambda)x \end{aligned} \tag{5.37}$$

where $\lambda = (\lambda_1, \ldots, \lambda_p)^T$ with $\underline{\lambda}_i \leq \lambda_i \leq \overline{\lambda}_i, \forall\, i = 1, \ldots, p$, is the collection of all the online measured time-varying parameters. Here, the research focus is restricted to the case that all the state space matrices $A(\lambda)$, $B_f(\lambda)$ and $C(\lambda)$ depend on λ affinely. Then, Arcak's two DOF nonlinear observer, such as that shown in Eq. (5.21), can be extended to the following gain scheduled nonlinear observer form.

$$\begin{aligned} \dot{\hat{x}} = \;& A(\lambda)\hat{x} + B_f(\lambda)f[\hat{x} + L_2(\lambda)(y - C(\lambda)\hat{x})] + \Psi(y,u) \\ & +[L_1(\lambda) - B_f(\lambda)K_1L_2(\lambda)](y - C(\lambda)\hat{x}) \end{aligned} \tag{5.38}$$

The scheduled observer gains $L_1(\lambda)$ and $L_2(\lambda)$ are

$$\begin{aligned} L_1(\lambda) &= L_{1,0} + \lambda_1 L_{1,1} + \cdots + \lambda_p L_{1,p} \\ L_2(\lambda) &= L_{2,0} + \lambda_1 L_{2,1} + \cdots + \lambda_p L_{2,p} \end{aligned} \tag{5.39}$$

where $L_{1,i}$, $L_{2,i}$, $\forall\, i = 0, 1, \ldots, p$ are all the observer gains. The search for the convergent observer gains can be represented as the following SDP problem shown in Theorem 9.

Theorem 9 *Consider the nonlinear system in Eq. (5.37) and Arcak's two DOF gain-scheduled nonlinear observer in Eq. (5.38) (5.39). The Jacobian matrix of the Lipschitz*

continuous function $f(x)$ is lower and upper bounded by the matrices K_1 and K_2 in the domain of interest. Then, the observer error $e = x - \hat{x}$ is asymptotically stable if the following matrix inequality conditions are feasible

$$P \succ 0,$$

$$\begin{pmatrix} \overline{A}(\lambda)^T P + P\overline{A}(\lambda) & PB_f(\lambda) \\ B_f(\lambda)^T P & 0 \end{pmatrix} \tag{5.40}$$

$$-\begin{pmatrix} I - L_2(\lambda)C(\lambda) & 0 \\ 0 & I \end{pmatrix}^T M_1 \begin{pmatrix} I - L_2(\lambda)C(\lambda) & 0 \\ 0 & I \end{pmatrix} \prec 0, \quad \forall\, \lambda \in \Lambda$$

where Λ represents the polytopic space that contains the parameter vector λ. The multiplier matrix M_1 is the same as that defined in Eq. (5.23). The parameter dependent matrix $\overline{A}(\lambda)$ denotes

$$\overline{A}(\lambda) = A(\lambda) + B_f(\lambda)K_1 - L_1(\lambda)C(\lambda) \tag{5.41}$$

Proof: The proof is similar to that for Theorem 3 except that all the state space matrices are replaced with their corresponding parameter dependent ones shown in Eq. (5.37).

Remark 7 *This result is based on a single quadratic Lyapunov function (SQLF) [7] as $V(e) = e^T Pe$, $P \succ 0$. It is also possible to choose a parameter dependent quadratic Lyapunov function (PQLF) to reduce the conservatism. However, this choice will make the semidefinite condition in Eq. (5.40) become a bilinear matrix inequality (BMI), which is a NP hard problem in general.*

5.3.2 Gain-Scheduled Nonlinear Optimal *L2* Observer Design

Similar to the time invariant case, the nonlinear parameter varying system in Eq. (5.37) can be augmented as

$$\begin{aligned} \dot{x} &= A(\lambda)x + B_f(\lambda)f(x) + \Psi(y,u) + B_w(\lambda)w \\ y &= C(\lambda)x \\ y_p &= C_p(\lambda)x \end{aligned} \tag{5.42}$$

By applying the dissipativity condition in Eq. (5.31) and (5.32), the gain scheduled nonlinear optimal L_2 observer design problem can be reframed to the following semidefinite programming problem presented in Theorem 10.

Theorem 10 *Consider the nonlinear system in Eq. (5.42) and Arcak's two DOF gain-scheduled nonlinear observer in Eq. (5.38) (5.39). The Jacobian matrix of the Lipschitz continuous function $f(x)$ is lower and upper bounded by the matrices K_1 and K_2 in the domain of interest. The optimal L2 observer design can be formulated as the following*

semidefinite programming problem

$$min\ \gamma$$

$$subject\ to$$

$$P \succ 0, \quad \tau > 0$$

$$\begin{pmatrix} \overline{A}(\lambda)^T P + P\overline{A}(\lambda) + C_p^T(\lambda)C_p(\lambda) & PB_f(\lambda) & PB_w(\lambda) \\ B_f(\lambda)^T P & 0 & 0 \\ B_w(\lambda)^T P & 0 & -\gamma^2 I \end{pmatrix}$$

$$-\tau \begin{pmatrix} I - L_2(\lambda)C(\lambda) & 0 & 0 \\ 0 & I & 0 \\ 0 & 0 & 0 \end{pmatrix}^T \begin{pmatrix} 0 & -\frac{K_2^T - K_1^T}{2} & 0 \\ -\frac{K_2 - K_1}{2} & I & 0 \\ 0 & 0 & 0 \end{pmatrix} \begin{pmatrix} I - L_2(\lambda)C(\lambda) & 0 & 0 \\ 0 & I & 0 \\ 0 & 0 & 0 \end{pmatrix} \prec 0$$

$$\forall\, \lambda \in \Lambda \tag{5.43}$$

where τ is a scalar S-Procedure multiplier. Λ and $\overline{A}$ are the same with those defined in Theorem 9.

Proof: This proof is also similar to that for Theorem 8 except that all the state space matrices are replaced with their corresponding parameter dependent ones shown in Eq. (5.37).

5.3.3 Finite Dimensional Relaxation

The semidefinite conditions in Eq. (5.40) and (5.43) are indeed infinite dimensional LMI constraints due to their continuous dependence on the parameter λ. To make them numerically tractable, it is necessary to convert them to finite dimensional LMI constraints. In what follows, the construction of such a finite dimensional relaxation of Eq. (5.40) and (5.43) will be discussed in two cases.

a) C, C_p are constant matrices.

In this case, the LMIs in Eq. (5.40) and (5.43) depend on the parameter λ affinely. From the constraint $\underline{\lambda} \leq \lambda \leq \overline{\lambda}$, it is easy to see that the parameter space Λ is a polytopic convex set with 2^p vertices.

$$\lambda \in \mathbf{Co}\left\{\Lambda^k,\ \ k = 1, \ldots, 2^p\right\} \tag{5.44}$$

where Λ^k denotes the kth vertex of the polytope Λ, which is assumed to be known. Therefore, it is only necessary to guarantee the semidefinite constraint on all the 2^p vertices of Λ [54] [46].

Lemma 19 *Suppose $F(\lambda)$ represents the parameter dependent matrix on the left side of the semidefinite conditions in Eq. (5.40) or (5.43), where C and C_p are assumed to be constant matrices. $F(\lambda) \prec 0, \forall\, \lambda \in \Lambda$ is feasible if and only if the following LMIs are feasible.*

$$F(\Lambda^k) \prec 0, \quad \forall\, k = 1, \ldots, 2^p \tag{5.45}$$

b) $C(\lambda)$, $C_p(\lambda)$ are affine functions of λ.

In this case, the LMI conditions in Eq. (5.40) and (5.43) depend on the parameter λ quadratically. From the LPV literature, various relaxation methods, such as parameter space griding [31], multi-convexity relaxation [22], and linear fractional representation (LFR) [6] [10], can be applied here. The multi-convexity relaxation requires that the 2nd-order derivative of the parameter dependent LMI along the edges of the polytopic parameter space is positive semidefinite, which is a strong requirement in general. Therefore, some conservatism in the relaxation is inevitable. Parameter space griding method approximates the infinite dimensional LMI at a set of discrete points in the whole parameter space. The

denser the grid, the larger the dimension of the LMIs, which should always be avoided. If the grid is looser, it is possible to miss some critical points, which reduces the robustness of the relaxation. The LFR method aims at representing the quadratically parameter dependent LMI as a LFR form, where the parameter dependent block is usually a diagonal matrix. Then, the full-block S-Procedure can be utilized to derive a finite dimensional relaxation. Although, this method is powerful and easily to be extended to a high order parameter dependent case, it is generally a hard task to get a LFR representation of the parameter dependent LMI. Here, a more simple method to find a finite dimensional LMI relaxation for the quadratical parameter dependent matrix inequality will be introduced.

Suppose $F(\lambda)$ represents the parameter dependent matrix on the left side of the semidefinite conditions in Eq. (5.40) or (5.43), which is a quadratic matrix function of λ

$$F(\lambda) = F_0 + \sum_{i=1}^{p} \lambda_i F_i + \sum_{i=1}^{p}\sum_{j=1}^{p} \lambda_i \lambda_j F_{ij} \prec 0 \tag{5.46}$$

where F_0, F_i, F_{ij}, $i, j = 1, \ldots, p$ are all symmetric matrices. Similar to the quadratic form of a scalar quadratic polynomial, $F(\lambda)$ can be represented as the following matrix quadratic form.

$$F(\lambda) = \begin{pmatrix} I \\ \lambda_1 I \\ \vdots \\ \lambda_p I \end{pmatrix}^T \underbrace{\begin{pmatrix} F_0 & 0.5F_1 & \cdots & 0.5F_p \\ 0.5F_1 & F_{11} & \cdots & 0.5F_{1p} \\ \vdots & \vdots & \ddots & \vdots \\ 0.5F_p & 0.5F_{1p} & \cdots & F_{pp} \end{pmatrix}}_{G} \begin{pmatrix} I \\ \lambda_1 I \\ \vdots \\ \lambda_p I \end{pmatrix} \tag{5.47}$$

For Eq. (5.40) or (5.43), the multiplier matrix G contains only decision variables P, L_1, L_2 and τ.

To relax this parameter dependent semidefinite condition, it is desired to find a multiplier matrix V that represents the algebraic constraint for the parameter λ shown below.

$$\begin{pmatrix} I \\ \lambda \otimes I \end{pmatrix}^T V \begin{pmatrix} I \\ \lambda \otimes I \end{pmatrix} \prec 0 \tag{5.48}$$

Then, the search of the multiplier matrix V becomes critical to the quality of the relaxation. Next, two ways to construct such a qualified multiplier are discussed.

1) **Unstructured Full Block Multiplier** V_1

   In this method, the search of a multiplier matrix V_1 satisfying the algebraic condition in Eq. (5.48) resorts to the feasibility problem of a set of LMIs shown below [11] [19]

$$\begin{pmatrix} I \\ \Lambda^k \otimes I \end{pmatrix}^T V_1 \begin{pmatrix} I \\ \Lambda^k \otimes I \end{pmatrix} \prec 0, \ \ \forall\, k = 1, \ldots, 2^p \tag{5.49}$$

   where Λ^k denotes the kth vertex of the polytope Λ. Then, applying S-Procedure, the following LMI that guarantees the negative definiteness of $F(\lambda)$ in the whole parameter space Λ [6] [11] can be obtained.

$$G - V_1 \prec 0 \tag{5.50}$$

   The LMIs in Eq. (5.49) and (5.50) constitute the finite dimensional relaxation of the semidefinite condition in Eq. (5.46).

2) **Structured Multiplier** V_2

   Although the SDP solvers, such as SeDuMi1.3 or SDPT3, can be employed to find a qualified multiplier efficiently, giving a clear physical interpretation to those elements in V_1 becomes a difficult and abstract task. Moreover, the solver may return a conservative multiplier corresponding to an enlarged polytope, which is always undesirable. Next, the derivation of the multiplier V_2 in an analytical way, which avoids the unnecessary conservatism at the cost of more decision variables, is shown.

From the constraint $\underline{\lambda} \leq \lambda \leq \overline{\lambda}$, the matrix inequality for each λ_i has the following form

$$\begin{pmatrix} I \\ \lambda_i I \end{pmatrix}^T \underbrace{\begin{pmatrix} \underline{\lambda}_i \, \overline{\lambda}_i I & -\frac{\underline{\lambda}_i + \overline{\lambda}_i}{2} I \\ -\frac{\underline{\lambda}_i + \overline{\lambda}_i}{2} I & I \end{pmatrix}}_{U_i} \begin{pmatrix} I \\ \lambda_i I \end{pmatrix} \leq 0 \tag{5.51}$$

where $i = 1, \ldots, p$. I represents an identity matrix that has the same dimension with that in Eq. (5.47). The multiplier U_i is a known matrix with clear physical interpretations. Furthermore, similar to the S-Procedure for the scalar case where a positive scaling factor (S-Procedure multiplier) preserves the positivity or negativity of the quadratic polynomial inequality [58], a positive definite matrix scaling factor can be added into each block in the multiplier U_i. This addition to the multiplier U_i leads to the following general matrix inequality for each λ_i.

$$\begin{pmatrix} I \\ \lambda_i I \end{pmatrix}^T \underbrace{\begin{pmatrix} \underline{\lambda}_i \, \overline{\lambda}_i \, \Gamma_i & -\frac{\underline{\lambda}_i + \overline{\lambda}_i}{2} \Gamma_i \\ -\frac{\underline{\lambda}_i + \overline{\lambda}_i}{2} \Gamma_i & \Gamma_i \end{pmatrix}}_{\overline{U}_i} \begin{pmatrix} I \\ \lambda_i I \end{pmatrix} \leq 0 \tag{5.52}$$

Here, $\Gamma_i \succ 0, i = 1, \ldots, p$ is a full-block positive definite matrix with the same dimension as the identity matrix I in Eq. (5.51). It will be treated as a decision variable in the subsequent LMIs in Eq. (5.56).

Based on Eq. (5.52), an augmented matrix inequality with a higher dimension as shown in Eq. (5.53) that includes all the parameters $\lambda_1, \ldots, \lambda_p$ can be obtained.

$$\begin{pmatrix} I \\ \lambda_1 I \\ \vdots \\ I \\ \lambda_p I \end{pmatrix}^T \begin{pmatrix} \overline{U}_1 & & \\ & \ddots & \\ & & \overline{U}_p \end{pmatrix} \begin{pmatrix} I \\ \lambda_1 I \\ \vdots \\ I \\ \lambda_p I \end{pmatrix} \leq 0 \tag{5.53}$$

To match the matrix vectors in Eq. (5.47), the following transformation matrix T can be applied.

$$\begin{pmatrix} I \\ \lambda_1 I \\ \vdots \\ I \\ \lambda_p I \end{pmatrix} = \underbrace{\begin{pmatrix} I & 0 & 0 & \cdots & 0 \\ 0 & I & 0 & \cdots & 0 \\ & & \vdots & & \\ I & 0 & 0 & \cdots & 0 \\ 0 & 0 & 0 & \cdots & I \end{pmatrix}}_{T} \begin{pmatrix} I \\ \lambda_1 I \\ \vdots \\ \lambda_p I \end{pmatrix} \tag{5.54}$$

Then, the multiplier matrix V_2 can be derived as follows:

$$V_2 = T^T \begin{pmatrix} \overline{U}_1 & & \\ & \ddots & \\ & & \overline{U}_p \end{pmatrix} T \tag{5.55}$$

Similar to the unstructured multiplier case, the S-Procedure can be used to construct the finite dimensional relaxation of the semidefinite condition in Eq. (5.46) as

$$G - V_2 \prec 0, \quad \Gamma_1, \ldots, \Gamma_p \succ 0 \tag{5.56}$$

In summary, two methods to build the multiplier matrix V in Eq. (5.48) and their corresponding finite dimensional relaxation of the parameter dependent LMI condition in Eq. (5.40) and (5.43) have been discussed. The structured multiplier V_2 has a clear physical interpretation and fewer LMI conditions than the unstructured multiplier V_1. But the LMIs in Eq. (5.56) have much more decision variables than those in Eq. (5.49) and (5.50) due to the additional full-block matrix scaling factors $\Gamma_1, \ldots, \Gamma_p$ whose size depend on the order of the original nonlinear system in Eq. (5.37). Therefore, it is recommended to use the structured multiplier V_2 and LMIs in Eq. (5.56) in the case of lower order systems. For

a higher order system with a few scheduling parameters, it is more convenient to use the unstructured multiplier V_1 and LMIs in Eq. (5.49) and (5.50).

5.4 Simulation Examples

In this section, two observer design examples will be used to demonstrate the applications of the theoretical results discussed in this chapter.

5.4.1 Van der Pol Oscillator

First, the Van der Pol oscillator is used as an example for observer design for time invariant nonlinear systems. Its ordinary differential equation model is shown below [8].

$$\ddot{y} - \mu(1 - y^2)\dot{y} + y = 0, \quad \mu = 1.0 \tag{5.57}$$

By defining the state variables x_1 and x_2 as $x_1 = y$, $x_2 = \dot{y}$, its state space representation is

$$\begin{aligned} \begin{pmatrix} \dot{x}_1 \\ \dot{x}_2 \end{pmatrix} &= \begin{pmatrix} 0 & 1 \\ -1 & 0 \end{pmatrix} \begin{pmatrix} x_1 \\ x_2 \end{pmatrix} + \begin{pmatrix} 0 \\ 1 \end{pmatrix} \mu(1 - x_1^2)x_2 \\ y &= \begin{pmatrix} 1 & 0 \end{pmatrix} \begin{pmatrix} x_1 \\ x_2 \end{pmatrix} \end{aligned} \tag{5.58}$$

where $f(x) = (1 - x_1^2)x_2$ is the nonlinear memoryless function. Arcak's two DOF nonlinear observer of Eq. (5.3) has the following form.

$$\begin{aligned} \begin{pmatrix} \dot{\hat{x}}_1 \\ \dot{\hat{x}}_2 \end{pmatrix} &= \begin{pmatrix} 0 & 1 \\ -1 & 0 \end{pmatrix} \begin{pmatrix} \hat{x}_1 \\ \hat{x}_2 \end{pmatrix} + \begin{pmatrix} 0 \\ 1 \end{pmatrix} \mu f(\hat{x} + L_2 C e) \\ &+ L_1(y - C\hat{x}) \end{aligned} \tag{5.59}$$

where $e = x - \hat{x}$. The sector condition for e and $\phi(t, e)$ can be derived from the lower and upper bounds of the Jacobian matrix $(\partial f(x)/\partial x)$ in the operation domain.

$$\left(\frac{\partial f(x)}{\partial x}\right) = \begin{pmatrix} -2x_1x_2, & 1 - x_1^2 \end{pmatrix} \tag{5.60}$$

Suppose $(x_1,\ x_2) \in [-5,\ 5] \times [-5,\ 5]$. The matrices K_1 and K_2 in Eq. (5.6) are

$$\begin{aligned} K_1 &= \begin{pmatrix} min(-2x_1x_2), & min(1 - x_1^2) \end{pmatrix} \\ &= \begin{pmatrix} -50, & -24 \end{pmatrix} \\ K_2 &= \begin{pmatrix} max(-2x_1x_2), & max(1 - x_1^2) \end{pmatrix} \\ &= \begin{pmatrix} 50, & 1 \end{pmatrix} \end{aligned} \tag{5.61}$$

Finally, Theorem 3 can be applied to search for the convergent observer gains L_1, L_2. This convex semidefinite programming problem can be solved by SDPT 3 with YALMIP as the interface [9]. The L_1, L_2 gain results are shown below in Eq. (5.62).

$$\begin{aligned} L_1 &= \begin{pmatrix} 17.5846, & 63.8993 \end{pmatrix}^T \\ L_2 &= \begin{pmatrix} 0.3639, & 0.6864 \end{pmatrix}^T \end{aligned} \tag{5.62}$$

To verify convergence, the observer is forced to start from a different initial condition than the true process in the simulation. The results for the individual state observations are shown in Fig. 5.2 below. The whole phase portrait in the state space can be seen in Fig. 5.3. It is clear that the observer states converge to the system states at a rather quick speed.

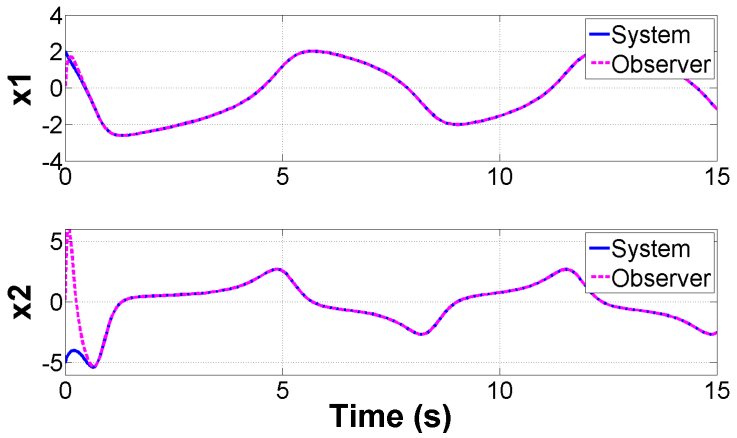

Figure 5.2: Simulation Results for The State Observation

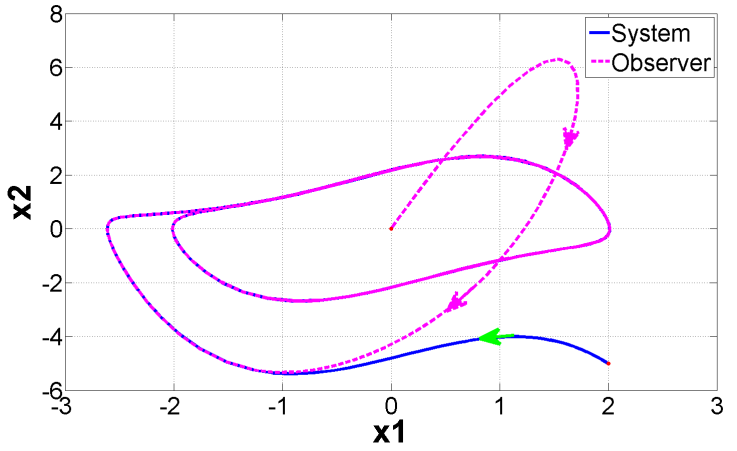

Figure 5.3: Simulation Results for The Phase Portrait

5.4.2 Slip Angle Estimation

The second example is the vehicle tire slip angle estimation problem, which is a challenging task in automotive active safety system. Previous research results in this field are based on one of the two assumptions shown below:

1. Linear tire model in which the tire-road friction force is proportional to the slip angle;

2. Nonlinear tire model with constant longitudinal velocity [34];

In this section, it will be shown that both the nonlinear tire model and variation of the longitudinal velocity can be considered simultaneously by applying the gain-scheduled nonlinear observer design methodology developed in this chapter.

Nonlinear Tire Model

Tire-road friction force is a critical external input source in various automotive active safety systems, such as anti-lock braking systems (ABS), traction control (TC) and electronic stability control (ESC) [39]. However, tire-road friction is a very complex physical phenomenon, which is represented by various complicated mathematical models, such as Magic Formula, Dugoff tire model [16] and LuGre tire model [25]. These highly nonlinear models make the design of the controller or observer a very challenging task.

In this example, the following nonlinear tire model for the lateral tire-road friction force under the assumption of parabolic normal pressure distribution [34] is adopted.

$$F_y(\alpha) = \begin{cases} \mu F_z(3\theta\alpha - 3\theta^2\alpha^2 sgn(\alpha) + \theta^3\alpha^3), & if\ |\alpha| \leq \frac{1}{\theta} \\ \\ \mu F_z sgn(\alpha) & if\ |\alpha| > \frac{1}{\theta} \end{cases} \tag{5.63}$$

with the definition of θ as

$$\theta = \frac{4a_c b_c k}{3\mu F_z},$$

where α is the slip angle of the wheel. μ and F_z represent the tire-road friction coefficient and normal load of the wheel. a_c is half-length of contact patch, b_c is half-width of the contact patch, and k is isotropic stiffness of tire elements per unit area of the belt surface. $1/\theta$ represents the value of slip at which a saturation of lateral tire force is reached. Unlike other highly cited tire models, such as the Magic formula, this polynomial representation of the tire model makes it easy to estimate the lower and upper bounds of the Jacobian matrix $(\partial f_y/\partial\alpha)$. A typical curve of the nonlinear lateral tire-road friction model in Eq. (5.63) with $\mu = 0.85$, $F_z = 6000N$, $\theta = 4.5$ is shown in Fig. 5.4 below.

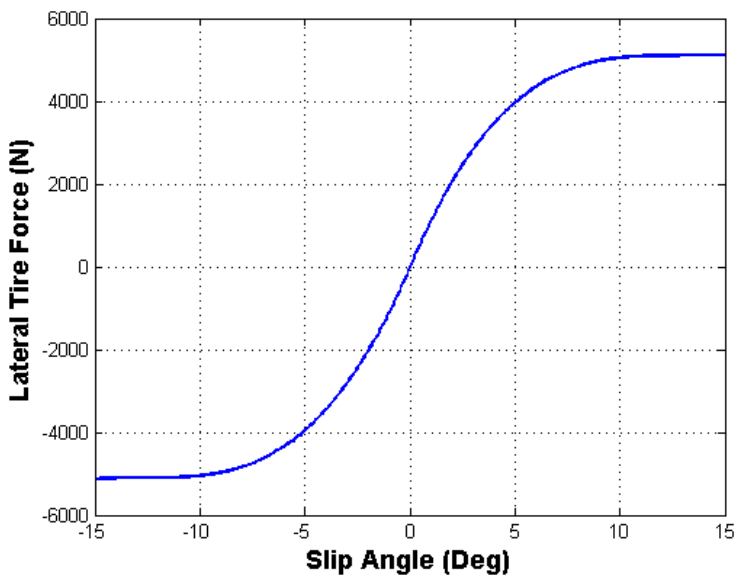

Figure 5.4: A typical curve of the nonlinear tire model in Eq. (5.63)

Nonlinear Parameter Dependent Bicycle Model

Based on the tire model in Eq. (5.63), the standard state equations of the nonlinear bicycle model can be derived as shown in Eq. (5.37), where the slip angles of the front and rear wheels α_f, α_r are chosen as the state variables [34]. The affine parameter varying state space matrices $A(\lambda)$, $B_f(\lambda)$, $B_w(\lambda)$, the measured input function $\Phi(y, u)$ and the nonlinear

state function $f(\alpha_f, \alpha_r)$ are shown below

$$A(\lambda) = \begin{pmatrix} -\frac{\dot{v}_x}{v_x} - \frac{c_{1f}}{v_x}\left(\frac{1}{M} + \frac{a^2}{I_z}\right) & \frac{c_{1r}}{v_x}\left(\frac{ab}{I_z} - \frac{1}{M}\right) \\ \\ \frac{c_{1f}}{v_x}\left(\frac{ab}{I_z} - \frac{1}{M}\right) & -\frac{\dot{v}_x}{v_x} - \frac{c_{1r}}{v_x}\left(\frac{1}{M} + \frac{b^2}{I_z}\right) \end{pmatrix} \tag{5.64}$$

$$B_f(\lambda) = \begin{pmatrix} -\frac{1}{v_x}\left(\frac{1}{M} + \frac{a^2}{I_z}\right) & \frac{1}{v_x}\left(\frac{ab}{I_z} - \frac{1}{M}\right) \\ \\ \frac{1}{v_x}\left(\frac{ab}{I_z} - \frac{1}{M}\right) & -\frac{1}{v_x}\left(\frac{1}{M} + \frac{b^2}{I_z}\right) \end{pmatrix} \tag{5.65}$$

$$B_w(\lambda) = \frac{1}{v_x}\begin{pmatrix} -\frac{1}{M} & -\frac{a}{I_z} \\ \\ \frac{1}{M} & -\frac{b}{I_z} \end{pmatrix} \tag{5.66}$$

$$\Phi(y, u) = \begin{pmatrix} \frac{\dot{v}_x}{v_x} & 1 & 1 \\ \\ 0 & 0 & 1 \end{pmatrix}\begin{pmatrix} \delta \\ \dot{\delta} \\ r \end{pmatrix} \tag{5.67}$$

$$f(\alpha_f, \alpha_r) = \begin{pmatrix} c_{2f}\alpha_f^2 sgn(\alpha_f) + c_{3f}\alpha_f^3 \\ \\ c_{2r}\alpha_r^2 sgn(\alpha_r) + c_{3r}\alpha_r^3 \end{pmatrix} \tag{5.68}$$

where M, I_z, a, b are the mass, yaw inertia, the length of front end and rear end to the CG of the vehicle. $c_{i,f}$, $c_{i,r}, i = 1, 2, 3$ are the coefficients of the polynomial tire models in Eq. (5.63) for the front and real tires. v_x, $\dot{v}_x$ are the longitudinal velocity and acceleration, which are assumed to be the measured signals. r, δ, $\dot{\delta}$ are the yaw rate, steering angle and its derivative, which are treated as the measured input signals. W_F and W_T denote those unmeasured disturbance force and torque inputs, such as air drag or uncertain inertia forces. The affine scheduling parameter λ is composed of two elements λ_1 and λ_2 which are defined as

$$\lambda_1 = \frac{1}{v_x}, \quad \lambda_2 = \frac{\dot{v}_x}{v_x} \tag{5.69}$$

The variation range of λ_1, λ_2, such as $\underline{\lambda}_1 \leq \lambda_1 \leq \overline{\lambda}_1$, $\underline{\lambda}_2 \leq \lambda_2 \leq \overline{\lambda}_2$, can be estimated from the following physical constraints in the real applications based on desired dynamic range for the observer to operate.

$$15kph \leq v_x \leq 150kph, \quad -8.0m/s^2 \leq \dot{v}_x \leq 8.0m/s^2 \tag{5.70}$$

Besides the above state equation, the kinematic relation between slip angles and the measured signals are shown in Eq. (5.71).

$$\delta - \frac{a+b}{v_x} r = \alpha_f - \alpha_r \tag{5.71}$$

This kinematic model is regarded as the output equation, which can be abstracted as

$$y = \begin{pmatrix} 1 & -1 \end{pmatrix} \begin{pmatrix} \alpha_f \\ \alpha_r \end{pmatrix} \tag{5.72}$$

Gain-Scheduled Nonlinear Observer

Here, the gain-scheduled observer in Eq. (5.38) is used to estimate the two slip angles α_f, α_r. The search of the observer gains resorts to the semidefinite problem in Theorem 10 for ensuring optimal *L2* performance, which aims at minimizing the effect of the unmeasured disturbance inputs W_F, W_T on the observer error. The output equation in Eq. (5.72) shows that the output matrix is constant, which implies that the LMI conditions in Eq. (5.40) and (5.43) depends on the scheduling parameter λ affinely. Therefore, Lemma 19 can be applied to derive the finite dimensional relaxation of the parameter dependent LMI conditions.

By using the SDP solver SeDuMi 1.3, the following results are obtained for the observer gains.

$$
\begin{aligned}
L_1(\lambda) &= \begin{pmatrix} 9.6103 \\ 10.1651 \end{pmatrix} + \lambda_1 \begin{pmatrix} -72.1241 \\ -84.5006 \end{pmatrix} + \lambda_2 \begin{pmatrix} -0.4527 \\ -0.5227 \end{pmatrix} \\
L_2(\lambda) &= \begin{pmatrix} 0.5307 \\ 0.4693 \end{pmatrix} + \lambda_1 \begin{pmatrix} 0.5170 \\ -0.5154 \end{pmatrix} + \lambda_2 \begin{pmatrix} -0.018 \\ 0.0187 \end{pmatrix}
\end{aligned}
\tag{5.73}
$$

where the scheduling parameters λ_1 and λ_2 are defined in Eq. (5.69). This gain-scheduled observer requires that both the longitudinal velocity and acceleration are measured online, which is available in today's automotive active safety systems [39]. The velocity and acceleration scheduled observer gains can also be represented as a set of smooth lookup tables, which are widely used in the automotive control systems [39]. The shape of these lookup tables is shown in Fig. 5.5 below, from which it can seen that the observer gains are dominated by the variation of the velocity especially in the low speed region. When the speed is above 60kph, the gains approach their steady states. This flat region also explains why previous research results with fixed observer gains can also give a good performance in the speed range above 60kph [34]. The change of acceleration has a relative minor effect on the scheduling of the gains at these speeds.

Simulation Result

The data from CarSim is used to verify the performance of the gain-scheduled nonlinear observer. To excite the tire-road friction force into nonlinear region, a sedan is required to follow the trajectory of the extreme "Fishhook" maneuver in the simulation test. The fishhook is an extreme maneuver to stress the vehicle dynamics to its limits. This type of maneuver could also represent an extreme avoidance maneuver. Its longitudinal velocity profile, which decreases from 78kph to 23kph gradually, is shown in Fig. 5.7.

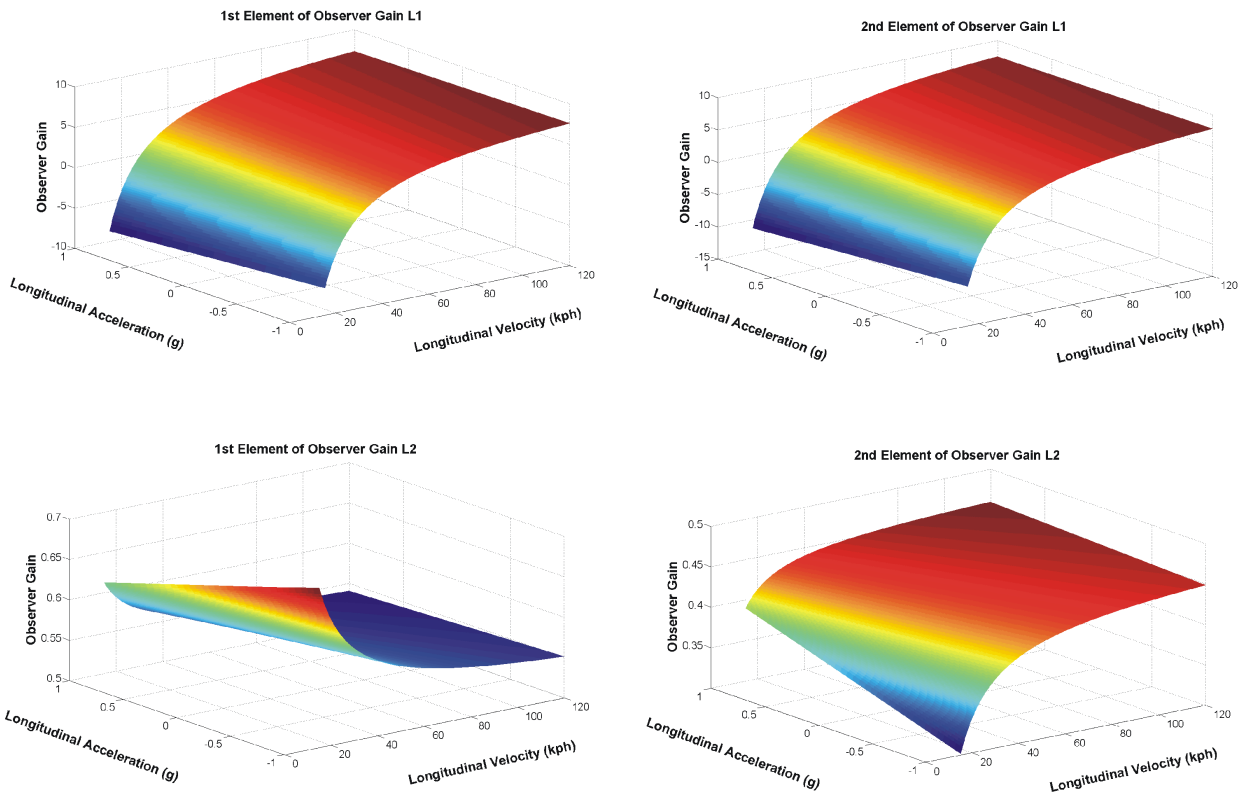

Figure 5.5: The lookup table for the longitudinal velocity and acceleration scheduled observer gains.

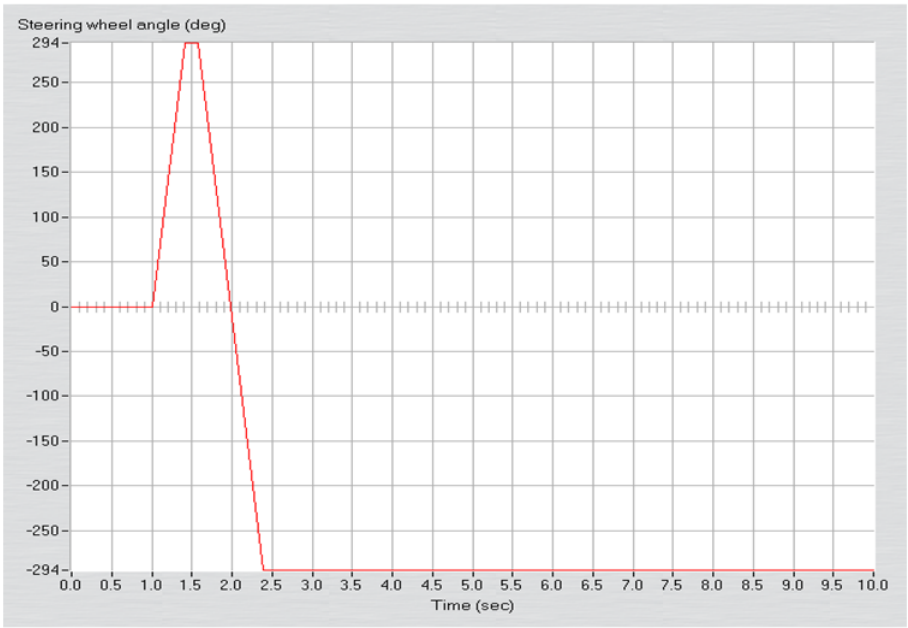

Figure 5.6: The steering angle of fishhook.

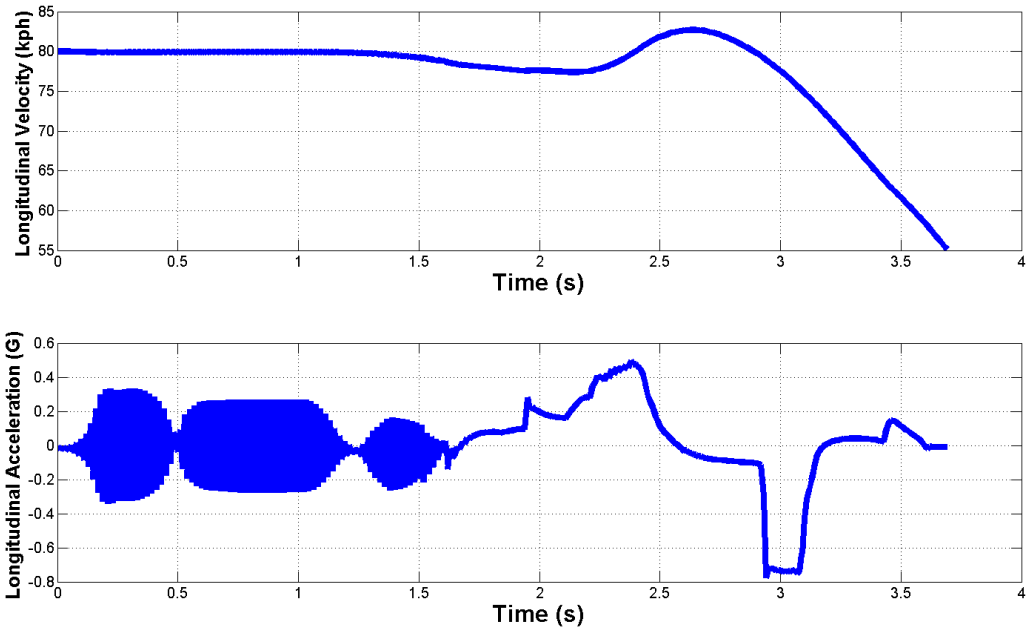

Figure 5.7: The longitudinal velocity and acceleration profile in the simulation.

To demonstrate the superiority of the nonlinear gain-scheduled observer, a LPV observer discussed in chapter 3 that is based on the linear tire-road friction model in Eq. (3.13) is also simulated. The simulation results are presented in Fig. 5.8. As in chapter 3, the two observers start to work 1 second later than the maneuver and at a different initial condition. Fig. 5.8 shows that the estimated slip angles from the gain-scheduled nonlinear observer converge to the true states quickly. When the front and rear slip angles reach beyond 5.7deg (0.1rad), the LPV observer cannot produce accurate estimation results. This observation is consistent with the tire model in Fig. 5.4 which shows that the relationship between slip angle and cornering force becomes nonlinear above 5.7deg (0.1rad).

5.5 Conclusions

In this chapter, a design framework that reframes the search of the optimal convergent observer gains for both the Extended Luenberger Observer and Arcak's two DOF nonlinear observer as a convex semidefinite programming problem has been developed. It has been

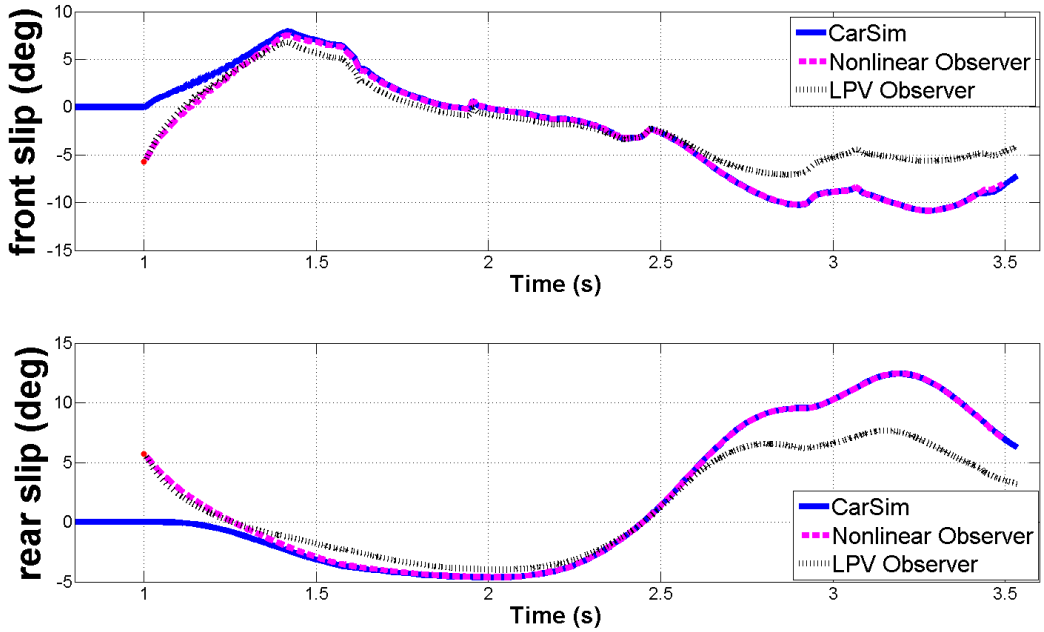

Figure 5.8: The simulation results of gain scheduled nonlinear observer and the LPV observer in the fishhook maneuver.

shown that the observer error dynamics can be modeled as a *Lure* type system with multivariable sector conditions from the bounded Jacobian matrices. Furthermore, this methodology is extended to design a gain scheduled observer for parameter varying nonlinear (PVNL) systems for the first time. Different finite dimensional relaxation methods for the parameter dependent LMIs are analyzed and compared. The simulation examples for both the time-invariant and parameter-varying nonlinear systems support the validity of the theoretical results.

Chapter 6

Conclusions and Future Work

6.1 Concluding Remarks

In summary, the application of LMI based optimization methods to develop model based vehicle state estimation algorithm has been developed in this dissertation. The three degree of freedom (DOF) bicycle model for estimating the non-measurable tire slip is the application example for the observers. However, all the observer design methodologies presented in this dissertation are formalized in a systematic manner, which allow them to be easily applied to other dynamical models besides the vehicle model.

First, the linear tire-road friction model was considered. The linear parameter varying (LPV) observer design methodology was then applied with the longitudinal velocity and acceleration treated as online measured time-varying scheduling parameters. Some robust design techniques, such H_2 and H_∞ norm optimization, for the uncertainty in the measured scheduling parameters were also proposed. Next, the gain-scheduled observer design method was augmented to interval estimation where the observer gain parameters are tuned in such a way that the observer error is a positive linear system. In this framework, the uncertain cornering stiffness is modeled as a disturbance input that perturbs the observer error. Instead of a single estimation trajectory for each state variable, the interval observer results in an envelope that covers all the possible state trajectories when the cornering stiffness parameters vary in the pre-specified interval. In real-world applications, this envelope provides valuable information of worst-case bounds on the estimated values. Finally, a nonlinear observer design technique is developed to cope with the nonlinearity in the tire-road friction model. Similar to the LPV observer, the time invariant nonlinear observer was also augmented to a parameter varying nonlinear (PVNL) observer such that both nonlinear tire model

and time-varying longitudinal velocity and acceleration can be considered simultaneously. A new relaxation approaches for the infinite dimensional LMIs were also proposed. In the development of all these estimation algorithms, the search of convergent and optimal observer parameters were cast as a convex semidefinite programming problem.

All of the presented vehicle state estimation algorithms are verified using the simulation data from CarSim, a high-fidelity commerical simulation software package. The simulation results verify that the robust LPV observer produces better estimation results in the presence of measurement error of longitudinal velocity and acceleration. The gain-scheduled interval observer was shown to provide a robust estimation solution in the simulation of varying cornering stiffness parameters. It was also shown that the real slip angles are always constrained within the estimated envelope. In the simulation of aggressive maneuvers, such as a fishhook, the nonlinearity in tire-road friction becomes notable. The nonlinear observer showed superior performance over the linear observer in this case.

6.2 Future Work

6.2.1 Sensor Fusion with Camera, Radar and Lidar

In this dissertation, the vehicle state estimation algorithms are developed only based on inertial measurements, such as velocity and acceleration. It is far from the goal of advanced driver assistance systems (ADAS), which are expected to automate/adapt/enhance vehicle systems for safety and better driving. The latest ADAS technology can be based upon vision/camera systems, radar/Lidar systems, Vehicle-to-Vehicle (V2V) or Vehicle-to-Infrastructure systems. All of these state-of-the-art sensing systems provide an opportunity to improve the estimation accuracy and robustness against the model uncertainty.

Besides access to the vehicle states, those advanced sensing systems may also provide more precise measurements of the scheduling parameters, such as the longitudinal velocity and acceleration in the bicycle model. This could further improve the estimation accuracy of

the slip angle. Furthermore, the camera and radar can provide relative velocity with respect to other vehicles or pedestrians, which is vital information for prediction of crashes.

6.2.2 Moving Horizon Estimation using Multi-Parametric Programming

A Moving Horizon Estimator (MHE) computes an estimate at the current instant by solving an optimization problem based on information from a fixed-number of latest measurements collected over a finite horizon [52]. In this problem, the cost function to be minimized is traditionally described by the norm of the difference between real and predicted measurements over the horizon, a norm of the process noise over the horizon and a norm of the difference between an estimate at the beginning of the horizon and an a priori one. The main advantages of the MHE are that nonlinear systems are handled without linearization and constraints are directly incorporated during the optimization. However, the computation time of the MHE can be very lengthy due to its large number of decision variables. One remedy for this dilemma is to apply multi-parametric programming methods such that the complex online computation can be circumvented [15].

Multi-parametric programming is a technique for solving an optimization problem, where the objective is to minimize or maximize a performance criterion subject to a given set of constraints in which some of the parameters vary between specified lower and upper bounds. The main characteristic of multi-parametric programming are listed below [15].

- The variation of initial condition or process model parameters is modeled as the symbolic varying parameters in the cost function and constraint conditions;
- Both the objective function and optimal decision variables are returned as functions of the varying parameters which can be explicitly represented by lookup tables;
- The algorithm can also compute the regions in the parameter space where these functions are valid;

The motivation of using multi-parametric programming to address the vehicle state estimation problems is that both nonlinear dynamical model and time-varying parameters can be considered in a unified optimization framework [52]. Applying the multi-parametric programming method, one can obtain the optimal solution as a complete map of all the initial conditions and time-varying parameters. Hence, as the operating conditions vary, it is not necessary to repeat the optimization process for the new set of conditions, since the optimal solution is already available as a function of the operating conditions. This advantage of multi-parametric programming greatly facilitates its implementation on the embedded systems with low software and hardware complexity [15]. Therefore, this methodology has the potential to improve upon the estimation algorithm developed in this dissertation.

Bibliography

[1] F. E. Thau (1973). Observing the state of nonlinear dynamic systems. *International Journal of Control*, 17(3):471–479, 1973.

[2] S. Raghavan (1992). *Observers and compensators for nonlinear systems with application to flexible-joint robots*. Ph.D. Dissertation, University of California at Berkeley, Berkeley, CA 94720, U.S.A, 1992.

[3] A. Rantzer (1997). On the kalman-yakubovich-popov lemma. *Systems and Control Letters*, 28(1):7–10, 1997.

[4] R. Rajamani (1998). Observer design for lipschitz nonlinear systems. *IEEE Transactions on Automatic Control*, 43(3):397–401, 1998.

[5] A. Rantzer (2001). A dual to lyapunov's stability theorem. *Systems and Control Letters*, 42(3):161–168, 2001.

[6] C.W. Scherer (2001). Lpv control and full block multipliers. *Automatica*, 37(3):361–375, 2001.

[7] G. Balas (2002). Linear parameter-varying control and its application to aerospace systems. In *ICAS Congress Proceedings*, Toronto, Canada, 2002.

[8] H.K. Khalil (2002). *Nonlinear Systems*. Prentice Hall, Upper Saddle River, NJ, USA, 3rd edition, 2002.

[9] J. Lofberg (2004). Yalmip: A toolbox for modeling and optimization in matlab. In *Proceedings of 2004 IEEE International Symposium on Computer Aided Control Systems Design*, Taipei, 2004.

[10] C.W. Scherer (2005). Relaxations for robust linear matrix inequality problems with verifications for exactness. *SIAM Journal on Matrix Analysis and Applications*, 27(2):365–395, 2005.

[11] C.W. Scherer (2006). Lmi relaxations in robust control. *European Journal of Control*, 12(1):3–29, 2006.

[12] C.W. Scherer (2006). Robust h_2 estimation with dynamic iqcs: A convex solution. In *Proceedings of 2006 IEEE Conference on Decision and Control*, San Diego, CA, USA, 2006.

[13] D. Simon (2006). *Optimal State Estimation*. John Wiley & Sons, Hoboken, NJ, USA, 1st edition, 2006.

[14] S. Ibrir (2007). Circle-criterion approach to discrete-time nonlinear observer design. *Automatica*, 43(8):1432–1441, 2007.

[15] Michal Kvasnica (2009). *Real-Time Model Predictive Control via Multi-Parametric Programming: Theory and Tools*. VDM Verlag, Saarbrcken, Germany, 1st edition, 2009.

[16] R. Rajamani (2012). *Vehicle Dynamics and Control*. Springer, New York, USA, 2nd edition, 2012.

[17] M. Abbaszadeh and H. J. Marquez (2006). A robust observer design method for continuous-time lipschitz nonlinear systems. In *Proceedings of the 45th IEEE Conference on Decision and Control*, San Diego, CA, USA, 2006.

[18] B. Acikmese and M. Corless (2008). Stability analysis with quadratic lyapunov functions: Some necessary and sufficient multiplier conditions. *Systems and Control Letters*, 57(1):78–94, 2008.

[19] B. Acikmese and M. Corless (2011). Observers for systems with nonlinearities satisfying incremental quadratic constraints. *Automatica*, 47(7):1339–1348, 2011.

[20] J. H. Ahrens and H.K. Khalil (2009). High-gain observers in the presence of measurement noise: A switched-gain approach. *Automatica*, 45(4):936–943, 2009.

[21] P. Apkarian and R. J. Adams (1997). Advanced gain-scheduling techniques for uncertain systems. *IEEE Trans. on Control System Technology*, 6(1):21–32, 1997.

[22] P. Apkarian and H. D. Tuan (2000). Parameterized lmis in control theory. *SIAM Journal on Control and Optimization*, 38(4):1241–1264, 2000.

[23] M. Arcak and P. Kokotovic (2001). Nonlinear observers: a circle criterion design and robustness analysis. *Automatica*, 37(12):1923–1930, 2001.

[24] K. J. Astrom and B. Wittenmark (2008). *Adaptive Control*. Dover Publications, New York, USA, 2nd edition, 2008.

[25] E. Velenis M. Basset C. Canudas-de Wit, P. Tsiotras and G. Gissinger (2003). Dynamic friction models for road/tire longitudinal interaction. *Vehicle Systems Dynamics*, 39(3):189–226, 2003.

[26] E. Walter C. Durieu and B. Polyak (2001). Multi-input multi-output ellipsoidal state bounding. *Journal of Optimization Theory and Applications*, 111(2):273–303, 2001.

[27] S. K. Spurgeon C. Edwards and R.I. Patton (2000). Sliding mode observers for fault detection and isolation. *Automatica*, 36(4):541–553, 2000.

[28] S. Chebotarev D. Efimov, T. Raissi and A. Zolghadri (2013). Interval state observer for nonlinear time varying systems. *Automatica*, 49(1):200–205, 2013.

[29] R. Sheridan D. M. Bevly and J. C. Gerdes (2001). Integrating ins sensors with gps velocity measurements for continuous estimation of vehicle side-slip and tire cornering stiffness. In *Proceedings of American Control Conference*, Arlington, VA, 2001.

[30] C Edwards and S.K. Spurgeon (1998). *Sliding Mode Control: Theory And Applications*. CRC Press, FL, USA, 1st edition, 1998.

[31] A. Packard F. Wu, X.H. Yang and G. Becker (1996). Induced l2 norm control for lpv systems with bounded parameter variation rates. *International Journal of Robust and Nonlinear Control*, 6(9/10):983–998, 1996.

[32] X. Fan and M. Arcak (2003). Observer design for systems with multivariable monotone nonlinearities. *Systems and Control Letters*, 50(4):319–330, 2003.

[33] J.De. Leon-Morales G. Besancon and O. Huerta-Guevara (2006). On adaptive observers for state affine systems. *International Journal of Control*, 79(6):581–591, 2006.

[34] R. Rajamani G. Phanomchoeng and (2011) D. Piyabongkarn. Nonlinear observer for bounded jacobian systems, with applications to automotive slip angle estimation. *IEEE Transactions on Automatic Control*, 56(5):1163–1170, 2011.

[35] L. El Ghaoui and S. Niculescu (2000). *Advances in Linear Matrix Inequality Methods in Control*. SIAM, Philadelphia, PA, USA, 2000.

[36] A. Howel and K. Hedrick (2002). Nonlinear observer design via convex optimization. In *Proceedings of American Control Conference*, Anchorage, AK, USA, 2002.

[37] A. Rapaport J.L. Gouze and (2000) M.Z. Hadj-Sadok. Interval observers for uncertain biological systems. *Ecological Modelling*, 133(1-2):45–56, 2000.

[38] J.C. Doyle K. Zhou and K. Glover (1995). *Robust and Optimal Control*. Prentice Hall, New Jersey, USA, 1st edition, 1995.

[39] U. Kiencke and L. Nielsen (2000). *Automotive Control Systems*. Springer, New York, USA, 1st edition, 2000.

[40] A. J. Krener and A. Isidori (1983). Linearization by output injection and nonlinear observers. *Systems and Control Letters*, 3:47–52, 1983.

[41] A. J. Krener and W. Respondek (1985). Nonlinear observer with linearizable error dynamics. *SIAM Journal on Control and Optimization*, 23(2):197–216, 1985.

[42] O. Bernard M. Moisan and J.L. Gouze (2009). Near optimal interval observers bundle for uncertain bioreactors. *Automatica*, 45(1):291–295, 2009.

[43] D.G. Maksarov and J.P. Norton (2002). Computationally efficient algorithms for state estimation with ellipsoidal approximations. *International Journal of Adaptive Control and Signal Processing*, 16(6):411–434, 2002.

[44] F. Mazenc and O. Bernard (2011). Interval observers for linear time-invariant systems with disturbances. *Automatica*, 47(1):140–147, 2011.

[45] A. Megretski and A. Rantzer (1997). System analysis via integral quadratic constraints. *IEEE Transactions on Automatic Control*, 42(6):819–830, 1997.

[46] J. Mohammadpour and C.W. Scherer (2012). *Control of Linear Parameter Varying Systems with Applications*. Springer, New York, USA, 2012.

[47] M. Moisan and O. Bernard (2010). Robust interval observers for global lipschitz uncertain chaotic systems. *Systems and Control Letters*, 59(11):687–694, 2010.

[48] J. Bokor P. Seiler, B. Vanek and G.J. Balas (2011). Robust h filter design using frequency gridding, 2011.

[49] G. Phanomchoeng and R. Rajamani (2010). Observer design for lipschitz nonlinear systems using riccati equations. In *Proceedings of American Control Conference*, Baltimore, MD, USA, 2010.

[50] G. Calafiore R. Tempo and F. Dabbene (2012). *Randomized Algorithms for Analysis and Control of Uncertain Systems: With Applications*. Springer, New York, USA, 2nd edition, 2012.

[51] A. Rapaport and D. Dochain (2005). Interval observers for biochemical processes with uncertain kinetics and inputs. *Mathematical Biosciences*, 193(2):235–253, 2005.

[52] J. B. Rawlings and D. Q. Mayne (2009). *Model Predictive Control: Theory and Design*. Nob Hill Pub, Madison, WI, USA, 2nd edition, 2009.

[53] W. J. Rugh and J. S. Shamma (2000). Research on gain scheduling. *Automatica*, 36(10):1401–1425, 2000.

[54] C.W. Scherer and S. Weiland (2005). *Lecture Notes DISC Course on Linear Matrix Inequalities in Control*. April 2005 edition, 2005.

[55] C.W. Scherer and I.E. Kose (2008). Robustness with dynamic iqcs: An exact state-space characterization of nominal stability with applications to robust estimation. *Automatica*, 44(7):1666–1675, 2008.

[56] S. Skogestad and I. Postlethwaite (2005). *Multivariable Feedback Control: Analysis and Design*. Wiley-Interscience, New Jersey, USA, 2nd edition, 2005.

[57] S.P.Boyd and L. Vandenberghe (2004). *Convex Optimiation*. Cambridge University Press, Cambridge, UK, 2004.

[58] E.Feron S.P.Boyd, L.El Ghaoui and V.Balakrishanl (1994). *Linear Matrix Inequalities In Systems and Control Theory*. SIAM, Philadelphia, PA, USA, 1994.

[59] K. Sun and A. Parkard (2005). Robust h_2 and h_∞ filters for uncertain lft systems. *IEEE Transactions on Automatic Control*, 50(5):715–720, 2005.

[60] J.M. Bravo T. Alamo and E.F. Camacho (2005). Guaranteed state estimation by zonotopes. *Automatica*, 41(6):1035–1043, 2005.

[61] M.J. Redondo T. Alamo, J.M. Bravo and E.F. Camacho (2008). A set-membership state estimation algorithm based on dc programming. *Automatica*, 44(1):216–224, 2008.

[62] D. Efimov T. Raissi and (2012) A. Zolghadri. Interval state estimation for a class of nonlinear systems. *IEEE Transactions on Automatic Control*, 57(1):260–265, 2012.

[63] P. Seiler U. Topcu, A. Packard and G. Balas (2010). Help on sos. *IEEE Control Systems Magazine*, 30(4):18–23, 2010.

[64] A.J. van der Schaft (1996). *L2-Gain and Passivity Techniques in Nonlinear Control*. Springer, Berlin, 1st edition, 1996.

[65] J.G. VanAntwerp and R.D. Braatz (2000). A tutorial on linear and bilinear matrix inequalities. *Journal of Process Control*, 10(4):363–385, 2000.

[66] Y. Wang and D. M. Bevly (2012). Robust observer design for lipschitz nonlinear systems using quadratic polynomial constraints. In *Proceedings of 51st IEEE Conference on Decision and Control (CDC)*, Maui, Hawaii, 2012.

[67] X. Xia and W. B. Gao (1989). Nonlinear observer design by observer error linearization. *SIAM Journal on Control and Optimization*, 27:199–216, 1989.

[68] H. Gao B. Du Z. Shu, J. Lam and (2008) L. Wu. Positive observers and dynamic output-feedback controllers for interval positive linear systems. *IEEE Transactions on Circuits and Systems – I*, 55(10):3209–3222, 2008.

[69] A. Zemouche and M. Boutayeb (2009). A unified adaptive observer synthesis method for a class of systems with both lipschitz and monotone nonlinearities. *Systems and Control Letters*, 58(4):282–288, 2009.

[70] A. Zemouche and M. Boutayeb (2012). Observers design for discrete-time lipschitz nonlinear systems. state of the art and new results. In *Proceedings of 51st IEEE Conference on Decision and Control (CDC)*, Maui, Hawaii, 2012.

[71] A. Zemouche and M. Boutayeb (2013). On lmi conditions to design observers for lipschitz nonlinear systems. *Automatica*, 49(2):585–591, 2013.

[72] A. Zemouche and G. Iulia Bara (2008) M. Boutayeb. Observers for a class of lipschitz systems with extension to h_∞ performance analysis. *Systems and Control Letters*, 57(1):18–27, 2008.